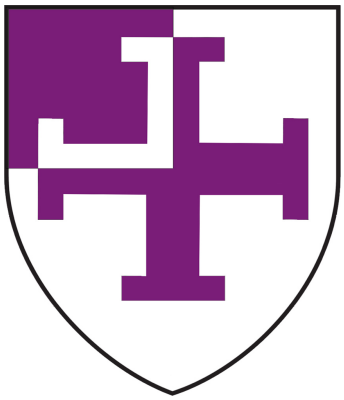

The Role of p97/VCP Co-factor UBXD8/FAF2 in DNA Damage Response

MSc by Research Thesis

Supervised by
Prof Kristijan Ramadan
and
Dr Ignacio Torrecilla

Susan Kilgas

St. Cross College

CRUK/MRC Oxford Institute for Radiation Oncology
Department of Oncology
University of Oxford

Trinity Term 2017

ACKNOWLEDGEMENTS

I would like to thank my supervisor, Professor Kristijan Ramadan, for offering me the opportunity to conduct exciting research in his group. Kristijan's enthusiasm, his lively and energetic presence and love for science are contagious and influenced my work positively throughout my degree. I am grateful for many of his insightful discussions and guidance, which have shaped me strongly as a young scientist.

I will always be thankful for the postdoctoral researcher in the group, Ignacio Torrecilla, who was my mentor during the year. Ignacio is an excellent scientist, who offered me his support, assistance and feedback. He helped me to become better as an independent thinker about my experiments and my results. Thank you for cooperating with me on an exciting project, which was made possible by your SILAC work.

I thank all the rest of the members Ramadan group: John Fielden, Bruno Rodrigues Vaz, Marta Popovic, Annamaria Ruggiano, Giyun Yoo, Katherine Wiseman, Abhay Narayan Singh, Swagata Halder and Judith Oehler. It was wonderful sharing the laboratory with all of them. They provided me with the friendship that I needed. I wish them all the best in their future careers.

Lastly, I would like to thank my family for their emotional support and for making it possible for me to study for this degree.

DECLARAITON

This dissertation is submitted for the degree of Master by Research in Oncology. I hereby declare that the results presented in this thesis are my own, except the results in Figure 3-1 and Figure 3-2, which describe the preliminary data that provided the basis for my project. The individuals responsible for this work are acknowledged in the figure legends. The dissertation does not exceed the prescribed word limit.

ABSTRACT

The homohexameric AAA ATPase p97, also known as valosin-containing protein (VCP), is a fundamentally important molecular chaperone in DNA damage repair. It interacts with its co-factors and uses ATPase activity to control ubiquitin- and SUMO-mediated protein turnover and degradation. SILAC-based quantitative mass spectrometry identified that the p97 co-factor UBXD8/FAF2 significantly increases its interaction with p97 on chromatin during cell recovery after ionising radiation. UBXD8, also known as Fas-associated factor 2 (FAF2), was also shown to have a putative SUMO-interacting motif (SIM). The literature so far has described UBXD8 as an endoplasmic reticulum (ER)-associated degradation protein and a p97 recruitment factor for *de novo* fatty acid synthesis in lipid droplets. Its role on chromatin after DNA damage, however, is unknown. This thesis characterises a role of UBXD8 in DNA damage response and observes how its function relates to p97 on DNA damage sites.

This study discovered that UBXD8 and p97 regulate levels of SUMO-1 and SUMO-2/3 on DNA damage. Depletion of either leads to the accumulation of sumoylated substrates over 6 hours after DNA damage induction. The kinetics of SUMO regulation is similar in the absence of UBXD8 and p97, raising the possibility that UBXD8 works in a complex with p97 to remove sumoylated proteins from chromatin. The study further demonstrated that UBXD8 itself is recruited to and regulates the recruitment of p97 to DNA damage, consequently having an effect on ubiquitylation.

These results introduce a potential novel component in DNA damage response. The potential clinical benefit of studying p97 and its co-factors is the specific targeting of p97 function in DNA repair that could provide a way to sensitise cancer cells to radiotherapy.

Contents

1. INTRODUCTION 1

1.1 Genomic Instability in Cancer 1

1.2. DNA Damage Response (DDR) Pathways 2

1.2.1 DNA Double Strand Break Repair: Non-Homologous End Joining (NHEJ) 6

1.2.2 DNA Double Strand Break Repair: Homologous Recombination (HR) 7

1.2.3 DNA Double Strand Break Repair: Alternative Non-Homologous End Joining (alt-NHEJ) 9

1.3. Regulation of DNA Damage Response by Ubiquitin and SUMO 9

1.3.1 Regulation of Ubiquitylation 10

1.3.2 Regulation of Sumoylation 13

1.3.3 The Role of SUMO in DNA Damage Response and Double Strand Break Repair 18

1.3.4 Crosstalk Between SUMO and Ubiquitin in DNA Damage Response 20

1.4. VCP/p97 in Genome Stability 23

1.4.1. The Structure and Function of VCP/p97 23

1.4.2 p97 Associated Co-factors 25

1.4.3 The Role of p97 in DNA Damage Repair 26

1.5. p97 Cofactors Connected to Thesis 29

1.5.1 UBXD8/FAF2 Structure and Function 29

1.6. Therapeutic Applications of DDR Proteins 31

1.7. Aims of the Thesis 34

2. MATERIALS AND METHODS 35

2.1 Solutions and Reagents 35

2.1.1 Antibodies 35

2.1.2 Buffers 36

2.2 Cell Lines and Cell Culture 38

2.2.1 Cell Lines 38

2.2.2 Culture Conditions 38

2.3 RNA Interference and Plasmid Transfection 38

2.3.1 siRNA Transfections 38

2.3.2 Plasmid Transfections 39

2.3.3 Generation of Cell Lines 40

2.4 Induction of DNA damage and Chemical Treatments 41

2.4.1 Laser-induced DNA Damage 41
2.4.2 Ionising Radiation (IR) 41
2.4.4 Chemical Treatments 41
2.5 Immunofluorescence (IF) 42
2.5.1 Image Acquisition and Analysis 42
2.6 Protein Analysis 43
2.6.1 Cell Lysis 43
2.6.2 SDS-PAGE 43
2.6.3 Western Blotting 44
2.7 Cloning 45
2.7.1 Restriction Enzyme Digestion 47
2.7.2 Transformation of Bacteria 48
2.7.3 Plasmid Purification 49
2.8 Statistical Analysis 50
3. RESULTS 1: UBXD8 IS A POTENTIAL NOVEL COMPONENT IN THE DNA DAMAGE RESPONSE 51
3.1. UBXD8 is Recruited to Sites of DNA Damage 55
3.2. Absence of UBXD8 Causes Hyperaccumulation of Sumoylated Substrates After DNA Damage Induction 59
3.3. UBXD8 Depletion Increases the Number of SUMO Foci After Ionising Radiation 66
3.4. Discussion 69
4. RESULTS 2: UBXD8 AND p97 WORK TOGETHER IN THE REGULATION OF SUMO ON DNA DAMAGE 70
4.1. Absence of p97 Leads to Hyperaccumulation of Sumoylated Substrates After DNA Damage Induction 70
4.2. p97 Recruitment to DNA Damage Depends on UBXD8 76
4.3. UBXD8 Depletion Leads to Hyperaccumulation of K48-linked Polyubiquitylated Substrates 78
4.4. Discussion 80
5. DISCUSSION 82
5.1. SUMO Regulation by UBXD8 and p97 82
5.2. Targeting p97-UBXD8 in Drug Discovery 87
References 90

1. INTRODUCTION

1.1 Genomic Instability in Cancer

Genome instability is inherent in most human cancers and is recognised as a fundamental enabling characteristic of cancer hallmark capabilities (Hanahan and Weinberg, 2011). Most tumours have mutations in their coding regions (insertions, deletions, frameshift mutations, missense and nonsense mutations), chromosome end-to-end fusions or alterations in chromosome numbers (Cancer Genome Atlas Research et al., 2013; Forbes et al., 2011; Stratton et al., 2009). These genomic aberrations display staggering inter-tumour heterogeneity, though advances in tumour genomic profiling technologies have enabled to uncover mutations in crucial "driver" genes that initiate the development of several cancers (Vogelstein et al., 2013). When mutated, these "driver" genes lead to disruptions in a variety of cellular processes, including the essential genome maintenance machinery responsible for: sensing DNA damage and activating the DNA damage response (DDR), directly repairing the damage or inactivating mutagenic molecules to avoid damage (Ciccia and Elledge, 2010; Harper and Elledge, 2007; Jackson and Bartek, 2009; Kastan, 2008). This confers a selective advantage to cancer and impacts on how tumours respond to therapy. During the course of tumour progression, cancerous cells acquire additional mutations that are not directly contributing to disease, but are a form of collateral damage resulting from defective maintenance of genomic integrity. These mutations are called "passenger" mutations (Vogelstein et al., 2013). Large-scale genomic and expression analyses have identified at least 450 DDR related genes that are directly involved in the maintenance of genome stability. Several DDR genes have a direct causal link to cancers and cancer predisposition syndromes. These include Ruijs-Aalfs Syndrome,

Bloom syndrome, Lynch syndrome (hereditary non-polyposis colorectal cancer or HNPCC), Werner syndrome, ataxia telangiectasia, Rothmund-Thomson syndrome and Nijmegen breakage syndrome (Lessel et al., 2014; Pearl et al., 2015). Similarly, a large proportion of cancers such as pancreatic cancer, breast cancer and ovarian adenocarcinoma have defects in homologous recombination (HR), a DNA repair pathway that resolves double strand breaks (DSBs) (Antoniou et al., 2008; Kanchi et al., 2014; Rustgi, 2014). In most cases, however, the specific DDR defects are poorly characterised.

There are several ways in which defective DDR is proposed to cause cancer progression. One hypothesis is activation of oncogenes and inactivation of tumour suppressor genes. Active oncogenes such as RAS and MYC stimulate firing of replication forks, eventually leading to replication stress, fork collapse and DSB formation due to the exhaustion of the available deoxyribonucleoside triphosphate (dNTP) pools. Cells consequently activate DDR and recruit repair factors to DSBs. When some DDR components are dysfunctional, such as in the above-mentioned syndromes, the damaged DNA is not correctly repaired - and in the case of tumour suppressor inactivation - the cells proceed through cell cycle with damaged DNA, leading to mutagenesis (Halazonetis et al., 2008). Current hypotheses propose that DDR defects are selected by the need to cope with high levels of replication stress (Bartkova et al., 2006; Halazonetis et al., 2008) and by the adaptive advantage caused by a high mutational load in tumourigenesis (Burrell et al., 2013; Cahill et al., 1999).

1.2. DNA Damage Response (DDR) Pathways

The variety of genotoxic lesions caused by both exogenous and endogenous sources are matched by the complexity of DNA repair mechanisms. The collective term for these is the

DNA damage response (DDR), which consists of separate but interconnected intra- and intercellular signalling pathways arising from detection of DNA damage, leading to accumulation of DNA repair factors and resulting in repair of lesions. Events in DDR affect fundamental cellular processes such as DNA replication and transcription, cell cycle, senescence and apoptosis (Ciccia and Elledge, 2010). This is to ensure faithful replication of genetic material and prevent any damage from being transmitted to the next cellular generation. Figure 1-1 below summarises the core DNA repair mechanisms:

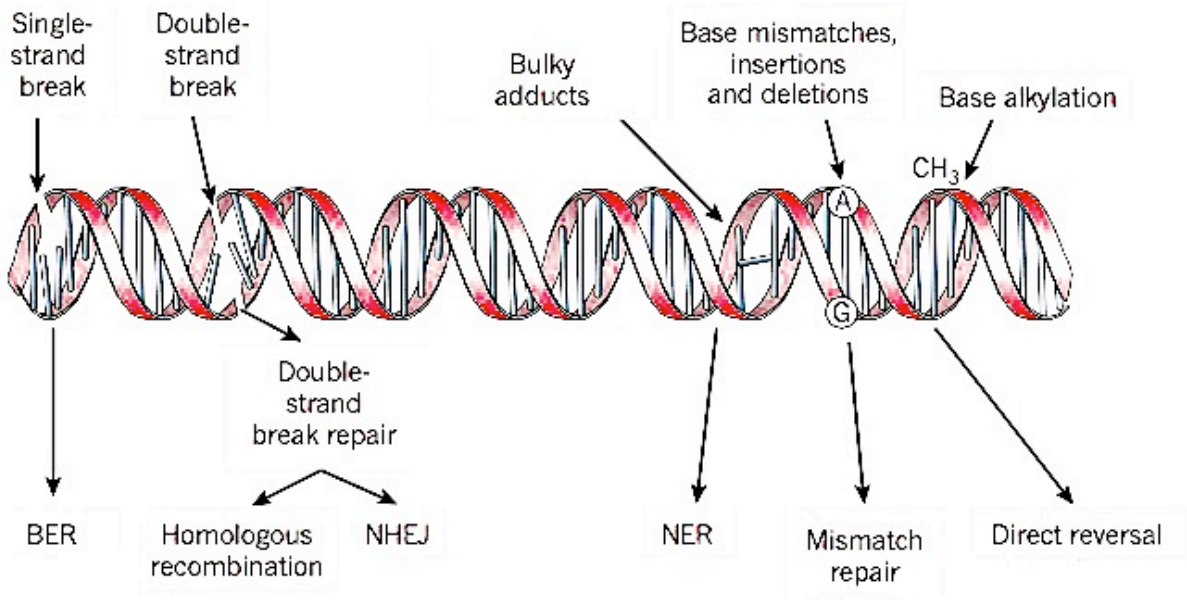

Figure 1-1. Overview of the main DNA lesions and their repair mechanisms. DNA can be damaged in several ways and each lesion is specific. Consequently, cells have evolved to respond to each type of damage in a specific way. A simple lesion such as base alkylation can be reversed directly with an enzymatic reaction, whereas more complicated lesions require a series of enzymes and proteins to repair the damage. DNA double-strand breaks (DSBs) are the most cytotoxic lesions and are repaired by two major pathways – HR and NHEJ. **Abbreviations:** HR, homologous recombination; NHEJ, non-homologous end joining; BER, base excision repair; NER, nucleotide excision repair. The figure is adapted from (Lord and Ashworth, 2012).

As shown in figure 1-1, base alkylation is one of the simpler changes that can occur to DNA structure. This can be repaired by a direct enzymatic reversal with the enzyme O^6-methylguanine DNA methyltransferase (MGMT) (Mishina et al., 2006). Other subtle changes such as base deamination and oxidative lesions caused by reactive oxygen species are repaired by base excision repair (BER). The principle of BER is to excise the damaged base using a lesion specific DNA glycosylase. The apurinic/apyrimidinic (AP) endonuclease creates a nick in DNA at the AP site, eventually leading to DNA resynthesis and ligation. Poly(ADP-ribose) polymerases 1 and 2 (PARP1 and PARP2) are sensors and signal transducers for single-strand breaks (SSBs) (Robertson et al., 2009).

Bulkier lesions are repaired by nucleotide excision repair (NER). These lesions distort the native structure of DNA and are mostly caused by ultraviolet (UV) light, resulting in thymine dimers. They can be encountered either during transcription (transcription-coupled NER), where the lesion blocks RNA polymerase II, or the lesion is simply detected by sensing DNA helix distortions by the xeroderma pigmentosum, complementation group C - radiation sensitive 23 (XPC-RAD23) heterodimer (global-genome NER). The repair mechanism is similar to BER: the region around the lesion is excised by excision repair cross-complementing 1 (ERCC1) or ERCC4, the sequence is resynthesised using DNA polymerases (Pol δ/ε/κ) and the DNA is ligated using DNA ligase 1 (LIG1) or XRCC1-LIG3. The specific polymerases and ligases used depends upon the replication status of cells, with Pol ε and LIG1 mostly used in replicating cells and Pol δ/κ and XRCC1-LIG3 used in non-replicating cells (Marteijn et al., 2014).

While NER is equipped to remove intrastrand crosslinks such as thymine dimers, interstrand crosslinks (ICLs) completely prevent DNA strand separation, halting

replication and transcription. These lesions are very toxic and are repaired by the Fanconi anaemia (FA) pathway. Patients with defective ICL have early onset haemotological malignancies such as bone marrow failure and acute myeloid leukaemia (AML), and they are hypersensitive to ionising radiation (IR) and alkylating agents (Deans and West, 2011; Walden and Deans, 2014). The FA repair pathway consists of 19 genes: Fanconi anaemia group protein A-T (FANCA-FANCT), and biallelic mutations in 17 of them are directly causative to FA (Wang and Smogorzewska, 2015). The key to ICL repair is the monoubiquitination of FANCD2 – a form of posttranslational modification (PTM) that is required for FANCD2 to recruit downstream repair proteins to stalled replication forks. Loss of monoubiquitination of the FANCD2-FANCI heterodimer is a central defect in FA. (Ceccaldi et al., 2016).

As previously mentioned, most cancers display mutations in DNA coding regions. Mismatch repair (MMR) pathway repairs these insertions, deletions and improper base pairings in the genome. The key components in this pathway are the heterodimers MutS homolog 2 - MutS homolog 6 (MSH2-MSH6) and MSH2-MSH3 that recognise mismatches at the replication fork. The DNA surrounding the lesion is then excised by the endonuclease PMS2 and the exonuclease 1 (EXO1). DNA Pol δ then resynthesises the missing strands, and LIG1 ligates the broken ends. Unrepaired mismatches lead to microsatellite instability, a form of genetic hypermutability (Jiricny, 2006). This frequently occurs in colorectal cancers. In fact, large-scale genomic analyses of 15 human cancers revealed that colorectal cancer patients have the highest frequency of DDR gene defects per patient (Pearl et al., 2015).

Among the many types of DNA lesions, DSBs are the most cytotoxic. If left unrepaired, they result in extensive loss of genetic information, leading to mutagenesis and cell death. DSBs are formed and repaired during physiological processes such as meiosis and V(D)J recombination during lymphocyte maturation, but their main exogenous sources are IR and chemotherapeutic drugs. Cells have two major DSB repair pathways – non-homologous end joining (NHEJ) and homologous recombination (HR) (Alt et al., 2013; Khanna and Jackson, 2001). The initial important signalling event after DSB formation is the phosphorylation of the histone variant H2AX around one or more megabases of DNA break sites, which functions as a major recruitment signal for DNA repair proteins (Lukas et al., 2011; Rogakou et al., 1998). It is therefore a widely used marker of DNA damage in experimental methods such as laser induced micro-irradiation and ionising radiation.

1.2.1 DNA Double Strand Break Repair: Non-Homologous End Joining (NHEJ)

NHEJ is the main DSB repair pathway in mammalian cells. Its availability throughout the cell cycle and ability to ligate broken DNA ends independently of sequence makes it a an effective repair method, but its reliance on DNA end-trimming prior to ligation can lead to mutagenesis (Lieber et al., 2003). NHEJ is initiated within seconds after DSBs by the recruitment of the Ku70-Ku80 heterodimer (the Ku complex), which forms a ring-like structure on both DNA ends in a sequence-independent manner and recruits the catalytic subunit of DNA-dependent protein kinase (DNA-PKcs) to the site of damage (Mari et al., 2006; Uematsu et al., 2007). The Ku heterodimer then moves inwards, forms an active DNA-PK complex and allows DNA-PKcs to bridge the broken ends. This leads to the recruitment of downstream repair factors: X-ray cross-complementing protein 4 (XRCC4), LIG4 (Costantini et al., 2007), XRCC4-like factor (XLF) (Yano et al., 2008) and aprataxin and PNK-like factor (APLF) (Grundy et al., 2013). The nuclease Artemis processes 3'-

phosphoglycolate overhangs (Povirk et al., 2007) and DNA polymerases of the Pol X family – Pol μ and Pol λ –perform strand-filling (Lee et al., 2004; Mahajan et al., 2002). The polynucleotide kinase 3'-phosphatase (PNKP) further modifies DNA terminal ends to enable end-ligation by XRCC4, LIG4 and XLF. The XRCC4-LIG4 complex directly interacts with XLF, which promotes the function of this complex (Ahnesorg et al., 2006). Two other crucial proteins are the paralog of XRCC4 and XLF (PAXX) and APLF. PAXX promotes DNA ligation in vitro and assembly of NHEJ factors in a Ku dependent manner (Ochi et al., 2015), and APLF acts as scaffold promoting the recruitment of XRCC4-LIG4 and XLF (Grundy et al., 2013).

1.2.2 DNA Double Strand Break Repair: Homologous Recombination (HR)

HR requires the presence of sister chromatids, because it uses a homologous DNA template to synthesise a new strand. It is considered to be an error-free way of repairing DSBs, but is restricted to G2 and S phases of the cell cycle. HR is initiated by displacement of the Ku complex and recruitment of the MRE11-RAD50-NBS1 complex (MRN complex) (Lee et al., 2016). The MRN complex recognises DSBs and performs DNA end-trimming near break sites with the 3'-5' exonuclease activity of the protein meiotic recombination 11 (MRE11). CtBP-interacting protein (CtIP) then resects DNA in a 5'-3' direction, generating 3' single-strand overhangs (Cannavo and Cejka, 2014). Subsequent end-resection by the 5'-3' exonucleases EXO1 and Bloom syndrome protein-DNA2 (BLM-DNA2) then generates long single stranded DNA (ssDNA), (Eid et al., 2010; Nimonkar et al., 2011), which get bound and protected by replication protein A (RPA). RPA then interacts with breast cancer type 2 susceptibility protein (BRCA2) and is replaced by DNA repair protein RAD51 homologue 1 (Liu et al., 2014). BRCA2 is itself localised to damage sites via BRCA1 and partner and localiser of BRCA2 (PALB2), which

mediate the interaction between BRCA2 and RAD51 (Zhang et al., 2009). Once BRCA2 is replaced by RAD51, the resulting ssDNA filament performs homology search and strand invasion. This results in displacement loop (D-loop) formation, marking the stage where ssDNA has recognised a homologous sequence and formed heteroduplex DNA (hDNA). This then results in strand synthesis and subsequent RAD51 removal from hDNA by RAD54 (Wright and Heyer, 2014).

The repair pathway of choice between NHEJ and HR is mediated by the antagonistic relationship between BRCA1 and p53-binding protein 1 (53BP1). 53BP1 is present throughout the cell cycle, where it restricts DNA end resection and thereby favours the less accurate NHEJ pathway over HR (Bunting et al., 2010; Xie et al., 2007). BRCA1 is an inhibitor of 53BP1 in G2/S phases of the cell cycle. The first implication for the antagonistic relationship between BRCA1 and 53BP1 was shown on $BRCA1^{\Delta 11/\Delta 11}$ allele mice, demonstrating that tumourigenesis was alleviated when 53BP1 was simultaneously deleted (Cao et al., 2009).

Cells that have impaired BRCA2 or RAD51 function are unable to perform conventional HR and are directed to use an alternative and mutagenic form of it, called single strand annealing (SSA) (Stark et al., 2004). A crucial step in SSA is the end-resection mediated by CtIP, and proteins that limit end-resection such as Ku70/80 and 53BP1 therefore suppress SSA (Escribano-Diaz et al., 2013; Munoz et al., 2012). CtIP-mediated end-resection initiates RAD52 binding to the 3' ssDNA tails and annealing of these repeat sequences, creating overhanging flap structures in the process. These are then removed by the ERCC1-ERCC4 complex, and the ends of broken DNA are ligated by LIG3 (Gottlich et al., 1998; Motycka et al., 2004; Rothenberg et al., 2008).

1.2.3 DNA Double Strand Break Repair: Alternative Non-Homologous End Joining (alt-NHEJ)

Alternative NHEJ (alt-NHEJ), also called microhomology-mediated end joining (MMEJ) or micro-SSA is a mutagenic form of DSB repair similar to SSA as they are both based on annealing of short homologous repeats flanking DSBs. Initially, just like in SSA, alt-NHEJ is promoted by CtIP-mediated end-resection and inhibited by Ku70/80. At later stages of repair, alt-NHEJ functions differently, being significantly less dependent on RAD52-mediated annealing and ERCC1-ERCC4 mediated DNA excision (Bennardo et al., 2008). The pathway depends mostly on PARP1, which acts as a break sensor and a signal transducer, leading to the recruitment of the MRN complex, XRCC1 and LIG3 (Audebert et al., 2004; Haince et al., 2008). EXO1 and BLM-DNA2 perform extensive end-resection and Pol λ preferentially fills in the gaps (Nick McElhinny et al., 2005; Truong et al., 2013). DNA is then ligated by either LIG1 or XRCC1-LIG3 (Paul et al., 2013).

1.3. Regulation of DNA Damage Response by Ubiquitin and SUMO

DNA damage response consists of a highly complex network of interconnected signalling proteins that recognise and repair damage sites. Naturally, this requires intricate fine-tuning of protein functions, which is achieved by various PTMs that activate or inhibit proteins, direct them to their correct subcellular compartments at the right time, influence their interactions with other proteins and control their disposal. PTMs such as phosphorylation, methylation, acetylation, neddylation, sumoylation and ubiquitylation occur and conduct the vast array of these cellular events at the site of DNA damage (Schwertman et al., 2016). Sumoylation and ubiquitylation - the covalent attachment of

SUMO and ubiquitin polypeptides, respectively-, are highly versatile and abundant chemical modifications in the maintenance of genomic stability. They play roles in all stages of DNA repair and their reversibility allows rapid changes to occur during this process, which is necessary for repair completion. If sumoylation and ubiquitylation are disrupted, the repair can either be delayed or remain incomplete, which increases the likelihood of cells accumulating more damage and eventually undergoing apoptosis. This happens because DNA damage repair proteins are not efficiently recruited to or extracted from break sites, leading to the disruption of dynamic protein exchange at the site of damage. For example, inherited defects in ubiquitylation lead to DDR deficiencies, illustrating the clinical importance of ubiquitylation in DDR (Jackson and Durocher, 2013; Schwertman et al., 2016). Understanding these complex PTMs could therefore aid both in the diagnosis and treatment of cancer.

1.3.1 Regulation of Ubiquitylation

Ubiquitylation is the covalent attachment of a 76-amino acid ubiquitin protein onto target proteins. This is a series of enzymatic reactions conducted by three classes of enzymes: ubiquitin-activating enzymes (E1s), ubiquitin-conjugating enzymes (E2s) and ubiquitin ligases (E3s). The importance and complexity of the ubiquitin code is illustrated by the activity of many enzymes: two E1 enzymes, over 35 E2s, over 600 E3 ligases and around 100 deubiquitinating enzymes (Grabbe et al., 2011; Komander and Rape, 2012). Overall, there exist more than 1,000 known components in the ubiquitin system and over 11,000 ubiquitylation sites on more than 4,000 proteins (Kim et al., 2011; Wagner et al., 2011). To add to the complexity of the possible signalling events, each ubiquitin contains 7 lysine residues (K6, K11, K27, K29, K33, K48, K63) and an amino terminus methionine 1 (M1), which can be used to form linear, branched, homogenous and mixed chains each with

different cellular outcomes. Proteins can be monoubiquitinated, multi-monoubiquitinated and polyubiquitinated (Bergink and Jentsch, 2009; Komander and Rape, 2012).

In the first enzymatic reaction, ubiquitin-activating enzyme E1 binds the C-terminal part of ubiquitin in an ATP-dependent manner. This reaction creates a thioester intermediate. Isopeptide linkage is then formed between the NH_2-group of a lysine residue in the target protein and the C-terminus of ubiquitin with the aid of an E2 conjugating enzyme and a catalysing E3 ligase (Spasser and Brik, 2012). Depending on the class of the E3 ligase, ubiquitin can be transferred from E2 to the substrate in different ways: (1) homologous to the E6-AP carboxyl terminus (HECT) type E3 ligases form a transient thioester with ubiquitin before transferring it to a substrate. Linkage specificity depends on E3 ligases; (2) RING and U-box containing E3 ligases are scaffold proteins that bind E2 conjugating enzymes and determine substrate specificity. (Komander and Rape, 2012) (3) RING/HECT hybrids, where RING1 recruits an E2 conjugating enzyme and ubiquitin is transported to a cysteine in RING2 domain before conjugating it to a substrate (Spratt et al., 2014). Once ubiquitin has been conjugated, it can form different types of ubiquitin chains. Adding a single ubiquitin protein typically affects the activity, localisation or complex formation of the target protein. For example, the DNA polymerase processivity factor proliferating cell nuclear antigen (PCNA) is monoubiquitylated, which influences its interaction with translesion synthesis (TLS) DNA polymerases - enzymes that are able to replicate past DNA lesions (Zhang et al., 2011). Homogenous polyubiquitin chains are connected through the same lysine or methionine residue. The type of lysine residue determines the cellular outcome: K48- and K11-linked polyubiquitin chains are degradation signals and proteins tagged with these are transported to the 26S proteasome. K63-linked polyubiquitin chains, however, usually regulate protein-protein interactions

and are important signals for the recruitment of proteins to DSBs (Chen and Sun, 2009). There is extensive crosstalk between ubiquitin and other PTMs in DSB repair, and one relevant to this study is the ubiquitin-SUMO mixed chain formation at the site of damage. Ring finger 4 (RNF4), a SUMO-targeted ubiquitin ligase (STUbL), ubiquitylates polySUMO chains and creates SUMO-ubiquitin mixed chains that act as signal for downstream repair proteins such as RAP80 (Guzzo et al., 2012; Hu et al., 2012). Figure 1-2 below summarises the main ubiquitin conjugations steps.

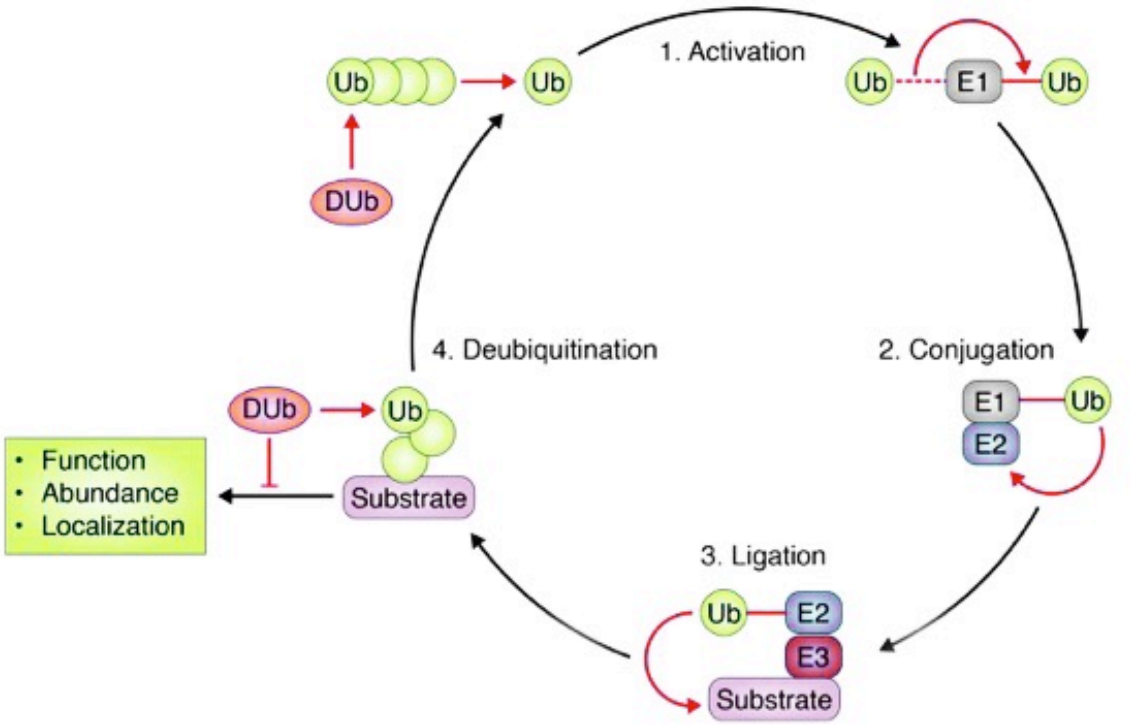

Figure 1-2. Overview of ubiquitin conjugation and deconjugation pathways. The ubiquitin activating E1 enzyme binds the C-terminus of ubiquitin. The E2 conjugating enzyme then binds ubiquitin and together with the E3 ligase ubiquitin is transferred onto a substrate, forming an isopeptide linkage. Several ubiquitin chains can form on one substrate. Ubiquitylation is a reversible reaction and specialised deubiquitination enzymes (DUBs) cleave off ubiquitin chains from substrates, thereby affecting substrate function, abundance and cellular localisation. The figure is adapted from (Heaton et al., 2016).

The ubiquitin code is recognised by specialised proteins with ubiquitin-binding domains (UBDs). Proteins can have several UBDs, and more than 20 different types of UBDs are known. The following UBDs are abundant in DDR proteins: ubiquitin-interacting motif (UIM), motif interacting with ubiquitin (MIU) and ubiquitin-binding zinc-finger (UBZ) (Dikic et al., 2009). For example, RAP80 contains two UIMs that confer specificity towards K63-linked polyubiquitin chains (Sims and Cohen, 2009). Just as there are several ubiquitin-binding domains, there are deubiquitinating enzymes, DUBs, involved in removing ubiquitin from target proteins. This confers the reversibility of ubiquitin modifications. DUBs are specialised isopeptidases that can remove entire chains from substrates, thereby reversing the signal and sending the proteins to be recycled or degraded. DUBs can be classified into six families, where five of them encode cysteine proteases and one encodes metalloproteases (Amerik and Hochstrasser, 2004; Mevissen and Komander, 2017). A well-characterised DUB is the cysteine protease ubiquitin-specific protease 1 (USP1), which deubiquitylates FANCD2 and its inactivation leads to FA phenotypes (Nijman et al., 2005). DUBs themselves are regulated by PTMs to ensure tight control of ubiquitylation and deubiquitylation events (Meray and Lansbury, 2007).

1.3.2 Regulation of Sumoylation

SUMO stands for small ubiquitin-like modifier. Like ubiquitin, SUMO can form mono, multi-mono, polymeric, branched and mixed chains (Tatham et al., 2001). It is functionally at least as diverse, being involved in the regulation of transcription, DDR, nucleocytoplasmic transport and chromosome segregation. Similarly to ubiquitylation, sumoylation is highly reversible and SUMO signals are antagonised by specific proteases, the sentrin-specific proteases (SENPs) (Gareau and Lima, 2010; Hendriks and Vertegaal, 2016).

SUMO conjugation system is analogous to the ubiquitin system, but with some important differences. SUMO is first activated in an ATP-dependent manner by the heterodimeric E1 activating enzyme SUMO-activating enzyme subunit 1-2 (SAE1-SAE2). ATP energy is used to adenylate the C-terminal glycine residue in SUMO, creating a thioester intermediate between SUMO and the cysteine residue in SAE2. Transesterification reaction then transfers SUMO from SAE2 to the E2 ubiquitin-conjugating enzyme 9 (UBC9). The thioester linked UBC9-SUMO then catalyses the formation of an isopeptide bond between the C-terminus of SUMO and the NH_2-group of a lysine residue in the target protein (Gareau and Lima, 2010). Figure 1-3 below summarises the main SUMO conjugation steps.

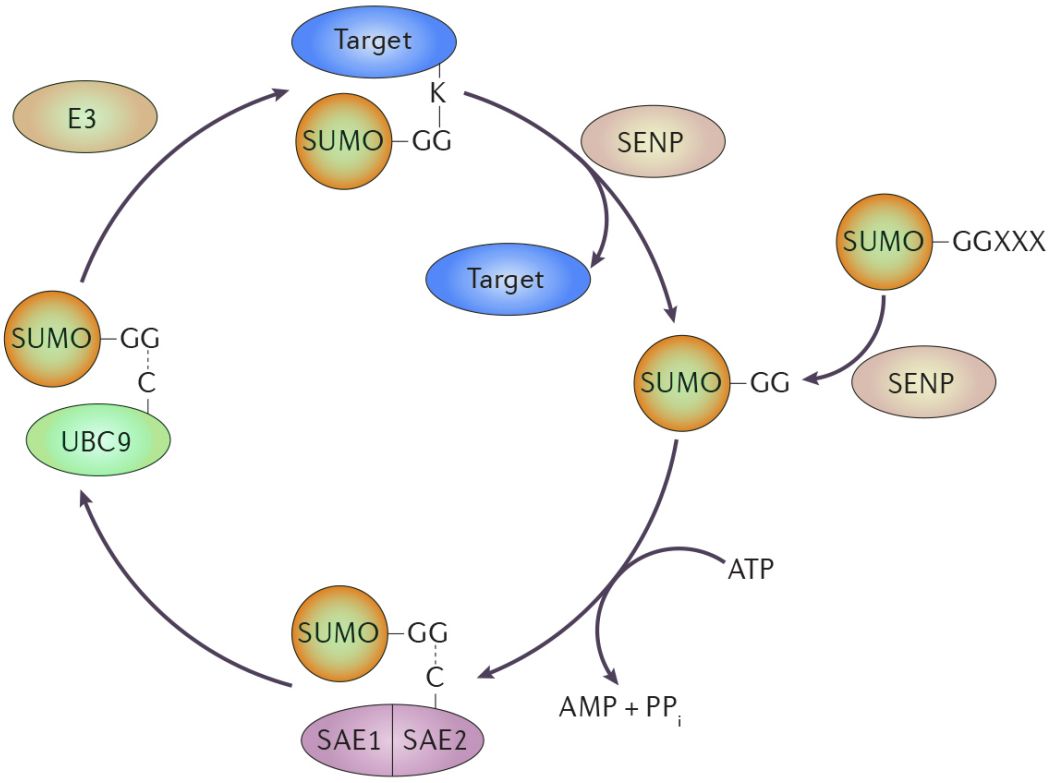

Figure 1-3. Summary of SUMO conjugation and deconjugation pathways. The first step in SUMO conjugation is the cleavage of the C-terminal extension, which is mediated by a specific protease named SENP. SUMO is then activated by the E1 activating enzyme SAE1-SAE2, which adenylates the C-terminal glycine residue of SUMO. This reaction is ATP dependent and releases AMP and PP_i in the process. SUMO is then transferred as part of a transesterification reaction from the heterodimeric E1 enzyme to the E2 conjugating enzyme UBC9. UBC9 can then directly transfer SUMO onto target proteins, although the reaction can be enhanced in the presence of an E3 ligase. SENPs then cleave SUMO from its substrates, thereby ensuring the reversibility of this PTM. **Abbreviations:** SENP, Sentrin-Specific Protease; SAE1-SAE2, SUMO-Activating Enzyme Subunit 1-2; UBC9, Ubiquitin-Conjugating Enzyme 9. The figure is adapted from (Hendriks and Vertegaal, 2016).

Contrary to the ubiquitin system, where mostly hundreds of E3 ligases determine substrate specificity (Hoeller et al., 2007), the SUMO system relies on its E2 conjugating enzyme, UBC9. E3 ligases are not necessarily important in the conjugation machinery (Sampson et al., 2001). For example, in a purified system, SUMO-1, SAE and UBC9 are sufficient to induce SUMO-1 binding to the nuclear factor of kappa light polypeptide gene enhancer in B-cell inhibitor, alpha (IκBα) (Desterro et al., 1998). The vast majority of SUMO targets occur within a consensus sequence ΨKxE/D, where Ψ signifies a bulky aliphatic residue

and x is any amino acid. UBC9 plays an important role of target selection by binding directly to this consensus sequence (Tatham et al., 2001). Overall, the number enzymes within the SUMO conjugation machinery is significantly smaller than in the ubiquitin system: one activating, one conjugating enzyme and twelve known E3 ligases (Garvin and Morris, 2017).

Similarly to SUMO conjugation system, SUMO-binding domains are less complex compared to the ubiquitin system. The most prevalent is the SUMO-interacting motif (SIM), which was first discovered by two-hybrid screens and mass spectrometry (Hannich et al., 2005; Minty et al., 2000; Song et al., 2004). SIM aligns as a parallel or antiparallel β-strand and consists of a hydrophobic core flanked by acidic amino acids and/or phosphorylated residues. It extends the SUMO β-sheet, thereby creating an interaction between the hydrophobic core of SIM and the hydrophobic pocket on SUMO (Reverter and Lima, 2005; Song et al., 2005). The SIM domain is found in various cellular proteins controlling DDR such as STUbLs, illustrating the importance of sumoylation in DNA damage repair (Kerscher, 2007; Perry et al., 2008). Additionally to SIMs, the MYM- and ZZ-type zinc-finger domains have been identified as novel SUMO-binding motifs. While the MYM-type domain interacts with the same SUMO-2 surface as SIMs, the ZZ-type domain has affinity for SUMO-1, representing a unique epitope for SUMO interaction that is spatially opposite to the SIM domain (Danielsen et al., 2012; Diehl et al., 2016; Guzzo et al., 2014).

Three SUMO isoforms are known to be involved in conjugation: SUMO-1, SUMO-2 and SUMO-3. SUMO-1 is regarded as the chain termination signal as it lacks the internal consensus sequence ΨKxE/D used for chain formation. It mostly forms a capping structure

on SUMO-2/3 chains, thereby preventing further chain elongation (Matic et al., 2008; Tatham et al., 2001). It is, however, shown that SUMO-2 can conjugate to SUMO-1 at various lysine residues and SUMO-1-SUMO-2/3 and SUMO-1-ubiquitin mixed chains occur, adding to the complexity of SUMO signalling (Hendriks et al., 2017; Hendriks and Vertegaal, 2016; Lamoliatte et al., 2017; Sun et al., 2007). SUMO-1 pools, however, are spatially more restricted compared to SUMO-2/3 pools. SUMO-1 is largely in the conjugated form within nuclear pores, whereas SUMO-2/3 isoforms exist as free proteins that undergo rapid conjugation upon cellular stress. This indicates that SUMO-2/3 signalling is more versatile than SUMO-1 signalling (Seeler and Dejean, 2003).

SUMO-2 and SUMO-3 have 97% sequence identity to each other and are 47% similar to SUMO-1 (Hendriks et al., 2015; Wang and Dasso, 2009). They are able form poly-SUMO chains and mixed chains with ubiquitin as they contain the ΨKxE/D consensus sequence in their N-terminal region, centered on K11 (Tatham et al., 2001). There is some evidence that separate types of SUMO chains exist, as linkages on other lysine residues have been detected in SUMO-2/3 (Hendriks et al., 2017; Hendriks and Vertegaal, 2016; Lamoliatte et al., 2017).

SUMO deconjugation is mediated by SENPs, and there are currently six known genes encoding SUMO-specific proteases in humans: SENP1, SENP2, SENP3, SENP5, SENP6 and SENP7 (Nayak and Muller, 2014). Three other enzymes have isopeptidase activity towards SUMO: desumoylating isopeptidases 1 and 2 (DESI-1 and DESI-2) are able to cleave SUMO-1 and SUMO-2/3 chains (Shin et al., 2012), and ubiquitin specific peptidase like 1 (USPL1) has a preference for SUMO-2/3 chains over SUMO-1 (Schulz et al., 2012). SUMO substrate specificity is partly influenced by the subcellular localisation of SUMO-specific proteases. For example, SENP1 and SENP2 are localised in the nuclear envelope

(Chow et al., 2014), whereas SENP7 is a critical component on heterochromatin, where it induces chromatin relaxation before HR (Garvin et al., 2013; Maison et al., 2012).

1.3.3 The Role of SUMO in DNA Damage Response and Double Strand Break Repair

The importance of SUMO in DSB repair is illustrated by the fact that SUMO-1 and SUMO-2/3 are present on DSBs, and that many of the DDR proteins are sumoylated: 53BP1, mediator of DNA damage checkpoint protein 1 (MDC1), BRCA1, RAP80 and the E3 ubiquitin ligase RNF168 (Galanty et al., 2009; Luo et al., 2012; Morris et al., 2009). The accumulation of RNF168 is suppressed in the absence of the SUMO E3 ligases protein inhibitor of activated STAT 1 (PIAS1) and PIAS4. Similarly, ubiquitin conjugates and downstream factors fail to accumulate in the absence of these ligases (Galanty et al., 2009; Morris et al., 2009), demonstrating that the function of sumoylation on sites of DNA damage is to regulate protein-protein interactions and enzymatic activities such as RNF8-RNF168 mediated functions crucial in ubiquitin-SUMO crosstalk at DSBs. Another SUMO E3 ligase, methyl methanesulfonate-sensitivity 21 (MMS21), is involved in DSB repair by promoting the activity of the structural maintenance of chromosomes 5-6 (CSMC5-SMC6) cohesion complex, involved in mediating HR between sister chromatids. MMS21 functions to increase sumoylation of the cohesion subunit RAD21 (Wu et al., 2012). Additionally to DSB repair, SUMO E3 ligases control the FA pathway and single strand break repair. PIAS1 promotes ICL repair via its interaction with sensitive to nitrogen mustard 1A (SNM1A), a 5'-3' exonuclease that digests past ICLs (Ishiai et al., 2004). Additionally, sumoylation promotes DNA repair by causing the accumulation of tyrosyl DNA phosphodiesterase (TDP1) on DNA breaks, a protein that removes stalled topoisomerase 1 from DNA ends (Hudson et al., 2012).

As SUMO-1 and SUMO-2/3 have only around 50% sequence identity and differ in their ability to form SUMO chains (Hendriks et al., 2015), they also perform distinct functions at the site of DSBs. Firstly, different recruitment kinetics to damage sites have been observed between SUMO-1 and SUMO-2/3, showing that DSB repair factors have different preferences for SUMO isoforms. For example, factors mostly associated with the early DNA damage response such as γH2AX, MDC1 and RNF168 are preferably modified by SUMO-1 (Chen et al., 2013; Danielsen et al., 2012; Luo et al., 2012), while later repair factors such as 53BP1, EXO1 and BRCA1 are equally modified by all three SUMO isoforms (Bologna et al., 2015; Galanty et al., 2009; Morris et al., 2009). One of the reasons for this difference in SUMO isoform kinetics is the activity of SUMO E3 ligases. PIAS4 is critical for SUMO-1 modification and is shown to be a involved in early DDR, whereas PIAS1 is necessary for SUMO-2/3 ligation in later stages of repair (Danielsen et al., 2012; Galanty et al., 2009; Luo et al., 2012). There is no functional redundancy between SUMO isoforms in DSB repair: SUMO-1 depleted cells show a stronger DSB repair defect in I-*Scel* reporter assays, but the depletion of SUMO-2/3 leads to radiosensitivity, suggesting that all isoforms are needed for efficient DSB repair (Hu and Parvin, 2014; Yin et al., 2012).

SUMO is responsible for the recruitment of DDR proteins to DSBs and influences the subcellular localisation of DNA repair factors. For example, RAD51 recruitment to DSBs is facilitated by its interaction with the sumoylated form of Bloom syndrome protein (BLM) helicase after fork stalling, thereby promoting homologous recombination (Ouyang et al., 2009). In another example, SUMO interacts with the FA scaffold protein synthetic lethal of unknown function protein 4 (SLX4) that is responsible for recruiting nucleases to DNA damage sites. The interaction between SLX4 and SUMO is necessary for SLX4

recruitment to collapsed replication forks (Guervilly et al., 2015). SUMO itself can also act as a scaffold for protein group recruitment in DDR. Sumoylation of the ATM and RAD3-related (ATR) kinase partner ATR interacting protein (ATRIP) regulates its interaction with its multiple binding partners after DNA damage, indicating that sumoylation plays a role in protein complex formation (Wu et al., 2014).

SUMO deconjugation pathways also have important roles in DNA break repair, particularly in HR. For example, SENP6 is known to keep RPA70, a protein that binds ssDNA intermediates, in a hyposumoylated state under normal conditions. Upon replication stress, SENP6 dissociates from RPA70, allowing it to be sumoylated, which then facilitates the recruitment of RAD51 to ssDNA (Dou et al., 2010). SENP7 influences chromatin compaction and therefore DSB repair efficiency by regulating sumoylation levels of KRAB domain-associated protein 1 (KAP1), a factor involved in the maintenance of heterochromatin. KAP1 is sumoylated under normal conditions, which provides a binding site for the ATPase chromodomain helicase DNA binding protein 3 (CHD3). CHD3 is part of the nucleosome remodelling and deacetylase (NuRD) complex involved in the maintenance of heterochromatin. Upon DNA lesions, KAP1 is rapidly phosphorylated by ATM, which decreases KAP1 sumoylation levels, leading to CHD3 release from the NuRD complex and chromatin relaxation, which allows for DSB repair to proceed (Garvin et al., 2013; Goodarzi et al., 2011; Noon et al., 2010).

1.3.4 Crosstalk Between SUMO and Ubiquitin in DNA Damage Response

There is extensive crosstalk between SUMO and ubiquitin in the DNA DSB repair. This is mediated by STUbLs, which are SUMO-targeted ubiquitin ligases. One of best-studied examples of this is the STUbL activity of RNF4, which ubiquitylates polysumoylated

substrates via an interaction between its N-terminal SIM and the sumoylated DDR proteins (Tatham et al., 2008). The major targets of RNF4 activity are 53BP1, MDC1 and RPA. RNF4 causes their turnover at break sites by the attachment of K48-linked polyubiquitin chains, leading to their subsequent extraction. The absence of RNF4 leads to inefficient recruitment of RAD51 (Galanty et al., 2012; Gibbs-Seymour et al., 2015; Luo et al., 2012). Additionally, RNF4 causes UBC13-dependent formation of K63-linked polyubiquitin chains, which is the predominant ubiquitylation signal for the recruitment of proteins to DSBs, and RNF4 depletion leads to a global decrease in K63-linked polyubiquitin signals at sites of DNA damage (Branigan et al., 2015; Yin et al., 2012). RNF4 targeted poly-SUMO chains are rapidly recognised by RAP80 through its UIM and SIM domains, leading to its recruitment to DSBs, where it is responsible for further recruitment of the BRCA1-A complex (Guzzo et al., 2012; Hu et al., 2012). Figure 1-4 below illustrates the role of SUMO in DDR.

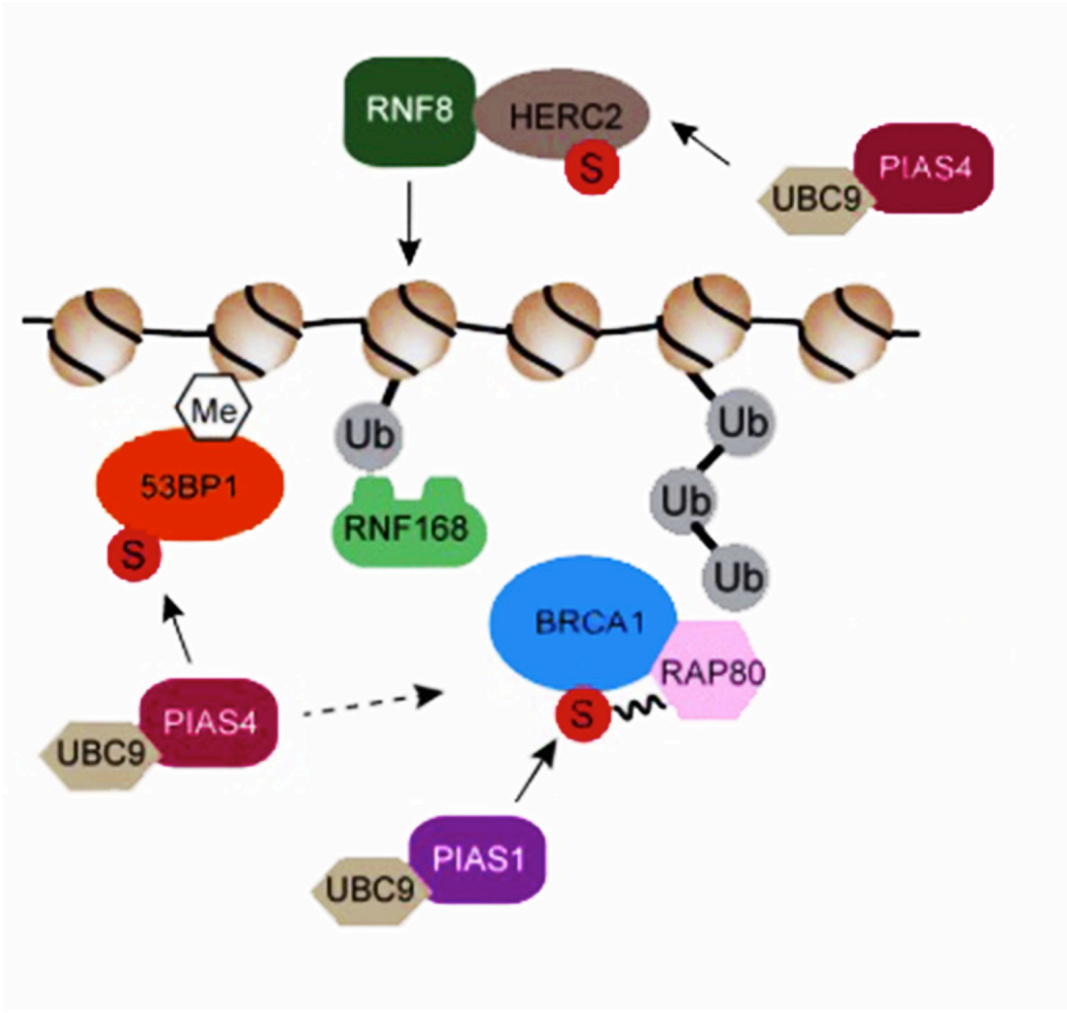

Figure 1-4. Examples of SUMO modifications on sites of DNA damage. SUMO targets several crucial DNA repair factors such as 53BP1, HERC2 and BRCA1. In this example, the SUMO E3 ligases PIAS1 and PIAS4 cause the formation of polySUMO chains on these proteins, which are then recognised by downstream mediators such as RAP80, eventually leading to recruitment of the BRCA1-A complex and RAD51 binding to RPA coated ssDNA. The absence of PIAS1 or PIAS4 has shown to significantly decrease both HR and NHEJ, resulting in hypersensitivity to IR. Depletion of RNF8 or RNF168 impairs the accumulation of all three SUMO isoforms, further demonstrating the global importance of sumoylation in DDR. **Abbreviations:** RNF, RING Finger; PIAS, Protein Inhibitor of Activated STAT; BRCA1, Breast Cancer Type 1 Susceptibility Protein; RAP80, Receptor Associated Protein 80; UBC9, Ubiquitin-Conjugating Enzyme 9; HERC2. HECT Domain and RCC1-Like Domain-Containing Protein 2; 53BP1, p53-Binding Protein 1. The figure is adapted from (Jackson and Durocher, 2013)

1.4. VCP/p97 in Genome Stability

1.4.1. The Structure and Function of VCP/p97

The homohexameric AAA ATPase valosin-containing protein (VCP)/p97 or Cdc48 in lower eukaryotes is a critical component of the ubiquitin-proteasome system (UPS). It uses energy from ATP to extract polybubiquitinated substrates from various cellular locations and protein complexes, leading to their degradation by the proteasome or to substrate deubiquitylation and recycling (Sauer and Baker, 2011). Its involvement in endoplasmic reticulum (ER)-associated protein degradation (ERAD) (Christianson and Ye, 2014), mitochondria-associated degradation (Taylor and Rutter, 2011), endosomal trafficking (Ramanathan and Ye, 2012), ribosomal quality control (Verma et al., 2013) and chromatin-associated degradation (CAD) (Franz et al., 2016; Ramadan et al., 2007) make it a central component of protein quality control. VCP/p97 cooperates with a variety of different co-factors that enable p97 to execute such diverse roles, providing pathway selectivity and substrate processing specificity. These co-factors operate on a bridging mechanism by bringing p97 to ubiquitylated substrates via their p97-interacting motifs and UBDs (Buchberger et al., 2015).

Structurally, p97 is a homohexamer with two ATPase domains forming a double ring. Each of the six subunits is composed of the following: N-terminal domain, AAA ATPase D1 and D2 domains that are separated by a linker domain, and a C-terminal tail. (DeLaBarre and Brunger, 2003). A recent seminal paper (Bodnar and Rapoport, 2017) elucidated the mechanism of substrate processing by the Cdc48 ATPase complex (Figure 1-5), where they demonstrated that there is extensive crosstalk between D1 and D2 rings during substrate translocation through the central pore of the Cdc48 hexamer and that the

final release of the processed substrate depends on deubiquitylation. Firstly, the K48-linked substrate binds to the co-factor complex ubiquitin fusion degradation 1 – nuclear protein localisation protein 4 (Ufd1-Npl4, or the UN complex), after which the Cdc48 unfolds the substrate using energy from ATP hydrolysis in D1, and passes it all the way through its central pore. The translocation process relies on ATP hydrolysis in D2, and the release of the K48-linked substrate requires partial trimming of ubiquitin chains by a Cdc48-associated deubiquitinase as well as ATP activity in D1. The remaining substrate can then be translocated through the pore and be released at the side of D2.

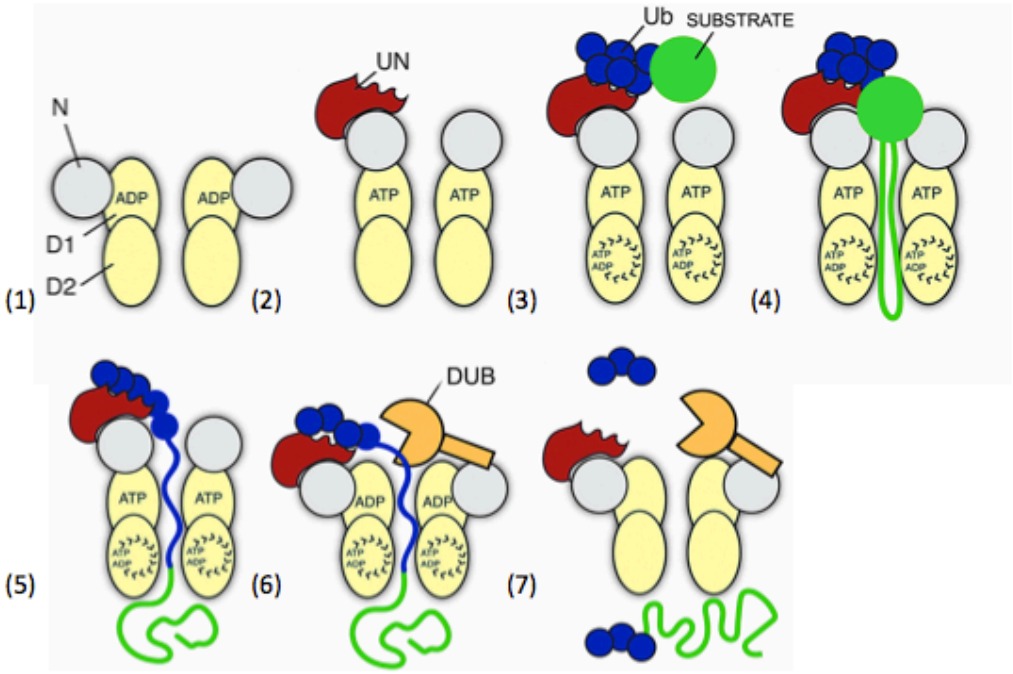

Figure 1-5. Model of Cdc48/p97 substrate processing. (1) The structure of Cdc48 consists of the N-terminal domain, D1 and D2 AAA domains, and a C-terminal tail. The D1 domain is ADP-bound. (2) Upon ATP binding, the N-terminus changes its confirmation and the UN complex Ufd1-Npl4 binds to the N-terminus. (3) K48-linked ubiquitylated substrates then bind the UN complex, (4) and the substrate unfolds and forms a loop that is translocated into the central cavity of Cdc48. (5) The binding of the substrate stimulates ATP hydrolysis in D2. This energy is then used to pull the substrate further, so that parts of ubiquitin chains enter into the cavity. (6) In order to fully release the substrate at the D2 side of the pore DUB activity is needed, which partially cleaves off ubiquitin chains, (7), allowing the remaining substrate to translocate through the cavity. **Abbreviations:** UN, Ufd1-Npl4; DUB, Deubiquitination Enzyme; Ub, Ubiquitin. The figure is adapted from (Bodnar and Rapoport, 2017).

Mutations in human p97 have been implicated in a variety of diseases, including colorectal, pancreatic and lung cancers (Haines, 2010). 2 % of familial amyotrophic lateral sclerosis cases (fALS) are due to mutations in the p97 gene, which is an autosomal dominant disease characterised by progressive degeneration of motor neurons, eventually leading to respiratory failure (Ishigaki et al., 2004). Inclusion body myopathy with Paget's disease of the bone and frontotemporal dementia (IBMPFD) is directly linked to p97 dysfunction and is an autosomal dominant negative condition leading to muscle weakness, osteolytic lesions and frontotemporal dementia (Watts et al., 2004). Consistently to the role of p97 in protein quality control, many of the diseases associated with p97 mutations lead to neurodegeneration as toxic protein aggregates accumulate in cells (Chapman et al., 2011).

1.4.2 p97 Associated Co-factors

p97 cooperates with several binding partners to mediate the variety of its functions. Around 30 different co-factors have been identified so far, by far the largest family containing ubiquitin regulatory X (UBX) or UBX-like domains. These UBX domains bind the N-terminus of p97 and assume the ubiquitin fold. There are 13 known UBX proteins in the mammalian system, but their functions are largely unknown (Alexandru et al., 2008; Buchberger et al., 2015). Other co-factors have the following domains/motifs: SHP motif, VCP interacting protein (VIP) motif, VCP-binding (VBM) motif, peptide *N*-glycosidase (PNGase)/ubiquitin-associated (PUB) domain and ubiquitin D (UBD) domain (Buchberger et al., 2015).

So far, three mutually exclusive p97 core complexes have been identified, each of which can have several functions by binding to different sets of accessory proteins that determine

the subcellular localisation of the complex or provide enzyme activities. The three core complexes are the $p97^{-Ufd1\text{-}Npl4}$, the $p97^{-p47}$ and the $p97^{-UBXD1}$ complex. Ufd1-Npl4 heterodimer associates with p97 to mediate protein quality control on sites of DNA damage, functions in ERAD and ribosomal quality control. It mediates the extraction of proteins with K48-linked polyubiquitin chains and directs the proteins to the proteasome (Verma et al., 2011; Ye et al., 2003). In contrast, the $p97^{-p47}$ and the $p97^{-UBXD1}$ core complexes have proteasome-independent functions and play a role in the ubiquitin-dependent membrane fusion and vesicular trafficking, respectively (Rabouille et al., 1998; Ritz et al., 2011).

Most of the co-factors bind to the N-terminal domain of p97, although domains have been identified that bind to the C-terminal tail. When co-factors bind the N-terminal part, six adaptors can be associated with the homohexameric structure of p97 at any one time. The three core complexes add a layer of complexity as they contain more than one binding site and thereby can occupy several N-terminal subunits at once, modifying the total number of adaptor proteins able to interact with p97 (Hanzelmann et al., 2011; Schuberth and Buchberger, 2008).

1.4.3 The Role of p97 in DNA Damage Repair

Seminal reports of p97 being involved in DDR came from the observations that p97 is physically recruited to DSBs and in the absence of p97 cells become hypersensitive to IR and delay DSB repair (Acs et al., 2011; Meerang et al., 2011). The $p97^{-Ufd1\text{-}Npl4}$ complex is recruited to DNA damage by K48-linked polyubiquitin signals formed by RNF8 (Meerang et al., 2011). The complex extracts polyubiquitinated proteins from chromatin and regulates the progression of DNA damage repair. For example, p97 removes sterically

trapped K48-linked Ku80 after NHEJ, and p97 depletion results in hyperaccumulation of both Ku80 and K48-linked polyubiquitin chains on DNA damage sites (van den Boom et al., 2016). Whether p97 also extracts Ku70 is currently unknown, although Ku70 is also ubiquitylated (Brown et al., 2015; Grundy et al., 2014; Postow et al., 2008). Additionally, the p97$^{\text{-Ufd1-Npl4}}$ complex extracts the ubiquitylated polycomb protein lethal(3)malignant brain tumour like protein 1 (L3MBTL1), thereby paving the way for the recruitment of downstream DDR factors such as 53BP1 (Acs et al., 2011). Other NHEJ factors are likely to be targeted by p97 as it has been shown to directly interact with ubiquitylated DNA-PKcs and the depletion of p97 in human cells results in overall decreased NHEJ efficiency (Jiang et al., 2013; Torrecilla et al., 2017).

Besides regulating NHEJ, p97 has additional roles in the coordination of HR. The p97$^{\text{-Ufd1-Npl4}}$ complex inactivation leads to impaired DNA end-resection, which disrupts the recruitment of RPA, BRCA1 and RAD51 (Meerang et al., 2011). One of the reasons for the impaired end-resection is hyperaccumulation of K48-linked Ku80, which directs the repair pathway of choice towards NHEJ. Since p97 extracts Ku in S/G2 phase, it favours HR over NHEJ (Feng and Chen, 2012; Ismail et al., 2015; van den Boom et al., 2016). Additionally, RNF8 leads to a hyperaccumulation of K48-linked ubiquitin chains on KAP1 during S/G2 phase, which is also recognised and extracted by the p97$^{\text{-Ufd1-Npl4}}$ complex. Phosphorylated KAP1 favours NHEJ over HR and removal of KAP1 during S/G2 phase by p97 directs the repair pathway of choice towards HR, leading to the recruitment of BRCA1 and RAD51 (Kuo et al., 2016).

The segregase activity of p97 is also required in transcription-coupled NER, where it extracts trapped RNA Pol II complexes that otherwise would mask DNA lesions and

prevent access of DNA repair machinery to UV-induced damage sites. RNA Pol II is first ubiquitylated by the E3 ligase cullin-3 (CUL3) (Chen et al., 2007; Ribar et al., 2007), which is a recruitment signal for the $Cdc48^{-Ufd1-Npl4}$ complex with the cofactors UBX4 and UBX5 (UBXD7 and UBXD9 in mammals). This complex then initiates chromatin-associated degradation of the main RNA Pol II subunit, retinol binding protein 1 (RBP1) (Verma et al., 2011). The final gap-filling DNA synthesis stage of NER, present in both transcription-coupled and global-genome NER, is also controlled by p97, where it extracts PCNA-bound chromatin licensing and DNA replication factor 1 (CDT1) and promotes its degradation to prevent DNA re-replication. Global-genome NER depends on two lesion sensors: damaged DNA-binding 2 (DDB2) and XPC, which recognise DNA damage in both transcribed and non-transcribed regions. The function of p97 in this process is to control the spatiotemporal turnover of these proteins, and the absence of p97 therefore leads to impaired repair of UV-induced lesions (Puumalainen et al., 2014; Raman et al., 2011; Ramanathan and Ye, 2011).

p97 also plays a role in the above-mentioned crosstalk between SUMO and ubiquitin in DNA DSB repair. The *S. pombe* variant of p97, Cdc48, is known to bind SUMO via a SIM domain in its co-factor Ufd1, and sumoylation of RAD22 (RAD52 in mammals) recruits Cdc48 to DNA damage (Kohler et al., 2013; Nie et al., 2012). STUbL targets and p97 work together to target DDR proteins to the proteasome. RNF4-mediated ubiquitylation of SUMO chains acts as a recruitment signal for p97, and the absence of either protein causes KAP1 stabilisation on chromatin, leading to heterochromatin formation and inhibition of DSB repair (Kuo et al., 2016). This leads to the question of whether downstream targets of RNF4 such as 53BP1 and BRCA1 are also extracted by p97, and if so, which co-factors

are regulating it. Whether human p97 is able to extract sumoylated substrates from DNA damage sites is currently unknown.

1.5. p97 Cofactors Connected to Thesis

1.5.1 UBXD8/FAF2 Structure and Function

UBX domain-containing protein 8 (UBXD8) or Fas associated factor family member 2 (FAF2) is a 445-amino acid protein belonging to a subfamily of hairpin proteins able to localise to both the ER and lipid droplets (LDs) (Schrul and Kopito, 2016). UBXD8 has major roles in the regulation of protein quality control and cellular energy homeostasis. It controls the degradation of several folding- or assembly-defective proteins as part of the ERAD pathway and acts as a recruitment factor for p97 in lipid droplet synthesis (Christianson et al., 2011; Mueller et al., 2008; Olzmann et al., 2013). The p97-UBXD8 complex is further indicated in the regulation of mRNA stability, where they mediate ubiquitin-dependent disassembly of messenger ribonucleoproteins (mRNPs) (Zhou et al., 2013).

Figure 1-6. UBXD8 domain architecture. UBXD8 is a 445-amino acid protein that has an N-terminal ubiquitin-associating (UBA) domain found in several UBX proteins. The ubiquitin associated (UAS) domain is responsible for the formation of homooligomers and its interaction with its binding partners depends on its positive surface charge. The linker region between the UBA and UAS domains forms a hairpin loop, which is responsible for UBXD8 insertion into the ER membrane. The UBX domain regulates the function of p97. The figure is adapted from (Kloppsteck et al., 2012).

Similarly to the p97 core complex protein p47, UBXD8 contains the ubiquitin-associating (UBA) domain (amino acids 1-66) in its N-terminus (Figure 1-6) (Kloppsteck et al., 2012),

and its predicted cytosolic localisation positions it well for ubiquitin binding. In a pulldown experiment using HEK294 cell lysates, the ectopically expressed UBA domain, however, did not bind polyubiquitin chains (Christianson et al., 2011). Further experiments are needed to conclude whether UBXD8 has ubiquitin binding ability.

UBXD8 is inserted into the ER-membrane via a hydrophobic extension between the UBA and UAS domain, known as the hairpin domain (amino acids 90-118) (Figure 1-6). Since UBXD8 shuffles between the ER and LDs, a targeted delivery mechanism exists responsible for UBXD8 integration into the correct membrane. The specificity is achieved via the hairpin domain, which binds directly to the peroxisome-biogenesis factor peroxisome assembly protein 19 (PEX19) after *de novo* synthesis of UBXD8. The interaction between the hairpin loop and PEX19 then ensures that UBXD8 is correctly targeted to ER membranes (Schrul and Kopito, 2016). Another layer of control is added by the ER-resident rhomboid pseudoprotease UBA domain containing 2 (UBAC2) protein, which acts as an ER receptor for UBXD8 that restricts UBXD8 translocation to LDs. The relative expression of both proteins in the ER correlates with the movement of UBXD8 between the ER and LDs. Once attached to LDs, UBXD8 in complex with p97 inhibits the adipose triglyceride lipase (ATGL), an enzyme mediating triacylglycerol hydrolysis (Olzmann et al., 2013).

The ubiquitin associated (UAS) domain (amino acids 122-277) is responsible for UBXD8 oligomerisation upon binding to long-chain unsaturated fatty acids (FAs), and this depends on the positive surface charge of the UAS domain (Figure 1-6). The interaction between UBXD8 and long-chain unsaturated FAs leads to the inhibition of FA synthesis via downregulating the transcription factor SREBP-1, an activator of cholesterol and FA

synthesis (Kim et al., 2013). Finally, the UBX domain (amino acids 360-445) is located in its C-terminus and binds the N-terminus of p97. As previously mentioned, UBX proteins regulate the function of p97 by forming a large interaction complex with up to six adaptors (Kloppsteck et al., 2012; Schuberth and Buchberger, 2008). The UBX domain is also necessary for p97 recruitment (Alexandru et al., 2008; Suzuki et al., 2012) and degradation of ERAD substrates (Phan et al., 2010).

Like several other UBX domain-containing proteins, UBXD8 is biochemically and structurally poorly characterised, so its potential cellular functions are anticipated to be much more complex. One of the indications for this comes from reports demonstrating UBXD8 involvement in human cancers. UBXD8 promotes the degradation of the tumour suppressor protein neurofibromin (Phan et al., 2010), which is indicated in the development of neurofibromatosis type 1 (NF1), a genetic disorder leading to the development of both benign and malignant tumours (Zhu and Parada, 2001). Functional neurofibromin inhibits the RAS oncogene pathway, and silencing UBXD8 leads to the same effect - it downregulates the RAS-mediated extracellular signal-regulated kinase (ERK) and protein kinase B (PKB) oncogenic pathways (Phan et al., 2010). Extensive biochemical and pre-clinical studies are needed to understand whether the UBXD family of proteins could be targets for discovery of novel targeted cancer therapies.

1.6. Therapeutic Applications of DDR Proteins

DNA damaging chemotherapies and radiotherapies are widely used cancer treatments, since cancer cells have higher proliferation rates and more endogenous DNA damage compared to normal cells, making them consequently more sensitive to genotoxic agents. It also makes them more reliant on the DNA damage repair pathways that they still retain

(Helleday et al., 2008; Jackson and Bartek, 2009), and this is why many of the DDR proteins represent attractive drug targets. One of the well-known examples is based on the concept of synthetic lethality, whereby simultaneous defects in two genes leads to cell death, whereas a single defect is compatible with life. This concept is best illustrated on BRCA1- and BRCA2-mutated cancers, where PARP inhibitors such as olaparib induce synthetic lethality. This is because BRCA-mutated cancers have a defective HR repair pathway, making them particularly reliant on BER. Inhibiting PARP therefore leads to greater cell death in cancer cells, but has minimal effect on normal tissues as they still have their HR pathway intact (Bryant et al., 2005; Farmer et al., 2005). Another example is the synthetic lethality with ATM and DNA-PK, where ATM inhibitors could increase the effectiveness of chemotherapy in p53-mutated cancers (Jiang et al., 2009).

Since aneuploidy is commonly observed in cancer cells (Storchova and Pellman, 2004), they also transcribe more proteins, many of which are mutated and misassembled, leading to proteotoxic stress. This inherent defect is exploited in the clinic with the proteasome inhibitor bortezomib, which is used in the treatment of multiple myeloma and mantle cell lymphoma (Deshaies, 2014). Similarly, p97 inhibitors have been developed that work on the same principle as proteasome inhibitors, increasing the proteotoxic stress in cancer cells and pushing them towards apoptosis (Anderson et al., 2015). Unfortunately, p97 is absolutely vital for several normal cellular processes and therefore its long-term use could lead to severe side effects. The study of p97 co-factors would allow a more specific control of its actions, such as inhibiting co-factors that control the recruitment of p97 to DNA damage sites after targeted ionising radiation.

A variety of enzymes within the DDR pathway have been studied for potential pharmaceutical applications. Deubiquitinating enzymes, DUBs, are a class of enzymes that regulate ubiquitylation in cells and thereby coordinate DDR. Several inhibitors exist for DUBs. For example, ubiquitin-specific protease 7 (USP7) deubiquitinates p53 and preclinical studies have demonstrated that P5091, an inhibitor of USP7 and USP47, induces apoptosis in multiple myeloma cells resistant to bortezomib (Chauhan et al., 2012; Weinstock et al., 2012). The research into the therapeutic applications of enzymes coordinating PTMs on DNA damage sites will be greatly facilitated when more pharmacological inhibitors become available. For example, a large number of cancers show an upregulation of the E2 ligase UBC9, which regulates sumoylation, and many approaches exist to target UBC9 (Mo and Moschos, 2005; Moschos and Mo, 2006).

The clinical use of DDR inhibitors is challenging as some patients develop resistance over time, and the addition of these inhibitors to conventional chemotherapies leads to additional side effects. It is also important to limit the iatrogenic effects of such therapies, as DDR inhibitors might increase the risk of developing secondary cancers. This could be avoided by controlling the time frame of drug administration (Lord and Ashworth, 2012). It is certainly necessary to study these drug effects in combination with targeted radiation, as radiation is more limited to a specific area near the tumour, and therefore the chances of developing additional side effects is smaller than in combination with chemotherapy.

1.7. Aims of the Thesis

Our group is interested in understanding the basic biochemical events in the p97 system occurring at the site of DNA damage after ionising radiation. It is looking to identify novel DNA damage response agents that could be clinically targeted as radiosensitising agents. Previous proteomics work identified that the protein UBXD8, previously known as the p97 co-factor functioning in ERAD and LD synthesis, increases its interaction with p97 on chromatin over 8 hours after ionising radiation. The group further identified that UBXD8 has a putative SIM domain. This provided the basis for this work.

The aims of this thesis are to understand whether UBXD8 in complex with p97 could facilitate the removal of sumoylated substrates from DNA break sites. UV-A laser micro-irradiation approach will be adopted to confirm UBXD8 recruitment to DNA damage. Its involvement in the regulation of sumoylation will be studied using both UV-A laser micro-irradiation and ionising radiation. These results will be compared with the effect of p97 on sumoylation, studying whether they affect sumoylation in a similar manner. Since UBXD8 is a known recruitment factor for p97 in the cytosol, it will also be studied whether it acts as a p97 recruitment factor on DNA damage and consequently what effect does this have on ubiquitylation.

2. MATERIALS AND METHODS

2.1 Solutions and Reagents

2.1.1 Antibodies

The list of antibodies used for western blotting and immunofluorescence are shown in tables 1 and 2 below:

Protein	Working Dilution	Source
UBXD8/FAF2 (Rabbit)	1:500	Non-commercial
SUMO-2 (Rabbit)	1:1,000	Cell Signaling
p97/VCP (Rabbit)	1:1,000	Proteintech
GFP (Rabbit)	1:10,000	Abcam
H2B (Mouse)	1:2,000	Cell Signaling
Vinculin (Mouse)	1:1,000	Abcam
β-actin (Mouse)	1:5,000	Ambion
Mouse-HRP	1:50,000	Sigma
Rabbit-HRP	1:50,000	Sigma

Table 1. Antibodies used for western blotting.

Protein	Working Dilution	Source
SUMO-1 (Rabbit)	1:400	Abcam
SUMO-2 (Rabbit)	1:200	Cell Signaling
UBXD8/FAF2 (Rabbit)	1:1,000	Non-Commercial
p97/VCP (Rabbit)	1:100	Proteintech
GFP (Rabbit)	1:1,000	Abcam
K48-linked Ub chains (Rabbit)	1:400	Genetech
γH2AX (Mouse)	1:500	Millipore
Alexa Fluor 488 donkey anti-rabbit	1:500	Invitrogen
Alexa Fluor 594 donkey anti-mouse	1:500	Invitrogen

Table 2. Antibodies used for immunofluorescence.

2.1.2 Buffers

Running Buffer: Tris/Glycine/SDS

10x running buffer was prepared by dissolving 30.0 g of Tris base and 144.0 of glycine in 1 L of ddH_2O. The buffer was then diluted to the working concentration (25 mM Tris; 190 mM glycine) with ddH_2O and supplemented with 0.1 % SDS.

Transfer Buffer

1x Tris/Glycine buffer was supplemented with 20 % methanol and 0.025 % SDS.

Tris-buffered saline with Tween 20 (TBS-T) buffer

10x TBS buffer was prepared by dissolving 88.0 g of NaCl and 24.0 g of Tris base in 800 mL ddH_2O. The pH was adjusted to 7.6 and the final volume was adjusted to 1 L with ddH_2O. TBS was then diluted to the working concentration (20 mM Tris, pH 7.5; 150 mM NaCl) with ddH_2O and supplemented with 0.1 % Tween 20 (Sigma).

Lysis Buffer: radioimmunoprecipitation assay buffer (RIPA buffer)

1x RIPA buffer was prepared using 50 mM Tris-HCl, 150 mM NaCl and 1.5 mM EDTA supplemented with the following inhibitors: 10 µg/mL aproptinin, 10 µg/mL chymostatin, 10 µg/mL leupeptin, 2.5 mM sodium orthovanadate, 4 mM sodium pyrophosphate and 20 mM sodium fluoride.

5x Laemmli Buffer (LB)

5x LB was prepared using 0.25 % bromophenol blue (SLS), 50 % glycerol (Fisher Scientific), 10 % SDS and 0.25 M Tris-HCl (pH 6.8). The buffer was diluted to the working concentration (50 mM Tris-HCl, pH 6.8; 2 % SDS; 10% glycerol; 0.05 % bromophenol blue) with ddH_2O and supplemented with 15 % β-mercaptoethanol.

1x Phosphate Buffered Saline Buffer (PBS buffer)

10x PBS was prepared using 80.0 g NaCl, 2.0 g KCl, 14.4 g Na_2HPO_4 and 2.4 g KH_2PO_4 dissolved in 800 mL ddH_2O. The pH was adjusted to 7.4 and the solution was increased to 1 L with ddH_2O. PBS was diluted to working concentration (137 mM NaCl; 2.7 mM KCl, pH 7.4; 12 mM phosphate) with ddH_2O.

2.2 Cell Lines and Cell Culture

2.2.1 Cell Lines

U-2 OS (U2OS) osteosarcoma, human embryonic kidney 293T (HEK293T) and HeLa cell lines were obtained from American Type Culture Collection (ATCC). Flp-IN/T-Rex HeLa construct was obtained from Stephen Taylor lab, Manchester (Tighe et al., 2008)

2.2.2 Culture Conditions

All cell lines were kept at 37 °C in a 5 % CO_2 humidified incubator and cultured in Dulbecco's Modified Eagle's Medium (DMEM; Gibco) supplemented with 10 % Foetal Bovine Serum (FBS; Sigma) and 1x Penicillin/Streptomycin (Gibco). Cells were passaged before they were confluent (typically when 80% confluent). Cells were washed using pre-warmed 1x PBS, trypsinised with pre-warmed 0.05 % trypsin (Thermo Fisher) in PBS and incubated until most cells had detached from the culture plate. Trypsinised cells were then resuspended in the equivalent of 2 volumes of pre-warmed complete DMEM and transferred to new a culture dish with fresh growth medium.

2.3 RNA Interference and Plasmid Transfection

2.3.1 siRNA Transfections

Cells were seeded to be approximately 60 % confluent on the day of transfection, typically 2.5–3.5x10^5 cells in a 6-well plate. Lipofectamine® RNAiMAX reagent (Invitrogen) was dissolved in 250 µL Opti-MEM (Gibco). The desired amount of the appropriate siRNA was dissolved in 250 µL Opti-MEM medium, the diluted siRNA was then added to the diluted Lipofectamine® RNAiMAX reagent in 1:1 ratio and incubated

for 15 minutes at room temperature (RT). The DMEM inside the 6-well plate wells was reduced to 1 mL before adding 500 µL of the siRNA-lipid complex to cells. Cells were left overnight at 37 °C and supplemented with 0.5 mL fresh DMEM on the following day. Experiments were carried out 48 or 72 hours after transfection. Depletion efficiency was assessed by western blotting. The list of siRNA sequences and working concentrations is provided in the table 3 below.

Name	Sequence (5' to 3')	Working Concentration	Reference
siLuciferase	CGUACGCGGAAUACUUCGA	20 nM	Microsynth AG
siUBXD8 #259	GACUUCUUAUUCUCCUUGATT	5 nM	Ambion
siFAF2_2	GCAUCGAAUCUAUGGAUCATT	5 nM	Ambion
sip97/VCP	AAGUAGGGUAUGAUGACAUUG	20 nM	QIAGEN

Table 3. siRNA sequences used.

2.3.2 Plasmid Transfections

3.75 µg of DNA sample was diluted in 1x PBS to make up 100 µL of solution. 4 µL of 25x PEI was diluted in 96 µL of 1x PBS, and the two solutions were mixed immediately, vortexed 3 times at low-speed and left at RT for 15 minutes. Meanwhile, the complete DMEM in wells was exchanged to 1.8 mL DMEM without FBS or Pen/Strep. 200 µL of PEI mixture was then added to wells and incubated at 37 °C for 4 hours. The growth medium was replaced by complete DMEM. Experiments were performed 24 hours after

transfection. Alternatively, cells were transfected with FuGENE® HD Transfection Reagent (Promega) according to the manufacturer's instructions.

2.3.3 Generation of Cell Lines

Stable transformants were created using HeLa cells containing a FRTTO site conferring resistance to zeocin and a Tet Repressor Protein (TetR) inducing resistance to blasticidin. Around 200,000 HeLa FRTTO cells were plated into a 6-well plate well to be approximately 90 % confluent on the day of transfection. The medium inside the wells was supplemented with 10 % FBS, 1x Penicillin/Streptomycin and contained no other antibiotics. The following day the cells were transfected using Lipofectamine® 2000. Transfection reaction contained the following:

A. 200 µL Opti-MEM + 6 µL Lipofectamine® 2000
B. 200 µL Opti-MEM + 4 µg DNA (3.6 µg of the pOG44/FRT recombinase plasmid and 0.4 µg of the pCDNA5-FRTTO-based construct)

Solutions A and B were mixed together and incubated at RT for 25 minutes. The mix was then added to cells in a drop-wise manner and incubated at 37 °C for 4 hours, after which fresh DMEM was added into wells. On the following day, cells were seeded into 15 cm dishes containing blasticidin (15 µg/mL) and hygromycin B (200 µg/mL). The medium was exchanged every few days until colonies started to overgrow. Colonies were then picked by scratching around and through the colony with a 200 µL pipette tip, and transferred to 12-well plates. The expression was tested by western blotting after 16 hours of doxycycline induction (1 µg/mL).

2.4 Induction of DNA damage and Chemical Treatments

2.4.1 Laser-induced DNA Damage

Cells were seeded into 6-well plates and cultured for 72 hours on 10 mm No. 1 cover glasses (VWR) before inducing UV-A laser micro-irradiation. Cells were sensitised to DSBs with Hoechst (10 μg/mL) for 20 minutes in complete DMEM. Coverslips were then transferred into a round glass-bottom with cell culture media and irradiated using 355 nm pulsed laser. Experiments were conducted using Nikon TE2000 with a 10x objective. Laser pulses were controlled manually, each lasting 5 nanoseconds (ns). The stage was moved by 25 μm in between each pulse. Laser energy at the source was adjusted using OD1 and OD2 filters, resulting in the final energy of approximately 30 mV. Coverslips were then transferred into 12-well plates with DMEM and cells were recovered at 37 °C for a specific amount of time. The coverslips were then washed once with PBS and fixed for immunofluorescence.

2.4.2 Ionising Radiation (IR)

Cells were irradiated with indicated gray (Gy) at a dose rate of 1.5 Gy/min using a Gamma-Service Medical GmbH GSR D1 irradiator. The cells were recovered at 37 °C for indicated times before fixing them for immunofluorescence.

2.4.4 Chemical Treatments

The allosteric p97 inhibitor NMS-873 (Sigma) was added to cell culture medium at a final concentration of 10 μg/mL. Cells were incubated for 2 hours at 37 °C before DNA damage induction.

2.5 Immunofluorescence (IF)

Cells were pre-extracted on ice for 5 minutes with 25 mM HEPES (pH 7.4), 50 mM NaCl, 1 mM EDTA, 3 mM MgCl2, 300 mM sucrose and 0.5 % Triton X-100. Cells were then fixed in 4 % formaldehyde for 15 minutes at RT, washed twice with 1x PBS and blocked overnight at 4 °C in 5 % BSA blocking buffer. Antibodies were dissolved in 2.5 % BSA in PBS, and coverslips were transferred onto 20 μL droplets of antibody solution on a parafilm in a wet chamber and incubated for 1 hour at RT. All antibody incubations besides the first primary antibody were conducted in dark. In between each antibody, cells were washed at least twice with 1x PBS for 5 minutes. Following incubation in the final antibody solution, samples were incubated in DAPI dye in PBS (1 μg/mL) for 20 minutes at RT. Coverslips were then dipped into ddH_2O, dried and mounted onto microscopy slides (Thermo Scientific) using FluoroMount-G hard mounting medium (Interchim).

2.5.1 Image Acquisition and Analysis

Images were acquired with a 60x objective Nikon Ni-E epifluorescent microscope. Images were analysed using ImageJ 1.46r, where the mean intensity at the site of DNA damage was determined by outlining the γH2AX signal and the signal intensity of the protein of interest was measured within the same region. Background signal was subtracted from the mean intensity at the site of DNA damage. Where necessary, well-defined foci in the nucleus were avoided to minimise interference with the normal background intensity. At least 60 cells were analysed per condition. All measurements were normalised to a specific time point in control cells to compare between independent experiments.

For ionising radiation-induced foci (IRIF) analysis, IRIF were quantified using ImageJ 1.46r, which automatically identifies cell nuclei and performs analysis on the existing area selection. Individual cell nuclei were selected using a wand tool with tolerance settings on 10.0. The images were processed by choosing "find maxima as single points", setting noise tolerance to 20.0. Foci number was determined by dividing integrated density (the product of mean gray value and area) by maximum gray value. At least 60 cells were selected per condition per experiment.

2.6 Protein Analysis

2.6.1 Cell Lysis

Cells were lysed using RIPA buffer supplemented with freshly added protease and phosphatase inhibitors: aproptinin (10 μg/mL), leupeptin (10 μg/mL), chymostatin (10 μg/mL), sodium pyrophosphate (4 mM), sodium orthovanadate (2.5 mM), sodium fluoride (20 mM). Lysed cells were centrifuged at 4 °C and 21,000 x g for 10 minutes. The supernatant was collected and protein concentrations were measured with the RC DC (reducing agent and detergent compatible) protein assay kit (BioRad) according to the manufacturer's instructions.

2.6.2 SDS-PAGE

SDS-PAGE gels were hand cast using the mini-PROTEAN Tetra Handcast System (Biorad). The percentage of gels prepared varied according to the size of proteins. The protocols used for separating and stacking gels are shown in table 4. 5 mL of separating solution and 1.5 mL of stacking solution was used per gel. 4x separating buffer was

prepared using 1.5 M Tris base and 0.4 % SDS (pH 8.8). The 4x stacking buffer was prepared using 0.5 M Tris base and 0.4 % SDS (pH 6.8).

Reagent	Stacking Gel (4 mL)	Separating Gel (8%; 12 mL)	Separating Gel (10%; 12 mL)
ddH2O	2.5 mL	5.8 mL	5.0 mL
4x Buffer	1.0 mL	3.0 mL	3.0 mL
30% Acrylamide	0.5 mL	3.2 mL	4.0 mL
10% APS	20 µL	60 µL	60 µL
TEMED	10 µL	8.0 µL	8.0 µL

Table 4. Stacking and separating gel recipes.

Samples were boiled for 5 minutes at 95 °C, centrifuged and vortexed before loading 30-50 µg of protein into wells. Protein samples were dissolved in 1x laemmli buffer supplemented with 15 % β-mercaptoethanol and adjusted to 50 µL with ddH_2O. Prestained dual colour protein standard (BioRad) was used to determine protein size. Samples were run in 1x running buffer at 90 V for 30 minutes and at 150 V for the remaining 1 hour.

2.6.3 Western Blotting

The SDS-PAGE gel sandwich was assembled according to the manufacturer's instructions (Biorad Mini Trans-Blot® electrophoretic transfer cell protocol). The buffer tank containing the gel sandwich was filled with ice-cold transfer buffer. The blot was run at 100 V for 75 minutes.

Nitrocellulose membranes were washed once with 1x TBS-T and blocked using 5 % skimmed milk solution in 1x TBS-T for 1 hour at RT. Membranes were incubated overnight at 4 °C in a suitable primary antibody solution in 5 % BSA in TBS-T. Membranes were then washed four times with 1x TBS-T and incubated for 1 hour at RT in the relevant peroxidase-conjugated secondary antibody solution containing 2.5 % skimmed milk in TBS-T. Membranes were washed again as above, incubated in clarity enhanced chemiluminescence (ECL) substrate (Biorad) for 5 minutes and the signal was detected using the ChemiDoc MP system (Biorad).

2.7 Cloning

Primer sequences and plasmids used are provided in tables 5 and 6 below:

Primer	Sequence (5' to 3')	T_m
nEGFP_FW	AAAAGGATCCATGGCGGCGCCTGAGGAGC	62
nEGFP_RV	AAAAGCGGCCGCTCATTCGTCAGTTAGGTCC	61
cEGFP_FW	AAAAGGATCCATGGCGGCGCCTGAGGAGC	62
cEGFP_RV	AAAAGCGGCCGCCCTTCGTCAGTTAGGTCCTGAAC	64

Table 5. Primer sequences and their melting temperatures.

Plasmid Name	Source
pcDNA5/FRT/TO cEGFP	Invitrogen
pcDNA5/FRT/TO nEGFP	Invitrogen
UBXD8-HA_3	K. Ramadan's lab

Table 6. Plasmids and their sources.

PCR reaction mix was set up as shown in table 7 and pcDNA5 was amplified using the primers shown in table 5.

The PCR thermocycler program was set to the following:

Stage	Temperature	Time
Early denaturation	95 °C	4 minutes
30 cycles	95 °C	30 seconds
	Primer Tm - 4 °C	30 seconds
	68 °C	1 minute/kb
Extension	68 °C	10 minutes
Maintenance	4 °C	∞

Steps 2-4 were repeated for 35 cycles.

Reagent	Final Concentration	x1 (µL)
ddH_2O	Up to 50 µL	28.5
5x PCR buffer	1x	10.0
2 mM dNTP mix (10x)	200 µM	5.0
10 µM FW primer (20x)	500 nM	2.5
10 µM RV primer (20x)	500 nM	2.5
2 u/µL DNA polymerase	1 u	0.5
Template DNA	1 ng -1 µg	1.0
Total volume		**50**

Table 7. PCR reaction mix reagents.

PCR products were purified using QIAGEN PCR purification kit according to the manufacturer's instructions. In summary, 5 volumes of buffer PB was added to 1 volume of PCR reaction mix. The sample was transferred into a QIAquick column attached to a 1.5 mL collection tube and centrifuged for one minute at 17,900 x g. The flow-through was discarded, 750 µL of buffer PE (10 mM Tris-HCl, pH 7.5; 80 % ethanol) was added to the column and centrifuged as above. Once the flow-through was discarded, the centrifugation step was repeated to remove residual wash buffer. QIAquick column was placed into a new 1.5 mL microcentrifuge tube and 25 µL of buffer EB (10 mM Tris-Cl, pH 8.5) was added into the column. The samples were then centrifuged and the amount of DNA was quantified using NanoDrop 1000 (Thermo Scientific).

2.7.1 Restriction Enzyme Digestion

Component	Quantity
10x NEBuffer 3.1	4 µL
BamH1 [NEB; 20 kU/mL]	0.5 µL
Not1 [NEB; 10 kU/mL]	1.0 µL
Plasmid	2 µg
Insert	1 µg
ddH_2O	Up to 40 µL
Total	**40 µL**

Table 8. Restriction enzyme digestion mix

An overnight digestion was performed at 37 °C. Restriction enzyme digestion products were run on an agarose gel. Insert bands were cut and purified using the QIAquick gel extraction kit (QIAGEN) according to the manufacturer's instructions. A ligation reaction was set up as shown in table 9 and carried out for 1 hour at 37 °C.

Component	Quantity
Plasmid	100 ng
Digest Insert	200 ng
T4 10x Buffer	2 µL
T4 Ligase (NEB; 400 kU/ml)	1 µL
ddH_2O	Up to 20 µL
Total	**20 µL**

Table 9. Components for ligation reaction.

2.7.2 Transformation of Bacteria

DH5α competent *Escherichia coli* from -80 °C were thawed on ice. 10 µL of plasmid was added to 1.5 mL of competent cells, and the mixture was incubated on ice for 20 minutes. Heat shock was applied for 1.5 minutes in a 42 °C water bath, after which the cells were recovered on ice for 5 minutes. Bacteria were transferred into Luria Bertani (LB) medium without antibiotics and incubated in a bacterial shaker (New Brunswick Scientific) at 37 °C, 250 rpm for 1 hour. Bacteria were centrifuged at 3000 x g for 3 minutes, the pellet was resuspended and the resuspension was spread onto agar plates (Sigma) containing ampicillin. Plates were incubated in a bacterial incubator (Binder) at 37 °C overnight and isolated bacterial colonies were picked up with a sterile pipette tip the following day for further amplification in 5 mL of LB containing 5 µL of ampicillin. Bacteria were incubated in a bacterial shaker at 37 °C, 250 rpm overnight. The bacteria were centrifuged at 4000 x g, 24 °C for 10 minutes.

2.7.3 Plasmid Purification

Plasmid purification was performed according to the QIAGEN plasmid mini/midi/maxiprep purification protocol. For miniprep, the bacterial pellet obtained from centrifugation was resuspended in 0.3 mL of resuspension buffer P1 (50 mM Tris-HCl, pH 8.0; 10 mM EDTA; 100 μg/mL RNase A) until the solution appeared clear. The solution was transferred into a 1.5 mL microcentrifuge tube and 0.3 mL of lysis buffer P2 (200 mM NaOH; 1% SDS) was added into the solution. The tube was inverted vigorously until the solution appeared homogenous and viscous. 0.3 mL of pre-chilled neutralisation buffer P3 (3.0 M CH_3CO_2K; pH 5.5) was added and the tube was inverted vigorously again until a fluffy white material was formed and the solution appeared less viscous. The tubes were then incubated on ice for 5 minutes and centrifuged at 17,900 x g for 10 minutes at 4 °C. The supernatant was loaded to a pre-equilibrated QIAprep spin column (equilibration buffer QBT: 750 mM NaCl; 50 mM MOPS, pH 7.0; 15 % isopropanol (v/v); 0.15 % Triton X-100 (v/v)) and was allowed to enter the resin by gravity flow. The spin column was washed with 750 μL of the wash buffer QC (1.0 M NaCl; 50 mM MOPS, pH 7.0; 15 % isopropanol (v/v)), and centrifuged for 3 minutes at 17,900 x g. Additional centrifugation step was performed to allow the column to dry. DNA was eluted into 1.5 mL microcentrifuge tubes by adding 50 μL of the elution buffer QF (1.25 M NaCl; 50 mM Tris-Cl, pH 8.5; 15 % isopropanol (v/v)) and centrifuged for 1 minute at 17,900 x g. The quantity and purity of DNA was measured with NanoDrop 1000 (Thermo Scientific). DNA was precipitated with 0.7 volumes of isopropanol. The solution was mixed and centrifuged at 17,900 x g for 30 minutes. The supernatant was removed and the DNA pellet was washed with 1 mL of 70 % ethanol and centrifuged again for 10 minutes at 17,900 x g. The supernatant was removed, the pellet was air-dried in an incubator at 37 °C for 30 minutes and re-dissolved in TE buffer (10 mM Tris-Cl, pH 8.0; 1 mM EDTA).

Clones were verified by sequencing (Source Bioscience).

2.8 Statistical Analysis

All statistical analysis was performed using GraphPad. Unpaired *t*-test was used with p-values indicated in the figures. For ionising radiation and UV-A laser micro-irradiation, values were plotted as mean ± SEM.

3. RESULTS 1: UBXD8 IS A POTENTIAL NOVEL COMPONENT IN THE DNA DAMAGE RESPONSE

Although the role of p97 in DNA damage repair is well known, many of its UBX domain-containing co-factors are functionally poorly characterised (Meerang et al., 2011). The biochemical mechanisms of p97 in DNA repair are therefore still underexplored. The $p97^{-Ufd1\text{-}Npl4}$ core complex is recognised in DNA repair, where it mediates the removal of K48-linked polyubiquitylated substrates such as Ku80 (van den Boom et al., 2016), L3MBTL1 (Acs et al., 2011) and KAP1 (Kuo et al., 2016), thereby paving the way for downstream DDR proteins. The $p97^{-Ufd1\text{-}Npl4}$ complex inactivation, however, impairs the recruitment of many essential HR proteins such as RPA, BRCA1 and RAD51 (Meerang et al., 2011), showing that the role of p97 in DNA damage is more complex than previously anticipated. It can be hypothesised that additional p97 co-factors form a complex with p97 on DNA damage sites and coordinate repair in specific ways.

To better understand the function of p97 in DNA damage repair, the laboratory performed stable isotope labelling with amino acids in cell culture (SILAC)-based mass spectrometry analysis of p97-interactome kinetics after IR. Cells were fractionated and separated into cytosolic, nucleosolic and chromatin compartments to see which proteins are increasing their interaction with p97 specifically in the nucleus and on chromatin after IR. HEK293T cells were exposed to 10 Gy IR and recovered for 30 minutes (early DDR) or 8 hours (late DDR) after radiation exposure. The cells were then collected and fractionated before pull-down experiments and mass spectrometry analysis.

As expected, the Ufd1-Npl4 complex increases its interaction with p97 in the nucleus after 30 minutes and 8 hours of IR exposure (data not shown). Interestingly, UBXD8 came out as one of the top hits on chromatin, where it increased its interaction with p97 over 8 hours after IR (Figure 3-1). UBXD8 has previously been involved in lipid droplet synthesis and known as the p97 recruitment factor in the cytosol. The mass spectrometry analysis suggests it might have an additional role in DNA break repair. In the cytosol, the interaction between p97 and UBXD8 was decreased 30 minutes after radiation exposure, and then increased slightly after 8 hours of recovery. The chromatin fraction, however, showed a consistent and a strong increase in interaction. These results were confirmed by immunoprecipitation. Further experiments demonstrated that UBXD8 depletion causes a delay in 53BP1 foci resolution (Figure 3-2), and that UBXD8 possesses a putative SIM domain. These results led to the hypothesis that UBXD8 in complex with p97 could facilitate the removal of sumoylated substrates from DNA break sites.

A

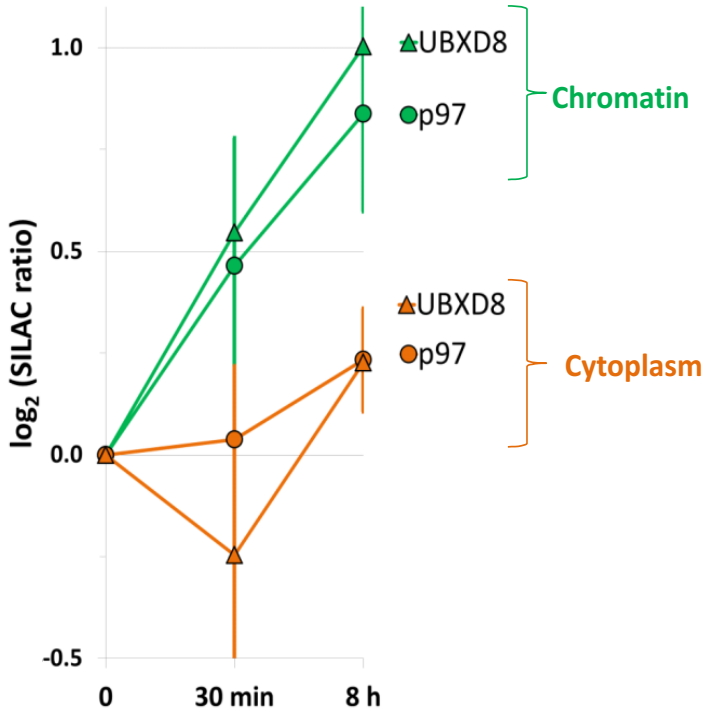

B

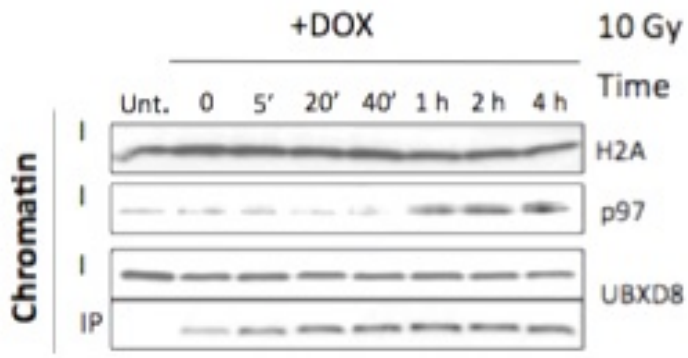

Figure 3-1. UBXD8 increases its interaction with p97 on chromatin after ionising radiation. (A) SILAC ratio of UBXD8 interacting with p97 on chromatin and in cytosol after 10 Gy IR. HEK293T cells were irradiated and recovered for 30 minutes or 8 hours. Interaction between p97 and UBXD8 is shown in untreated controls (time point 0), or after 30 minutes and 8 hours of recovery from IR. N= 3 independent experiments. The data are represented as Mean ± SD (B) Confirmation of the SILAC-based mass spectrometry data by immunoprecipitation. Myc/Strep-tagged p97 HEK293T cells were doxycycline (DOX)-induced, treated with 10 Gy IR and recovered over 4 hours. UBXD8 increases its interaction with p97 on chromatin after irradiation. H2A serves as the loading control. The data is representative of n=3 independent experiments. **Abbreviations:** I, input; IP, immunoprecipitation. Data in (A) and (B) were created by Dr Ignacio Torrecilla.

A

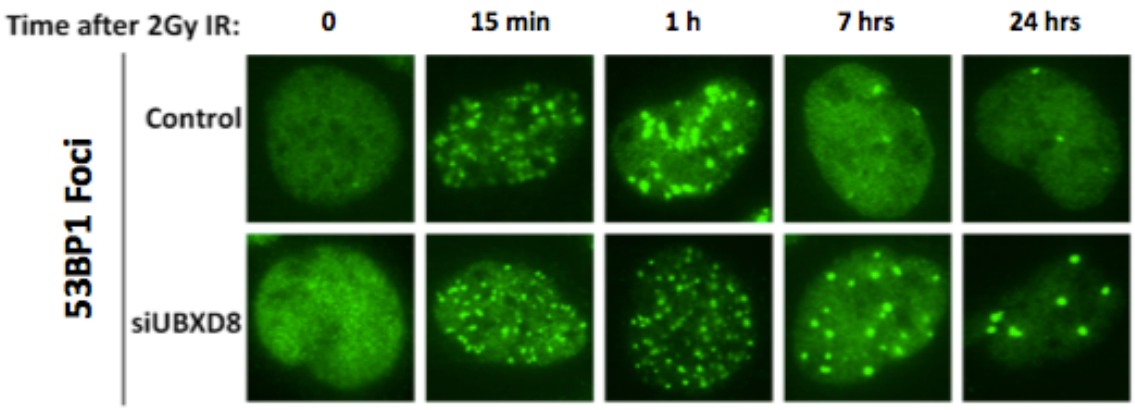

B

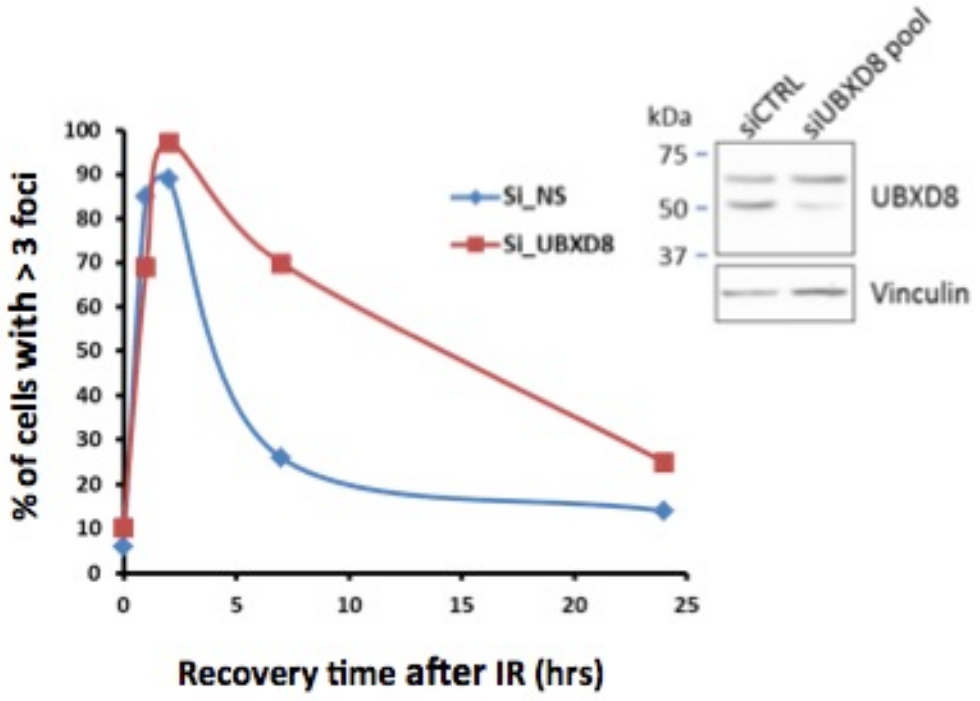

Figure 3-2. UBXD8 is involved in 53BP1 foci resolution after ionising radiation. U2OS cells were irradiated with 2 Gy IR, recovered over 24 hours, fixed and analysed by immunofluorescence. (A) Representative immunofluorescence images of the number of 53BP1 foci in UBXD8 depleted cells compared to controls. UBXD8 depletion causes persistence of 53BP1 foci after 2 Gy IR, lasting over 24 hours. (B) Quantification of the percentage of cells with more than three 53BP1 foci in siLuciferase and UBXD8 depleted cells over 24 hours. Western blot confirms UBXD8 depletion. N=1 independent experiment. Unpublished data by Dr Abhay Singh.

3.1. UBXD8 is Recruited to Sites of DNA Damage

Many DDR factors physically accumulate and can be visualised on DNA break sites, so it was tested whether UBXD8 is present on DNA damage. For this, two independent approaches and cell lines were used. Firstly, U2OS cells were transiently transfected for 72 hours with an N-terminal GFP-tagged mammalian UBXD8. DNA damage was induced in live U2OS cells by creating a localised damage region with UV-A laser micro-irradiation (355 nm). Cells were pre-sensitised to DSBs with Hoechst and recovered after damage for 6 hours and 8 hours. UBXD8 recruitment to DNA damage was monitored in fixed cells using a GFP antibody. As indicated in figure 3-3, UBXD8 co-localises with the γH2AX signal at sites of UV-A laser-induced DNA damage 6 and 8 hours after damage induction, demonstrating that UBXD8 is physically present on DNA damage. To confirm previous findings, Flp-IN/T-Rex HeLa cells were created that stably express UBXD8-nGFP upon doxycycline induction. Similarly, GFP antibody was used to monitor UBXD8 on DNA damage sites, and previous results were confirmed as shown in figure 3-4. The GFP antibody specificity was tested using Flp-IN/T-Rex HeLa doxycycline inducible cells stably expressing an empty GFP vector. As indicated in figure 3-5, there was no GFP recruitment that co-localised with the γH2AX signal in negative controls, demonstrating that the antibody effect is specific. GFP and UBXD8-GFP expressions were verified by western blotting. Altogether, these results demonstrate that UBXD8 is physically associated with DNA damage and therefore most likely plays a role in DNA break repair.

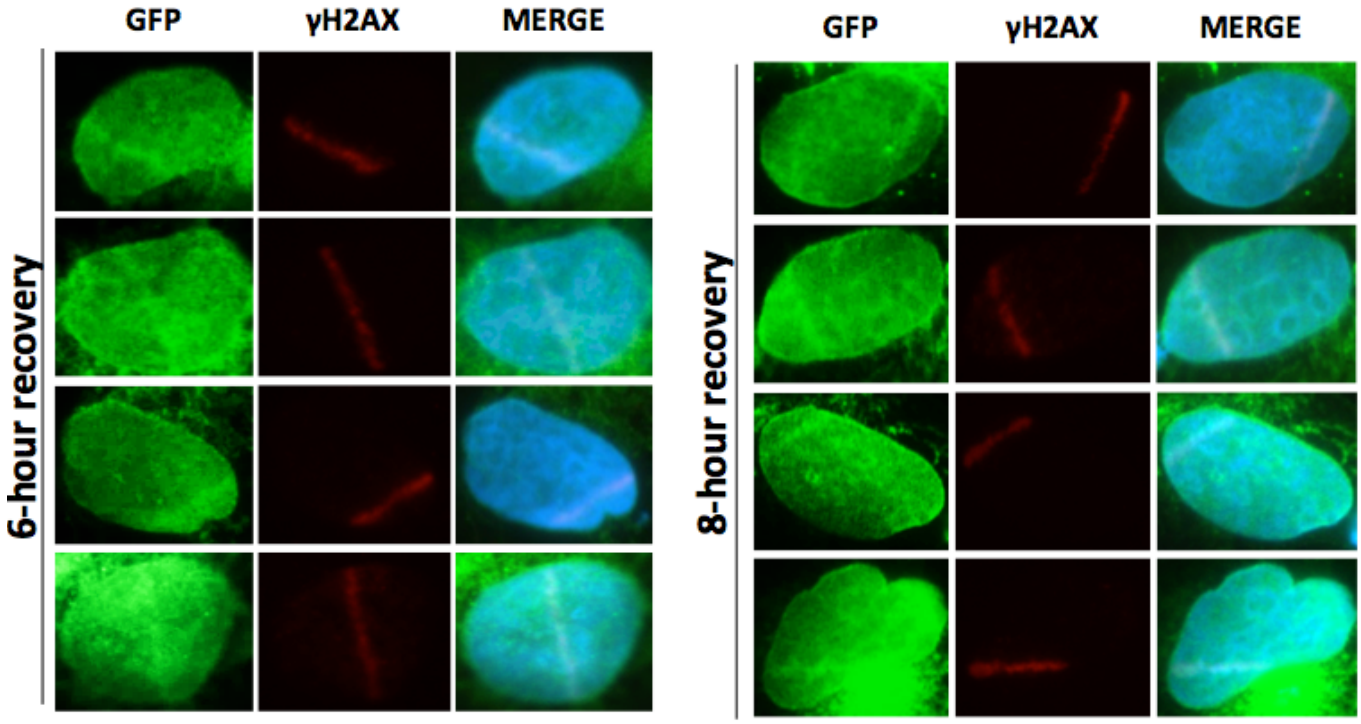

Figure 3-3. UBXD8 physically accumulates at DNA damage sites. U2OS cells were transfected for 72 hours with UBXD8-nEGFP plasmid. Cells were sensitised to DSBs with Hoechst and the recruitment of UBXD8 was visualised 6 and 8 hours after UV-A laser micro-irradiation. Cells were fixed and stained for GFP and γH2AX. GFP co-localises with the DNA damage marker γH2AX, demonstrating the recruitment of UBXD8 to UV-A induced DNA damage sites. N=2 independent experiments.

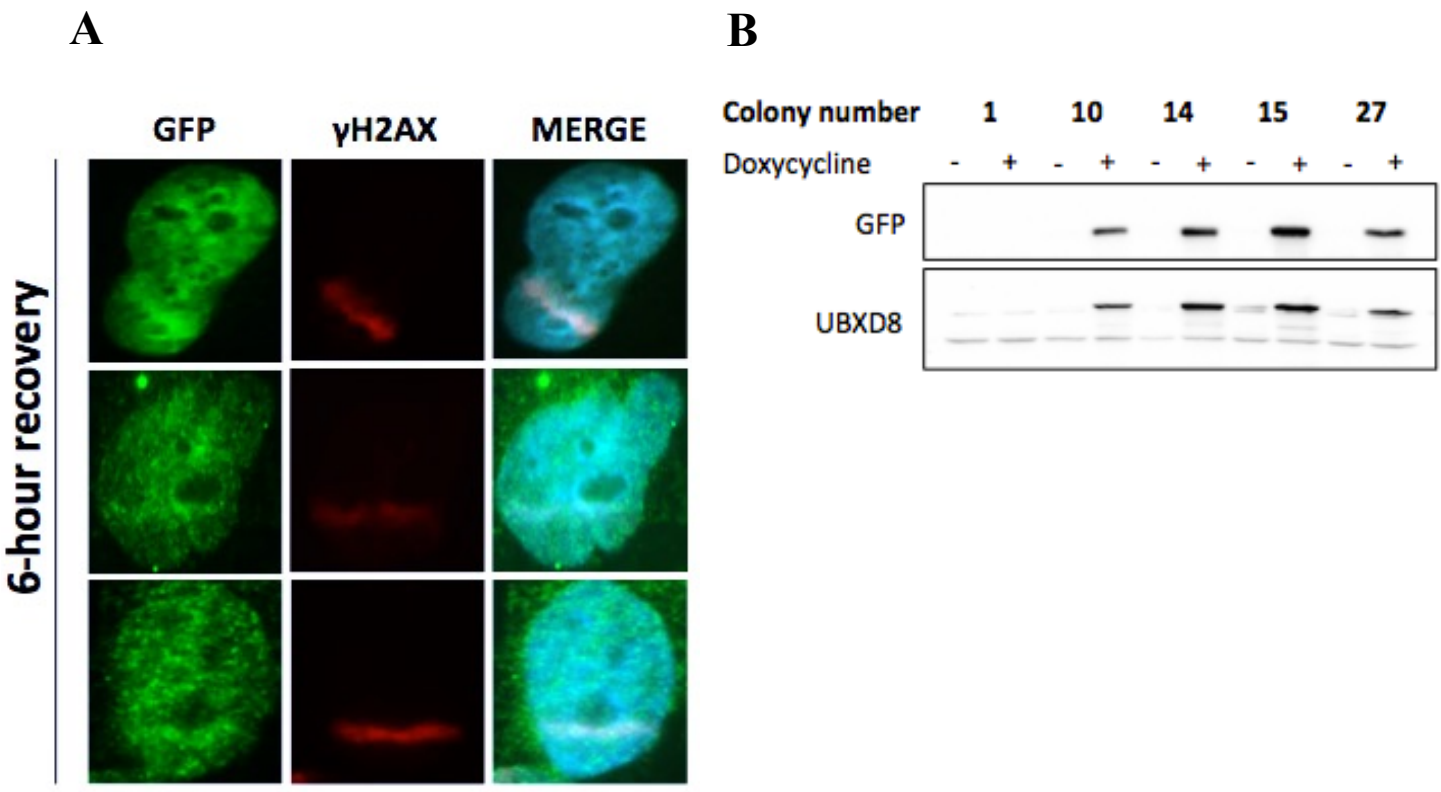

Figure 3-4. UBXD8 is recruited to DNA damage sites in stable transformed cells. (A) Flp-IN/T-Rex HeLa cells stably expressing UBXD8-nEGFP upon doxycycline induction were sensitised to DSBs with Hoechst and subjected to UV-A laser micro-irradiation. The recruitment of UBXD8 to DNA damage was visualised after 6 hours of cell recovery. Cells were fixed and stained for GFP and γH2AX. (B) Western blot demonstrating obtained stable cell line colonies expressing GFP-tagged UBXD8 upon doxycycline induction. Cells were induced with doxycycline 16 hours prior to UV-A laser micro-irradiation. Colony number 27 was used in this experiment. N=1 independent experiment.

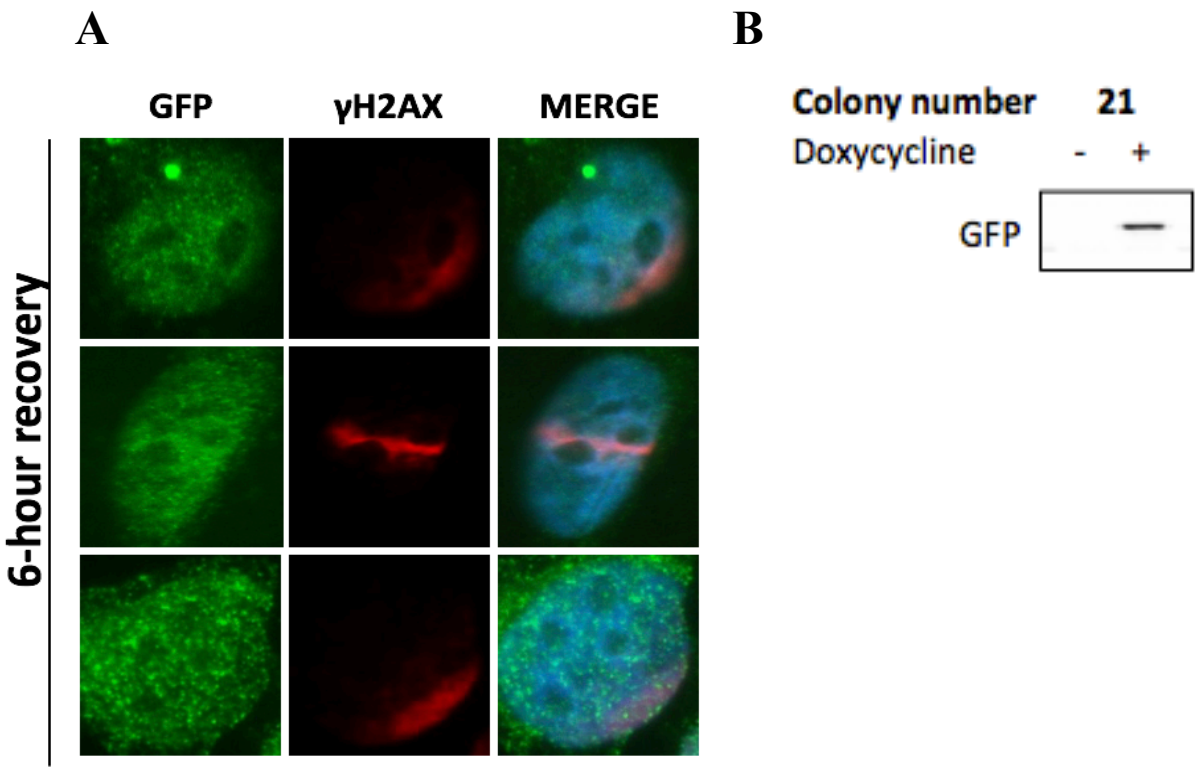

Figure 3-5. Representative images of control cells stably expressing GFP empty vector. (A) Flp-IN/T-Rex HeLa doxycycline inducible cells stably expressing empty GFP were used to demonstrate specificity of the above results showing UBXD8 recruitment to DNA damage sites. Cells were sensitised to DSBs with Hoechst, UV-A micro-irradiated and recovered for 6 hours. Cells were fixed and stained for GFP and γH2AX. No co-localisation of GFP and γH2AX was observed. (B) Western blot showing GFP expression in doxycycline inducible Flp-IN/T-Rex HeLa cells. Doxycycline was added to cells 16 hours prior to DNA damage induction. N=1 independent experiment.

3.2. Absence of UBXD8 Causes Hyperaccumulation of Sumoylated Substrates After DNA Damage Induction

SUMO-1 and SUMO-2/3 isoforms accumulate at sites of DNA damage, where they target several DDR components including 53BP1 and BRCA1 (Galanty et al., 2009). Sumoylation of substrates has been thought to stabilise chromatin-bound proteins (Jentsch and Psakhye, 2013), but in order to control DNA damage repair in a timely manner, these sumoylated substrates also have to be removed. Given that UBXD8 has now been shown to physically localise to DNA damage sites and has a putative SIM domain, it was tested whether UBXD8 is involved in the removal of sumoylated substrates from DNA damage sites.

U2OS cells were depleted of UBXD8 for 72 hours and depletion efficiency was assessed by western blotting (Figure 3-6). Cells were pre-sensitised with Hoechst, exposed to UV-A laser micro-irradiation (355 nm) and recovered for different times over 6 hours. Cells were then fixed and stained for SUMO-1, SUMO-2/3 and γH2AX. Signal intensity was measured at DNA damage sites, which colocalised with γH2AX. As shown in figures 3-6 and 3-7, UBXD8 depleted cells led to an overall increase in sumoylated substrates over 6 hours, compared to control treated siLuciferase cells. SUMO-1 hyperaccumulation started after half an hour of recovery and was detectable by 1 hour after damage, where UBXD8 depleted cells showed a signal increase of around 40% compared to siLuciferase controls. Between 1 hour and 6 hours of recovery, there was a further hyperaccumulation of SUMO-1, increasing about 88% from controls. Overall, control cells showed a slight decrease in SUMO-1 intensity over time. SUMO isoforms are known to give a relatively strong signal over several hours after damage. In the absence of UBXD8, however, there is hyperaccumulation of SUMO-1 and no clearing of the signal was observed.

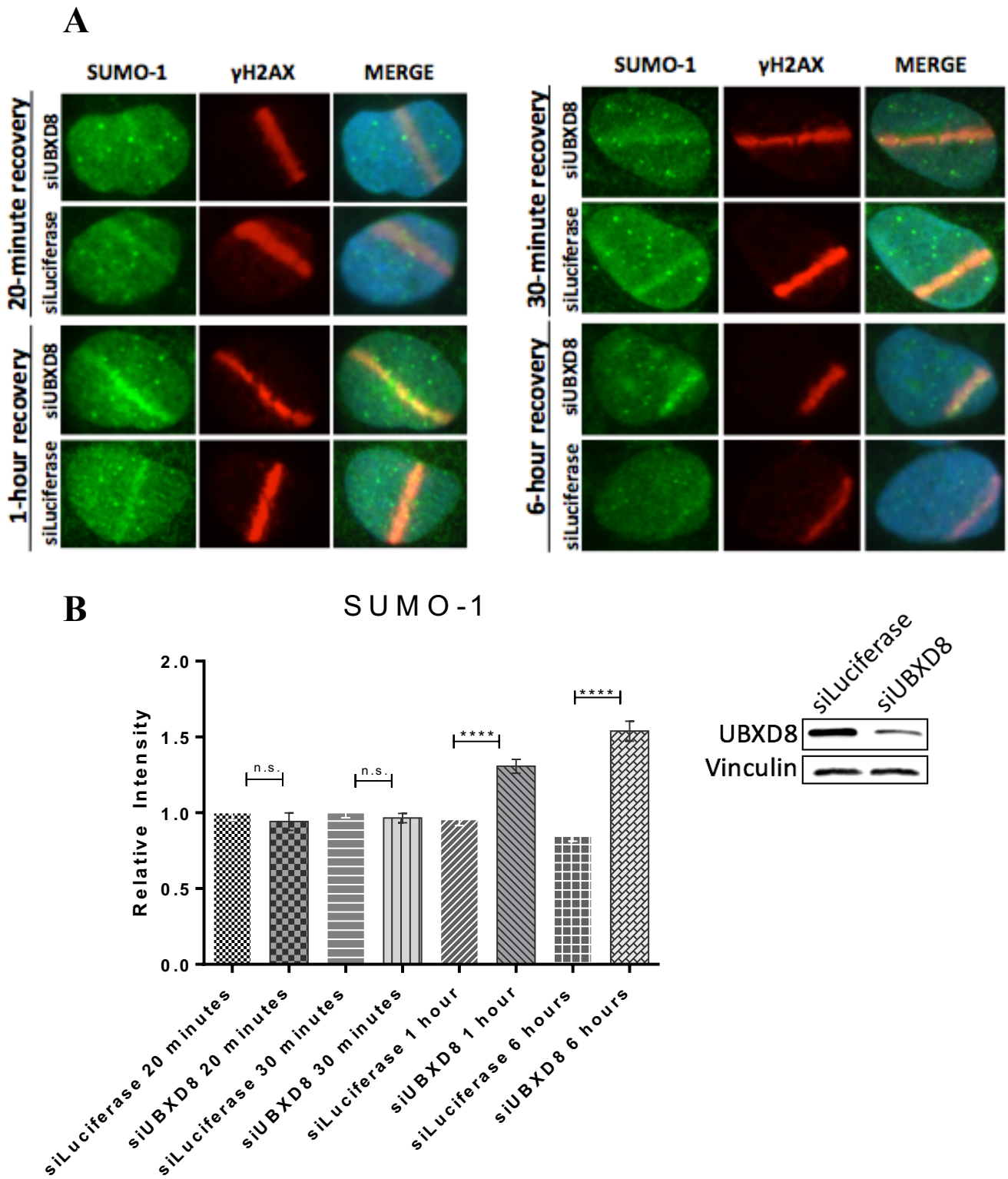

Figure 3-6. SUMO-1 accumulates on DNA damage in the absence of UBXD8. (A) Representative immunofluorescence images showing SUMO-1 accumulation at sites of DNA damage in UBXD8 depleted cells over 6 hours after damage induction. U2OS cells were either control depleted (siLuciferase) or UBXD8 depleted over 72 hours. Cells were sensitised to DSBs with Hoechst for 20 minutes, subjected to UV-A laser micro-irradiation and recovered over 6 hours. Cells were then fixed and stained for SUMO-1 and γH2AX. (B) Quantification of immunofluorescence data over n=3 independent experiments. At least 60 cells were analysed per experiment and condition. Western blot shows depletion efficiency and vinculin serves as the loading control. Data is represented as Mean ± SEM. **** $p < 0.0001$; n.s. $p > 0.05$

SUMO-2/3 kinetics differed slightly from SUMO-1 (Figure 3-7), already showing SUMO-2/3 hyperaccumulation 30 minutes after DNA damage induction in the absence of UBXD8. Compared to control levels, there was around 20% signal increase in UBXD8 depleted cells, rising to 30% increase after 1 hour and up to approximately 60% after 6 hours. Similarly, SUMO-2/3 signal intensity decreased over time in control cells, but increased and then persisted in the absence of UBXD8, indicating that UBXD8 is invloved in the clearing of SUMO-2/3 from DNA damage sites.

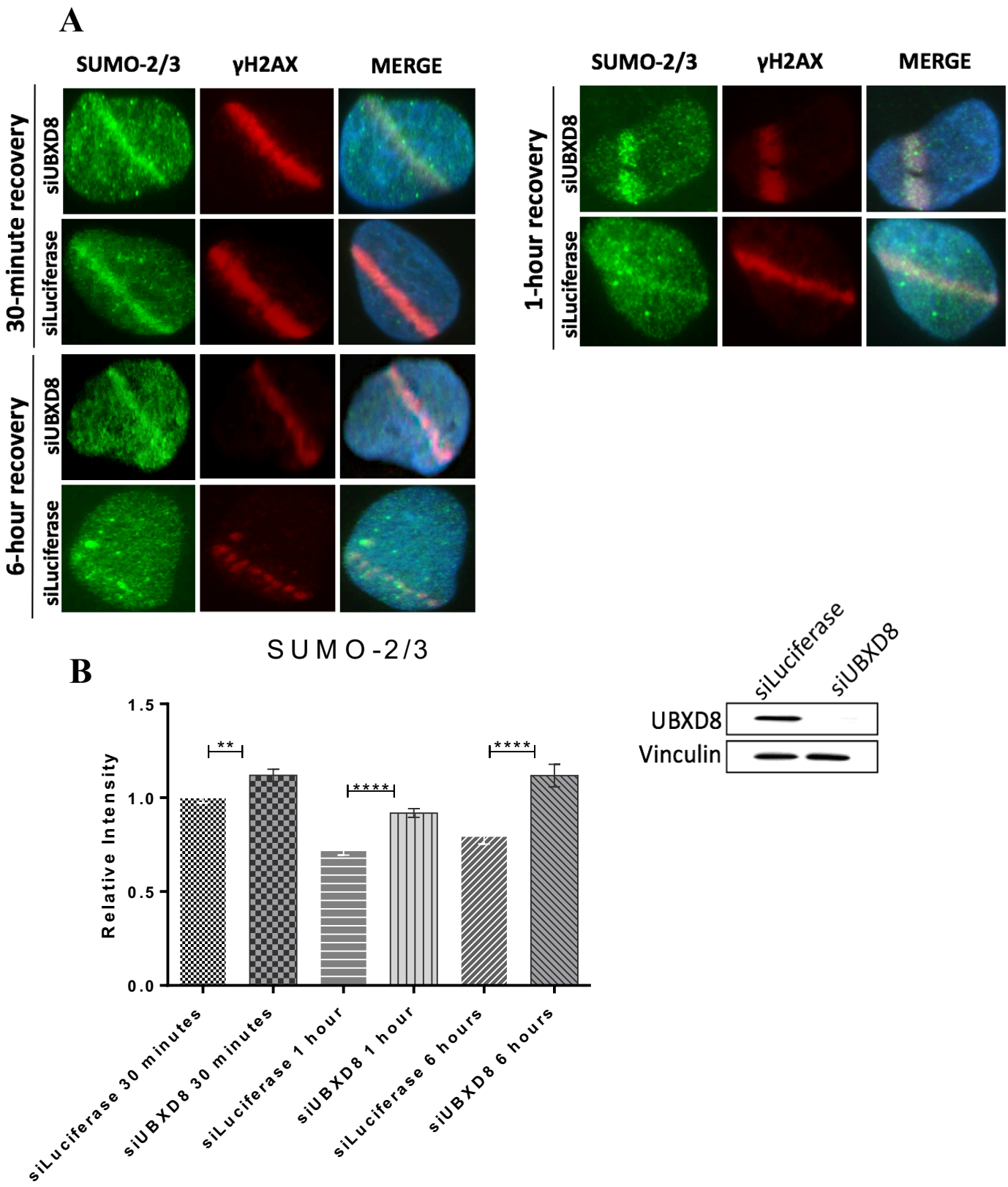

Figure 3-7. Depletion of UBXD8 leads to SUMO-2/3 accumulation on DNA damage. (A) Representative images showing SUMO-2/3 accumulation on DNA damage in the absence of UBXD8 over 6 hours of cell recovery. U2OS cells were control or UBXD8 depleted for 72 hours, sensitised to DSBs with Hoechst and subjected to UV-A laser micro-irradiation. Cells were then fixed and stained for SUMO-2/3 and γH2AX. (B) Quantification of immunofluorescence images over n=3 independent experiments. At least 60 cells were analysed per experiment and condition. Western blot demonstrates UBXD8 depletion and vinculin serves as the loading control. Data is represented as Mean ± SEM. ** $p < 0.01$; **** $p < 0.0001$

To confirm that these results are not cell line specific, HeLa cells were depleted and treated the same way. Cells were recovered for 1 hour to check the initial hyperaccumulation of both SUMO-1 and SUMO-2/3 in UBXD8 depleted cells. As seen in figure 3-8, there was a significant increase in SUMO-1 and SUMO-2/3 intensity 1 hour after DNA damage. Additionally, the effect of UBXD8 depletion on SUMO accumulation was assessed with two different siRNA sequences. Figure 3-9 demonstrates that using two independent siRNA sequences results in a similar SUMO accumulation. Overall, these results demonstrate that UBXD8 is associated in the removal of both SUMO-1 and SUMO-2/3, and the absence of UBXD8 leads to accumulation and persistence of SUMO on DNA damage sites.

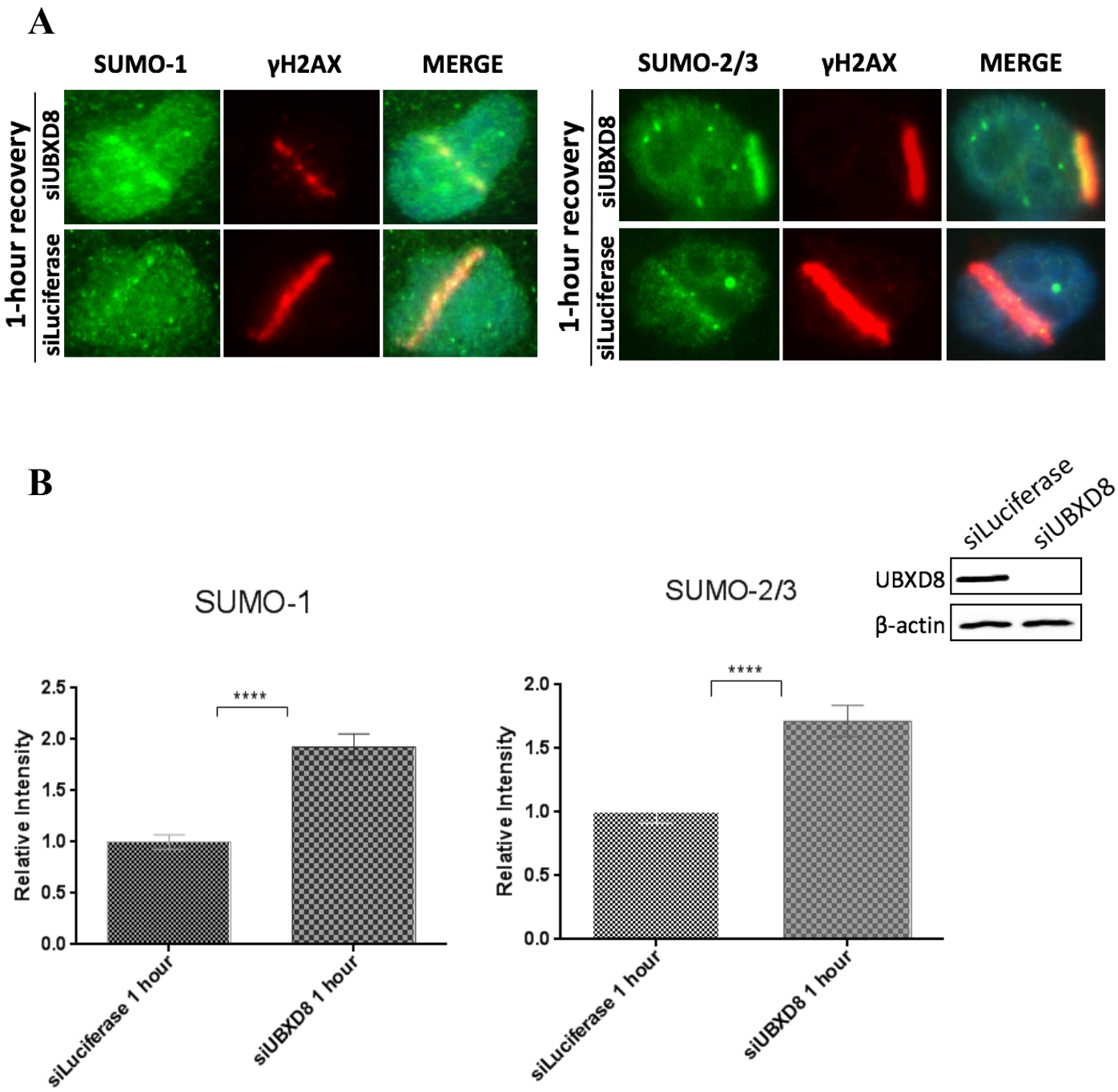

Figure 3-8. The effect of UBXD8 on SUMO accumulation is not cell line specific. (A) Immunofluorescence images demonstrating the accumulation of all three SUMO isoforms in the absence of UBXD8 in HeLa cells. Cells were UBXD8 and control depleted for 72 hours, UV-A laser microirradiated, fixed and stained for SUMO-1, SUMO-2/3 and γH2AX 1 hour after DNA damage induction. (B) Quantification of immunofluorescence images over n=2 independent experiments. At least 60 cells were analysed per condition and experiment. Western blot confirms UBXD8 depletion and β-actin serves as the loading control. Data is represented as Mean ± SEM. **** $p < 0.0001$

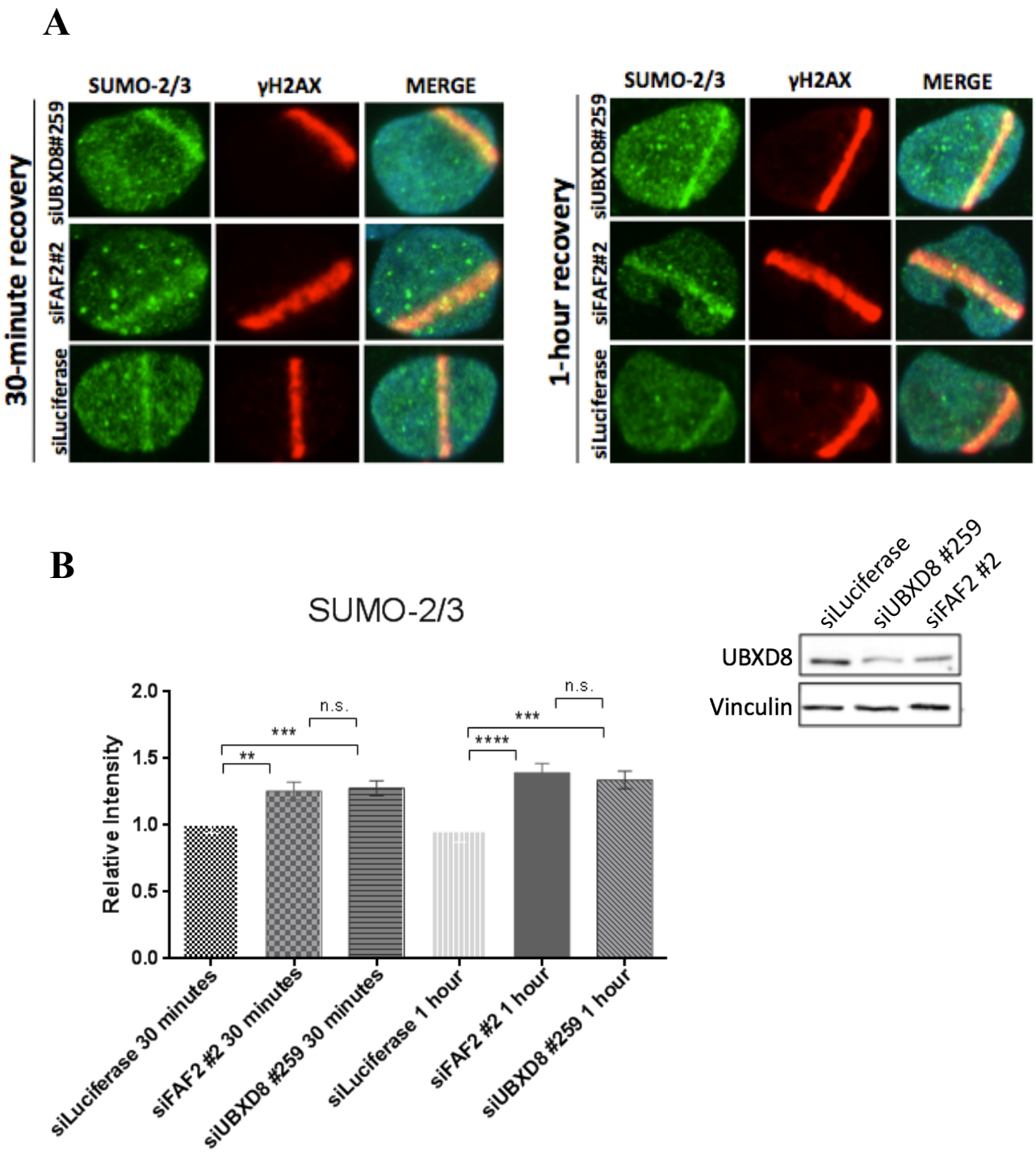

Figure 3-9. The effect of UBXD8 depletion on SUMO-2/3 accumulation with indicated siRNAs. (A) U2OS cells were depleted with two UBXD8 siRNAs and a control siRNA (siLuciferase) for 72 hours. Cells were sensitised by Hoechst, UV-A laser microirradiated, fixed and SUMO-2/3 accumulation was analysed by immunofluorescence 30 minutes and 1 hour after DNA damage induction. N=1 independent experiment. (B) Quantification of SUMO-2/3 intensity at the site of DNA damage. 100 cells were analysed per condition. Western blot confirms depletion and vinculin was used as the loading control. Data is represented as Mean ± SEM. ** $p < 0.01$; *** $p < 0.001$; **** $p < 0.0001$; n.s. $p > 0.05$

3.3. UBXD8 Depletion Increases the Number of SUMO Foci After Ionising Radiation

As IR is widely used in the treatment of several cancers, it was further tested whether UBXD8 depletion similarly leads to an increase in SUMO isoforms on DNA damage after IR. UBXD8 was depleted in U2OS cells for 72 hours, and depletion efficiency was confirmed by western blotting (Figure 3-10). Cells were treated with 2 Gy IR and collected at several time points over 6 hours. Cells were fixed and stained for SUMO-1, SUMO-2/3 and γH2AX.

After ionising radiation, the number of SUMO-1 and SUMO-2/3 foci significantly increased in UBXD8 depleted cells compared to siLuciferase controls (Figures 3-10 and 3-11). In non-irradiated cells, there was no difference in the number of SUMO foci between control and UBXD8 depleted cells. The controls reached their maximum number of SUMO-1 and SUMO-2/3 foci at 30 minutes, after which the number gradually declined back to non-irradiated levels by 6 hours. UBXD8 depleted cells, however, did not resolve their SUMO-1 or SUMO-2/3 foci, although the levels of SUMO-1 decreased over time in UBXD8 depleted cells, indicating the presence of additional factors. SUMO-2/3 foci, however, reached their maximum number at 30 minutes and remained similar after 6 hours of cell recovery. These results suggest that UBXD8 affects DSB repair kinetics by extracting SUMO from DNA damage sites after IR, as visualised by the number SUMO foci.

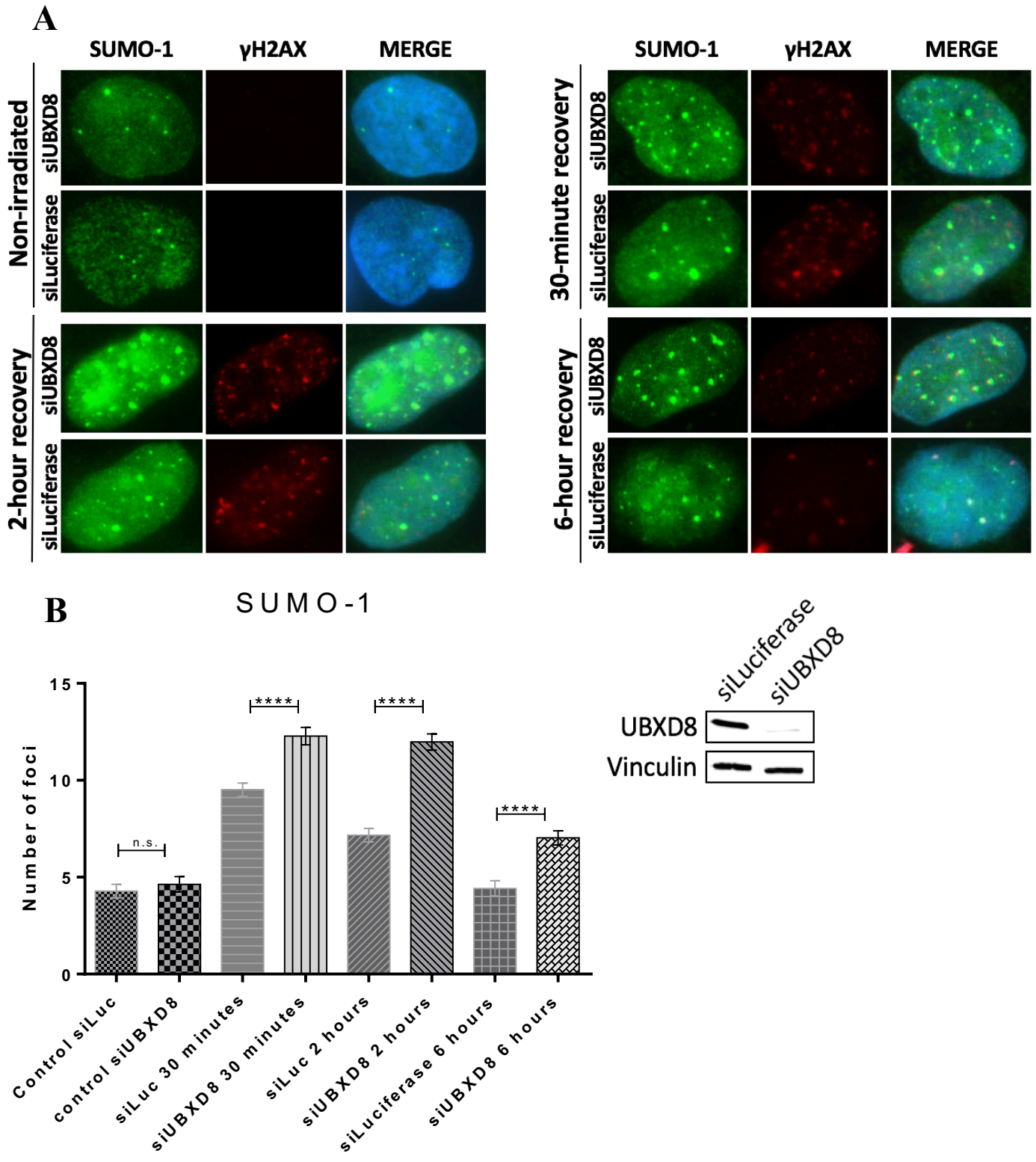

Figure 3-10. UBXD8 depletion increases the number of SUMO-1 foci after 2 Gy IR. (A) U2OS cells were control depleted and UBXD8 depleted over 72 hours, irradiated with 2 Gy IR, recovered over 6 hours, fixed and analysed by immunofluorescence. γH2AX is used as the DNA damage marker. N=2 independent experiments. (B) Quantification of immunofluorescence data. At least 100 cells were analysed per condition. Western blot confirms depletion and vinculin serves as the loading control. Data is represented as Mean ± SEM. **** $p < 0.0001$; n.s. $p > 0.05$

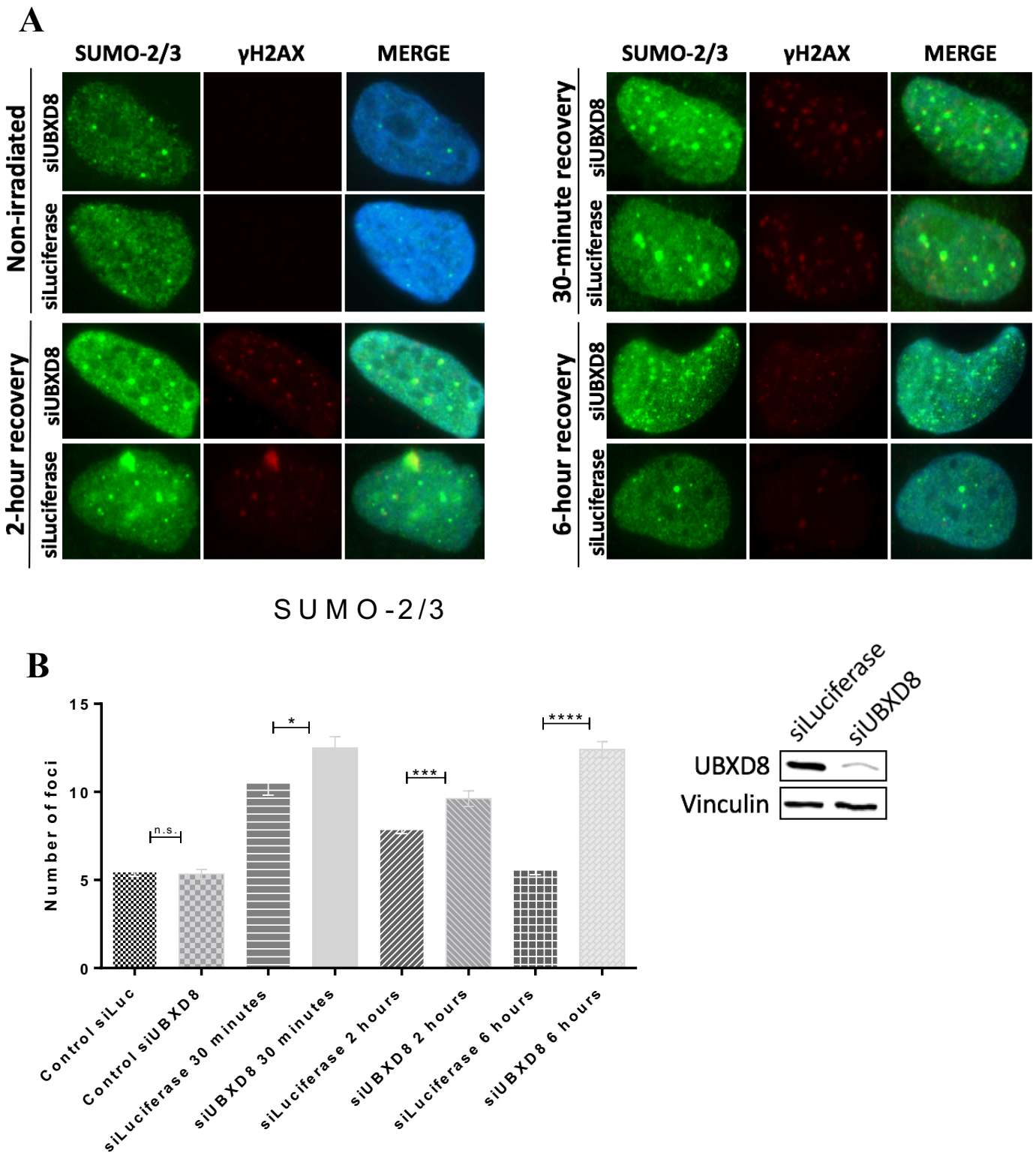

Figure 3-11. Absence of UBXD8 leads to an accumulative increase of SUMO-2/3 foci after 2 Gy IR. (A) Representative images of the number of SUMO-2/3 foci upon UBXD8 depletion after IR. U2OS cells were treated with siLuciferase or siUBXD8 over 72 hours, irradiated with 2 Gy IR and recovered over 6 hours. Cells were stained for SUMO-2/3 and γH2AX. (B) Quantification of the number of SUMO-2/3 foci. At least 100 cells were analysed per condition over n=2 independent experiments. Western blot shows depletion efficiency and vinculin is used as the loading control. Data is represented as Mean ± SEM. * $p \leq 0.05$; *** $p < 0.001$; **** $p < 0.0001$; n.s. $p > 0.05$

3.4. Discussion

The consistency between preliminary proteomics data and the aforementioned results strengthen the hypothesis that UBXD8 has a role in DNA damage response. SILAC-based mass spectrometry analysis coupled with immunoprecipitation experiments showed that UBXD8 is recruited to chromatin after ionising radiation, where it forms a complex with p97 (Figure 3-1). The above results demonstrated that UBXD8 is physically associated with DNA damage sites and is present at 6 and 8 hours after damage induction (Figures 3-3; 3-4). UV-A laser and IR experiments showing that the absence of UBXD8 leads to hyperaccumulation of all three SUMO isoforms is consistent with the observations that UBXD8 has a putative SIM domain (Figures 3-6; 3-7; 3-10; 3-11). The next step would be to confirm UBXD8 binding to SUMO in pulldown experiments and create SIM mutant cells to prove that the interaction is specific. This leads to the search of specific sumoylated substrates targeted by the p97-UBXD8 complex. Some clues about the potential substrates have come from preliminary data showing that the absence of UBXD8 delayed 53BP1 foci resolution (Figure 3-2). It is tempting to speculate that 53BP1 is one of the substrates, as it is shown to be sumoylated by both SUMO-1 and SUMO-2/3 after ionising radiation. Since 53BP1 foci formation upon UBXD8 depletion is not disrupted, it can be hypothesised that UBXD8 downstream of 53BP1. Additionally, the observations that UBXD8 is present on chromatin after 8 hours of ionising radiation (Figure 3-1) and UV-A laser-induced micro-irradiation (Figures 3-3; 3-4) suggests that UBXD8 could potentially act on proteins that are also later components of DDR. There are several possible candidates that can be identified by mass spectrometry with SIM mutants. Taken together, the data support a model where UBXD8 is a novel DDR protein extracting sumoylated substrates from sites of DNA damage.

4. RESULTS 2: UBXD8 AND p97 WORK TOGETHER IN THE REGULATION OF SUMO ON DNA DAMAGE

4.1. Absence of p97 Leads to Hyperaccumulation of Sumoylated Substrates After DNA Damage Induction

The first reports of the p97 system being able to recognise and extract sumoylated substrates came from studies in yeast. Models of *S. pombe* have shown that Cdc48 binds SUMO via the SIM domain in Ufd1. Additional evidence has come from *S. cerevisiae*, where Ufd1 also binds SUMO (Bergink et al., 2013; Nie et al., 2012). The $Cdc48^{-Ufd1-Npl4}$ core complex cooperates with STUbL by binding and processing both ubiquitylated and sumoylated substrates, for example in the removal of covalently bound topoisomerase 1 (TOP1)-DNA adducts (Heideker et al., 2011). It is currently unknown whether human p97 is able to recognise and process both ubiquitylated and sumoylated substrates. The preliminary results so far indicate that it is plausible that UBXD8 regulates sumoylation in complex with p97. To gain a further understanding into whether this possibility exists, the role of p97 in the regulation of sumoylation on DNA damage sites was studied.

U2OS cells were inhibited with the NMS-873 allosteric inhibitor for 2 hours. Cells were pre-sensitised to DNA damage using Hoechst and subjected to UV-A laser micro-irradiation (355 nm), after which they were recovered for several time points over 6 hours. Cells were fixed and the intensities of SUMO-1 and SUMO-2/3 were measured on laser-induced damage sites. Inhibition of p97 led to hyperaccumulation of both SUMO-1 and SUMO-2/3 over 6 hours. Similarly to UBXD8 depleted cells, the hyperaccumulation of SUMO-1 was detectable from 1 hour after DNA damage, with no significant change detected after 30 minutes of recovery (Figure 4-1). At 1 hour, SUMO-1 levels increased

approximately 169% from DMSO treated control cells. By 6 hours, the levels increased about 130% from control, showing there was a slight decrease in inhibitor treated cells between 1 hour and 6 hours of recovery. The control levels, however, peaked at 30 minutes as in UBXD8 depleted cells, after which there was a gradual decline in SUMO-1 levels.

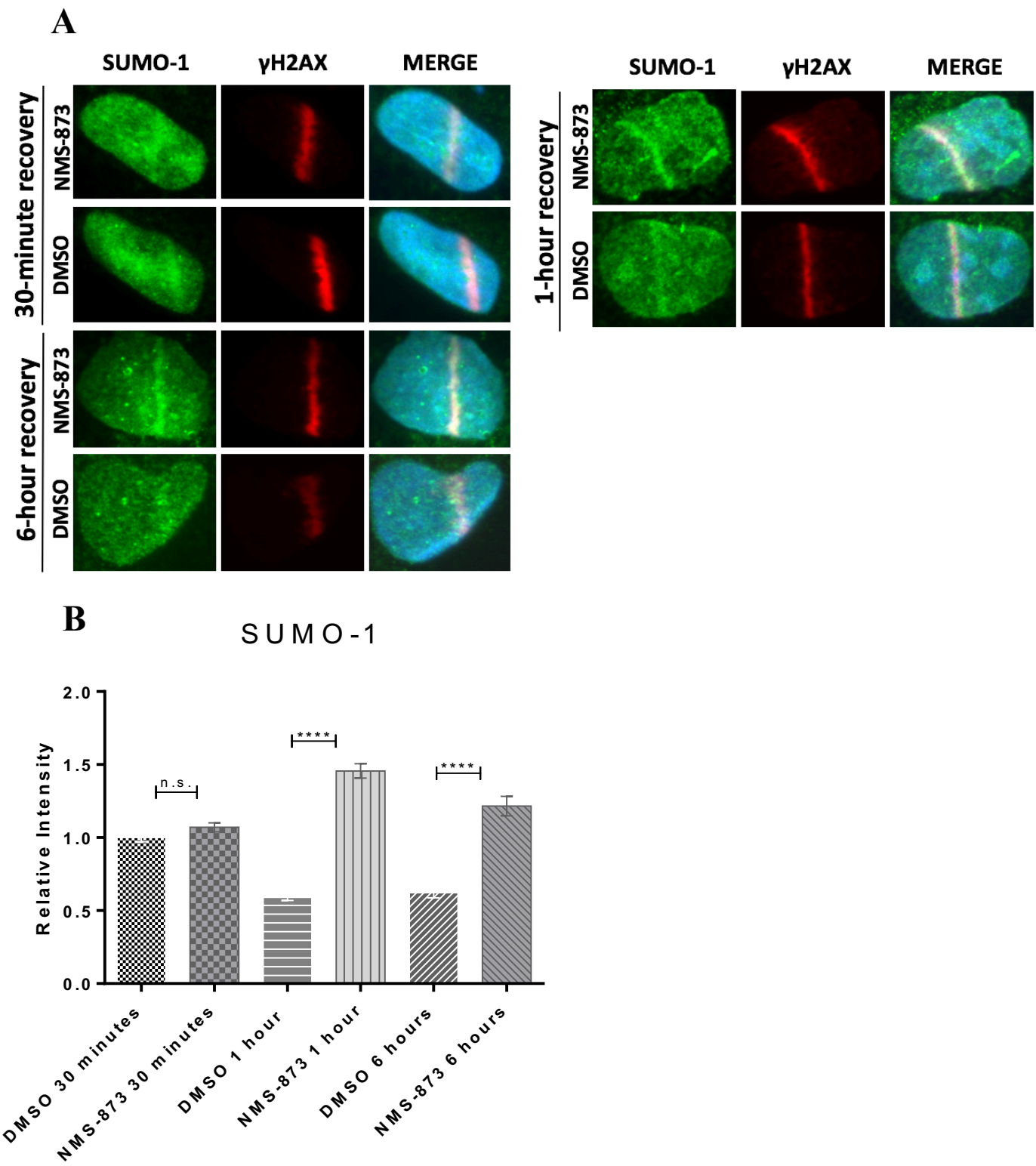

Figure 4-1. p97 inhibition leads to SUMO-1 accumulation on DNA damage. (A) Representative images of the effect that p97 inhibition has on SUMO-1 at the sites of DNA damage. Allosteric p97 inhibitor NMS-873 was applied to U2OS cells over two hours. Cells were then sensitised to DSBs with Hoechst, UV-A laser microirradiated and recovered over 6 hours. Cells were fixed and stained for SUMO-1 and γH2AX. Control cells were DMSO treated. (B) Quantification of immunofluorescence images. At least 60 cells were analysed per experiment and condition over n=3 independent experiments. Data is represented as Mean ± SEM. **** $p < 0.0001$; n.s. $p > 0.05$

SUMO-2/3 kinetics differed from SUMO-1 kinetics similarly to UBXD8 depleted cells (Figure 4-2). At 30 minutes after DNA damage induction, there was already a significant accumulation of around 47% compared to control cells. By 1 hour, the increase was around 63%, and at 6 hours the NMS-873 treated cells increased approximately 108% from DMSO controls. SUMO peaked at 30 minutes after DNA damage in DMSO controls and decreased gradually afterwards. To demonstrate that the accumulation of SUMO is not cell line specific, p97 was inhibited in HeLa cells with NMS-873 for two hours as above, and SUMO-1 and SUMO-2/3 hyperaccumulation was measured 1 hour after DNA damage induction (Figure 4-3). Overall, the absence of p97 has a very similar effect on SUMO levels to the absence of UBXD8.

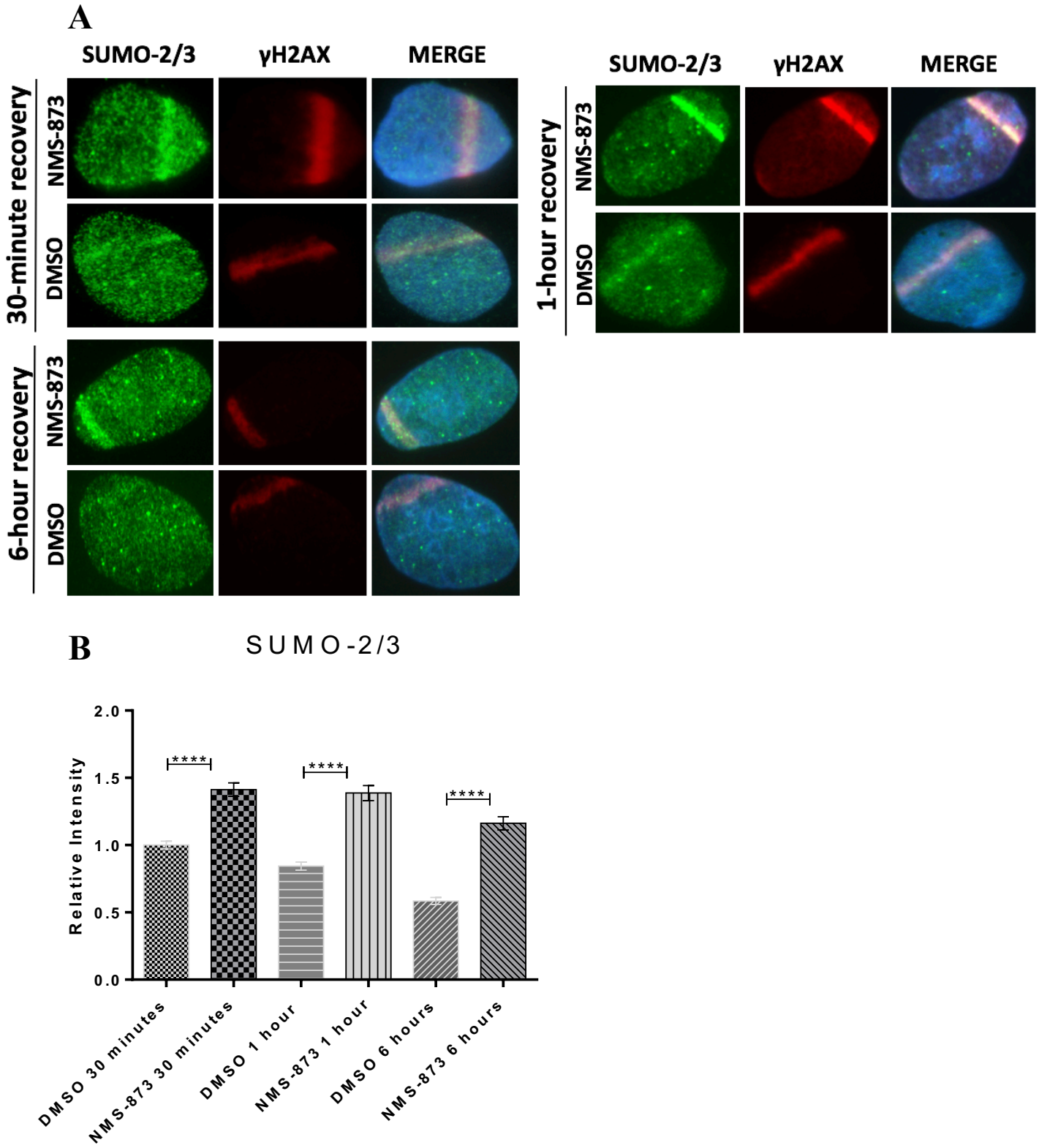

Figure 4-2. p97 inhibition results in SUMO-2/3 accumulation on DNA breaks. (A) Immunofluorescence images of SUMO-2/3 intensity at UV-A laser induced micro-irradiation sites. U2OS cells were treated with DMSO or an allosteric p97 inhibitor NMS-873 over two hours. Cells were sensitised to DSBs with Hoechst, microirradiated and fixed at several time points over 6 hours. (B) Quantification of SUMO-2/3 intensities upon p97 inhibition. At least 60 cells were analysed per condition. N=3 independent experiments. Data is represented as Mean ± SEM. **** $p < 0.0001$

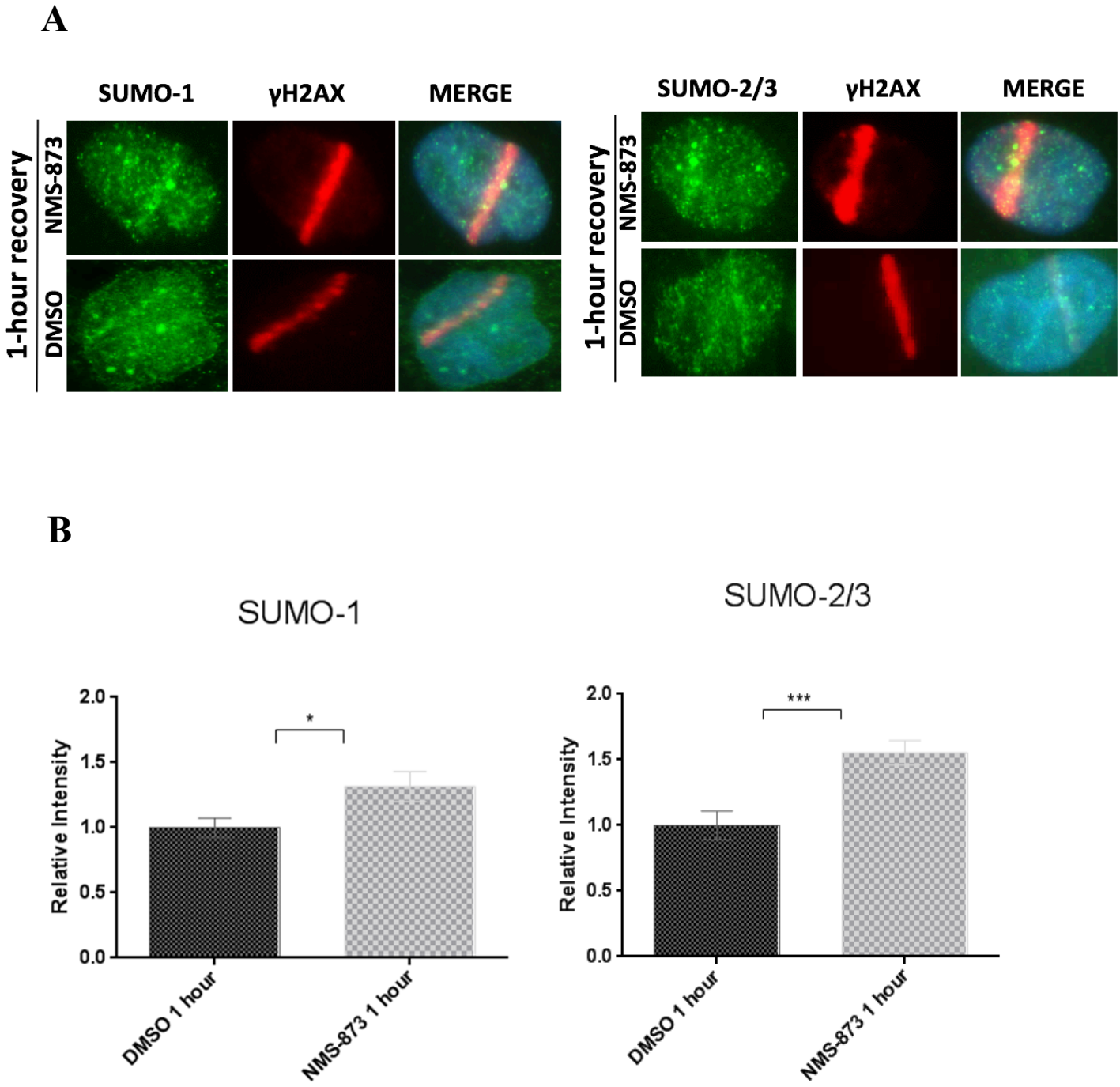

Figure 4-3. Confirmation of p97-induced SUMO accumulation on DNA damage in HeLa cells (A) Immunofluorescence images of SUMO-1 and SUMO-2/3 intensities at UV-A laser induced micro-irradiation sites 1 hour after damage induction. HeLa cells were treated with DMSO or the p97 inhibitor NMS-873 for two hours. Cells were sensitised to DSBs with Hoechst for 20 minutes and subjected to UV-A laser treatment. (B) Quantification of SUMO-1 and SUMO-2/3 intensities upon p97 inhibition. At least 100 cells were analysed over n=2 independent experiments. Data is represented as Mean ± SEM. * $p \leq 0.05$; *** $p < 0.001$

4.2. p97 Recruitment to DNA Damage Depends on UBXD8

The results so far have demonstrated that UXBD8 and p97 affect the removal of sumoylated substrates in a similar manner, suggesting that they might work in a complex. To test whether UBXD8 is responsible for p97 recruitment to DNA damage, U2OS cells were depleted of UBXD8 for 72 hours and DNA damage was induced using UV-A laser micro-irradiation (355 nm). Cells were recovered for 1 hour, fixed and stained for p97 and γH2AX. In the absence of UBXD8, p97 recruitment to DNA damage sites fell to approximately half of control levels (Figure 4-4), suggesting that UBXD8 acts upstream of p97 and is directly responsible for p97 recruitment. Depletion was confirmed by western blotting (Figure 4-4). Recruitment of p97 depends on RNF8 and Ufd1-Npl4 (Acs et al., 2011; Meerang et al., 2011), so it can be hypothesised that UBXD8 exists within the $p97^{Ufd1\text{-}Npl4}$ complex.

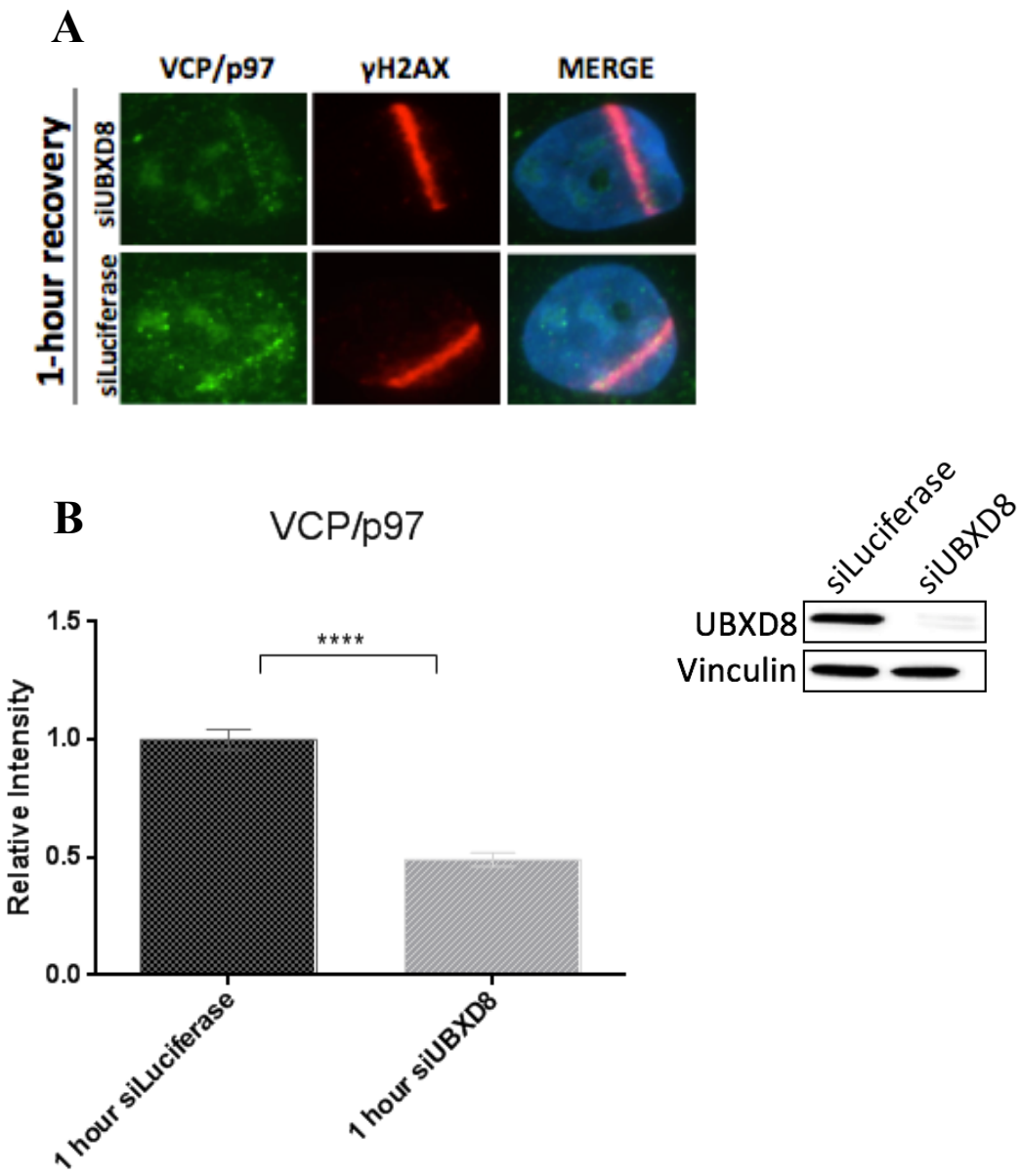

Figure 4-4. UBXD8 regulates p97 recruitment to sites of DNA damage. (A) Depletion of UBXD8 reduces p97 recruitment to UV-A laser induced micro-irradiation sites. U2OS cells were treated with siLuciferase or siUBXD8 for 72 hours. Cells were sensitised with Hoechst 20 minutes before UV-A laser treatment. Cells were recovered for 1 hour after DNA damage induction, fixed and stained for p97 and γH2AX. p97 recruitment to DNA damage sites was visualised by immunofluorescence. N=3 independent experiments. (B) Quantification of data represented in (A) over n=2 independent experiments. At least 100 cells were analysed per experiment and condition. **** $p < 0.0001$. Data is represented as Mean ± SEM. Western Blot confirms depletion and vinculin serves as the loading control.

4.3. UBXD8 Depletion Leads to Hyperaccumulation of K48-linked Polyubiquitylated Substrates

The N-terminus of UBXD8 has the UBA domain, which is highly conserved in residues for ubiquitin binding (Christianson et al., 2011). So far, however, it has not yet been shown that the UBA domain is able to bind ubiquitin. However, the above results demonstrated that UBXD8 is required for efficient recruitment of p97 to DNA damage. Knowing that compromising p97 function causes hyperaccumulation of K48-linked polyubiquitin chains on DNA break sites (Meerang et al., 2011), the effect of UBXD8 depletion on hyperaccumulation of K48-linked ubiquitin was investigated. U2OS cells were depleted of either p97 or UBXD8 and subjected to laser micro-irradiation. Cells were recovered for 5 minutes and 30 minutes, fixed and stained for K48 specific ubiquitin chains and for γH2AX. Depletion efficiency is shown by western blotting (Figure 4-5). As expected, depletion of p97 led to a rapid hyperaccumulation of K48-linked ubiquitin. 5 minutes after DNA damage induction, the increase from siLuciferase control cells was approximately 111%, and 30 minutes later the p97-depleted cells had around 82% more K48-linked polyubiquitin compared to controls (figure 4-5). UBXD8 depleted cells had a similar initial increase of approximately 111% 5 minutes after DNA damage induction, compared to siLuciferase treated cells. 30 minutes after damage, the effect of UBXD8 depletion was smaller than upon p97 depletion, but nevertheless there was around 40% increase in K48-linked chains compared to control cells (Figure 4-5). Overall, these results are consistent with the observations that UBXD8 is responsible for p97 recruitment to DNA damage sites, as both p97 and UBXD8 depletion lead to hyperaccumulation of K-48 linked polyubiquitin.

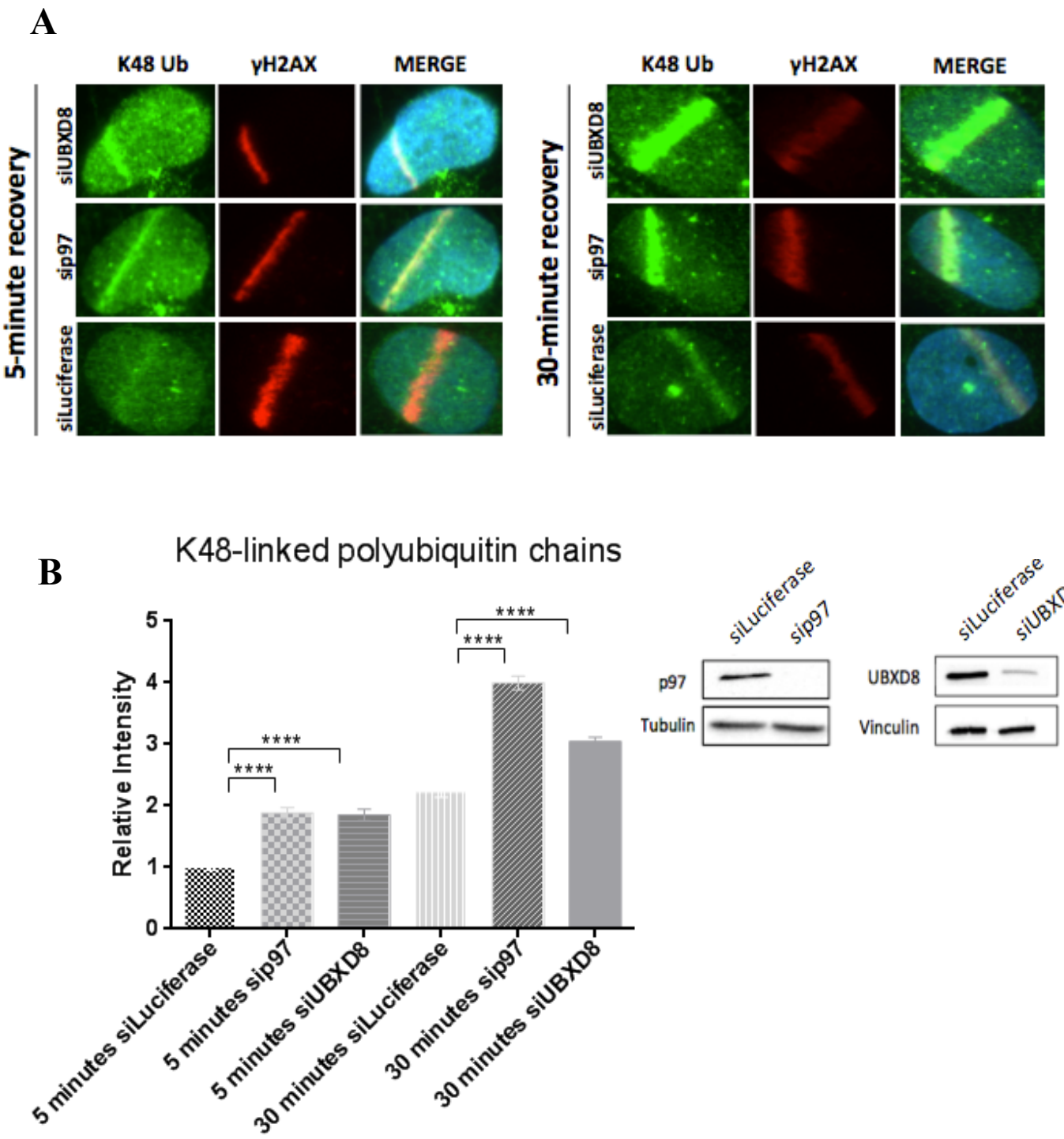

Figure 4-5. UBXD8 depletion causes hyperaccumulation of K48-linked ubiquitin on DNA damage sites. (A) U2OS cells were transfected with siRNA targeting UBXD8, p97 or control (siLuciferase). Cells were sensitised with Hoechst 20 minutes before UV-A laser induction and recovered for either 5 minutes or 30 minutes. Cells were fixed and K48-linked ubiquitin was visualised by immunofluorescence. Depletion of p97 served as a positive control. (B) Quantification of (A) in n=2 independent experiments. At least 100 cells were analysed per experiment and condition. **** $p < 0.0001$. Data is represented as Mean ± SEM. Western blot confirms depletions and tubulin and vinculin serve as loading controls.

4.4. Discussion

The absence of either UBXD8 or p97 leads to hyperaccumulation of all three SUMO isoforms over 6 hours after DNA damage induction (Figures 3-6; 3-7; 3-10; 3-11; 4-1; 4-2). The differences in SUMO-1 and SUMO-2/3 kinetics are also similar between UBXD8 depletion and p97 inhibition, showing a faster accumulation of SUMO-2/3 than SUMO-1. The resulting phenotypes, however, are stronger upon p97 inhibition. This could be because p97 has a variety of other functions in DDR, leading to additional indirect effects. For example, since p97 extracts polyubiquitylated substrates from chromatin and cooperates with the STUbL RNF4 (Bergink et al., 2013; Kuo et al., 2016), the stronger phenotypes can result because the mixed SUMO-ubiquitin chains are not being efficiently extracted. Since there are no indications that the UBA domain of UBXD8 is able to bind polyubiquitin chains (Christianson et al., 2011), the observation that the absence of UBXD8 leads to hyperaccumulation of K48-linked polyubiquitin substrates (Figure 4-5) is not necessarily a direct binding effect, but can result from a secondary effect of decreasing the levels of p97 on DNA damage. Further experiments, however, are needed to conclude that. Since the UBX domain in UBXD8 recruits p97 in the cytosol (Suzuki et al., 2012), it is tempting to speculate that a similar mechanism occurs in the nucleus. Although previous proteomics data has demonstrated that UBXD8 and p97 increase their interaction on chromatin upon IR (Figure 3-1), the complex in which UBXD8 exists needs to be elucidated. One possibility is that it is part of the core complex with Ufd1-Npl4, which could be tested by co-immunoprecipitation. The Ufd1-Npl4 core complex is also known in ERAD as is UBXD8 (Stolz et al., 2011), and p97 recruitment to DNA breaks is similarly decreased in the absence of UBXD8 as upon Ufd1-Npl4 depletion (Meerang et al., 2011). Additionally, comparing p97 recruitment between co-depleted cells and Ufd1-Npl4 and UBXD8 depleted alone would give an indication whether there is redundancy in the

system. Overall, the above results suggest that UBXD8 possibly in complex with p97 processes sumoylated and ubiquitylated substrates on DNA damage sites, and that UBXD8 is partly responsible for efficient p97 recruitment to DNA damage sites.

5. DISCUSSION

5.1. SUMO Regulation by UBXD8 and p97

This study identified UBXD8 as a potential novel component in the DNA damage response that is involved in the regulation of sumoylation and ubiquitylation at DNA break sites. Thus, it has been demonstrated that cells downregulated for UBXD8 have defective SUMO-1 and SUMO-2/3 clearance (Figures 3-6; 3-7; 3-10; 3-11), and the absence of its binding partner p97 leads to a similar hyperaccumulation of sumoylated substrates (Figures 4-1; 4-2). Furthermore, it was demonstrated that UBXD8 is upstream of p97, because it is partly responsible for the recruitment of p97 to DNA damage sites (Figure 4-4). Consequently, the absence of UBXD8 also affects K48-linked ubiquitin clearance (Figure 4-5). The importance of this study can be shown by the fact that ubiquitylation and sumoylation are both fundamental in the coordination of DNA damage repair. Attaching ubiquitin and SUMO onto target proteins leads to the recruitment of downstream repair proteins, and the resulting protein-protein interactions at DNA breaks allow recognition and repair of specific damage (Jackson and Durocher, 2013). If the process is dysregulated and ubiquitin and SUMO proteins are not effectively cleared from chromatin, the DNA break repair cannot be efficiently completed and cells are more likely to have induced radiosensitivity and to undergo apoptosis. Taken together, these results have identified a novel way in which sumoylation and ubiquitylation is regulated on DNA damage.

UBXD8 is one of the many co-factors of the molecular chaperone p97. The functions of p97 in DNA damage response are highly complex and much is currently unknown. One of the reasons for this is its large-scale influence on several DSB repair proteins, of which the molecular mechanisms are currently uncharacterised (Meerang et al., 2011). Additionally, up to six cofactors can bind to the N-terminus of p97 at any one time, giving it the ability

to specifically coordinate various cellular processes (Hanzelmann et al., 2011). Many of its co-factors are structurally and mechanistically under-characterised (Schuberth and Buchberger, 2008), which has a significant impact on how much is known about p97 functions. The preliminary data for this study identified p97-UBXD8 complex on DNA break sites (Figure 3-1), adding another layer of complexity to the function of p97 in DNA repair. Although the dual recognition of SUMO and ubiquitin in the p97 system has so far been only described in yeast (Nie et al., 2012), this study proposes that it is likely to exist also in human cells (Figure 5-1). In humans, it is known that p97 is involved in the extraction of SUMO-ubiquitin mixed chains by binding to ubiquitin. These SUMO-ubiquitin chains are formed by STUbLs, which attach ubiquitin proteins onto SUMO-2/3 chains (Tatham et al., 2008), but not onto SUMO-1 as SUMO-1 lacks the consensus sequence for conjugation (Ulrich, 2008). This study shows that there is likely to be an additional mechanism to STUbL in human p97 in the recognition and extraction of SUMO chains, because both SUMO-1 and SUMO-2/3 hyperaccumulation was observed upon UBXD8 depletion and inhibition of p97 (Figures 3-6; 3-7; 3-10; 3-11; 4-1; 4-2). Even though the UBA domain of UBXD8 has no known binding to ubiquitin, it can be hypothesised that once recruited to the sites of DNA damage, UBXD8 can target specific sumoylated substrates by recognising SUMO via its putative SIM domain and directing the substrate to p97, where translocation and substrate release occurs. Similarly to the processing of ubiquitylated substrates (Bodnar and Rapoport, 2017), SUMO chains could be trimmed by SENPs before fully releasing the substrates at the other side of the p97 pore, but these biochemical mechanisms need to be studied.

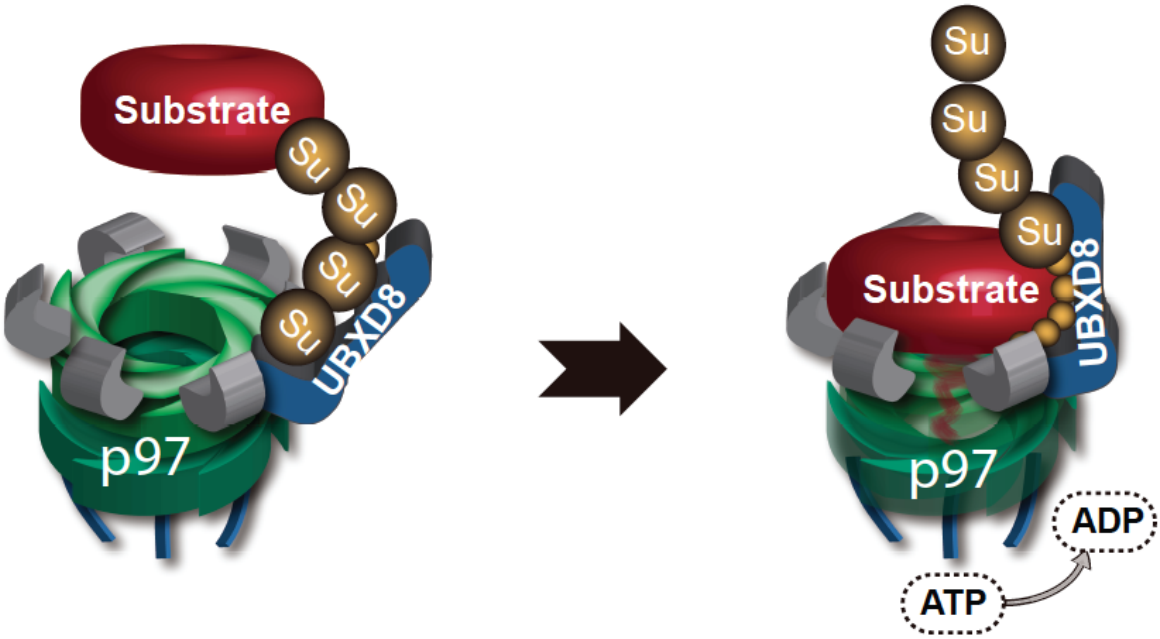

Figure 5-1. Hypothetical new model of p97 substrate processing. The conventional model of mammalian p97 substrate processing involves recognition of ubiquitylated substrates by p97 adaptors, which bring the substrates to p97 for processing. Using energy from ATP hydrolysis, the substrate is translocated through the p97 central cavity. This study demonstrates that one of the co-factors of p97, UBXD8, has a putative SIM domain and is recruited to DNA damage sites, where it regulates sumoylated substrates over several hours after DNA damage induction. The kinetics of SUMO-1 and SUMO-2/3 regulation was similar upon p97 inhibition, and it was further shown that UBXD8 partially recruits p97 to sites of DNA damage. Therefore, it could be hypothesised that the p97-UBXD8 complex identified on chromatin after IR plays a role in the recognition and processing of sumoylated substrates, and that there is a conserved dual recognition of ubiquitin and SUMO in p97 as formerly demonstrated in yeast.

The UBX domain of UBXD8 acts as a recruitment signal to p97 in the cytosol (Suzuki et al., 2012), so it can be hypothesised that a similar mechanism is used in the nucleus. This can be tested by creating UBX domain mutants and observing the recruitment of p97 to DNA damage sites, as well as confirming it biochemically by pulldown experiments in nuclear cell fractions. If UBXD8 acts upstream of p97, it leads to further questions about what complex is UBXD8 part of and how is UBXD8 itself recruited to DNA damage. It is a possibility that UBXD8 exists in the core Ufd1-Npl4 complex, as it does seem to affect

p97 recruitment to DNA damage in a similar way (Meerang et al., 2011). Whether it is part of the Ufd1-Npl4 complex can be tested by immunoprecipitation of the complex components, and by observing the potential redundancy in their recruitment of p97 to DNA damage. There is a possibility that UBXD8 exists within a novel complex.

The ability of UBXD8 to shuffle between subcellular compartments is mostly conferred by its hairpin loop domain, which binds PEX19 after *de novo* synthesis of UBXD8 (Schrul and Kopito, 2016). The exact molecular mechanisms responsible for its cellular trafficking are unknown. Concerning its recruitment to DNA damage sites, it could be studied whether UBXD8 mostly translocates from the cytosol to the nucleus or whether there is an existing nuclear pool of UBXD8. Knowing that most of UBXD8 is located in the cytoplasm (Wang and Lee, 2012), it will be difficult to detect any subtle changes in the movement between the two compartments. For example, monitoring UBXD8 decrease specifically in the cytosolic compartment after ionising radiation would give us an indication that a large amount of the protein is translocated into the nucleus. Furthermore, pre-extracting the cytosol and monitoring UBXD8 in the nucleus with a specific antibody under basal conditions in several cell lines would give an understanding whether UBXD8 has a resting nuclear pool. The results from this study demonstrate that the effect of UBXD8 depletion on the hyperaccumulation of K48-linked ubiquitin occurs within the first 5 minutes after DNA damage induction (Figure 4-5), indicating that an existing protein pool is necessary to cause these rapid cellular changes.

UBXD8 has the UAS oligomerisation domain (Kim et al., 2013), and oligomerisation influences the binding properties of several proteins (Hashimoto and Panchenko, 2010). The formation of homo-oligomers in UBXD8 might not only be important in the control of fatty acid synthesis in the cytosol (Kim et al., 2013), but could give it a degree of affinity

to bind SUMO. It could therefore be tested whether homooligomers of UBXD8 have higher affinity for sumoylated substrates. The specific substrates can then be identified by mass spectrometry analysis of UBXD8 SIM mutant cells after ionising radiation to see which interactions are lost upon SIM mutation. Current preliminary data suggests that one of the substrates could be 53BP1, as its foci resolution is disrupted in UBXD8 depleted cells and it is known to be heavily sumoylated by both SUMO-1 and SUMO-2/3 (Galanty et al., 2009). It is therefore plausible that the persistence of SUMO on 53BP1 is why 53BP1 is not extracted correctly from DSB sites. Since there is a global accumulation of sumoylated substrates over 6 hours after both UV-A micro-irradiation and IR, and UBXD8 is physically associated with break sites after 8 hours of DNA damage induction gives an appreciation that the effects of UBXD8 on DNA damage sites are quite complex and possibly several substrates are involved. The persistence of UBXD8 on DNA damage over 8 hours indicates that it has a function in later stages of DNA repair and/or in clearing of DNA repair components that fix DNA lesions, leading to an inability of these components to dissociate from break sites upon UBXD8 depletion.

Importantly, UVA laser causes complex DNA damage and it is not a specific marker of DSBs (Kong et al., 2009), although pre-sensitisation with Hoechst induces DSBs (Limoli and Ward, 1993). The indications that UBXD8 is involved in DSB repair come from mass spectrometry studies, where UBXD8 was identified on chromatin over 8 hours after 10 Gy of IR (Figure 3-1). Additionally, this study used IR as a source of DNA damage, which resulted in SUMO accumulation on DSB sites in UBXD8 depleted cells (Figures 3-10; 3-11). Its involvement in the regulation of 53BP1 foci clearance (Figure 3-2) also suggests that UBXD8 is a DSB repair protein. In order to specifically prove this, DSB repair can be analysed within the whole genome after IR in UBXD8 depleted cells using pulsed-field gel electrophoresis (PFGE) or a comet assay. Also, GFP-based HR and NHEJ reporter assays

can be performed upon UBXD8 depletion with relevant positive controls such as RAD51 and XRCC4 (Kim et al., 2005), respectively.

5.2. Targeting p97-UBXD8 in Drug Discovery

DNA damaging radiotherapy is widely used in cancer treatment (O'Connor, 2015). Its efficiency is reflected in its ability to cause DNA double strand breaks in tumour cells in a relatively localised manner, but nevertheless is associated with significant damage to normal surrounding tissues. Since cancer cells are compromised in ways they repair DNA damage, they are consequently more reliant on the DNA repair pathways that are still intact (Helleday et al., 2008; Jackson and Bartek, 2009). This notion has been therapeutically exploited as a concept of "synthetic lethality" (Lord et al., 2015). Taking this knowledge into radiobiology and targeting specific DNA damage repair pathways in combination with ionising radiation can lead to the development of novel cancer therapies, where normal cells would be minimally affected, but there would be an increased sensitivity of cancer cells to chemo-radiotherapy.

The p97 system is one of the major potential targets for therapy and there are a variety of possible co-factors that could affect a specific DSB repair function related to p97 (Anderson et al., 2015; Buchberger et al., 2015). Since p97 itself has a wide variety of crucial roles in normal cells (Meyer et al., 2012), its inhibition, especially long term, can lead to side effects. When, however, its co-factors are targeted in a manner where they affect a specific part of p97 function, the side effects could potentially be decreased. Taking UBXD8 as a potential example, when UBXD8 is depleted, the recruitment of p97 to the sites of DNA damage is decreased and its ability to extract ubiquitylated and/or sumoylated substrates from DNA repair sites are therefore compromised. The p97 function is not fully inhibited, but its ability to coordinate DSB repair is. Similarly to the concept of

synthetic lethality, when this would happen in normal non-irradiated cells for a short period of time, the cells are more likely to compensate and survive. Conversely, cancer cells exposed to ionising radiation, or cancers with defective DSB repair would be hypersensitive to p97 inhibitors. As sumoylated and ubiquitylated substrates accumulate on DNA break sites, the repair is slowed down (Hoeller et al., 2006), which makes cancer cells more sensitive to DNA damage caused by IR. Additionally, the preliminary proteomics data from this study demonstrated that immediately after IR, the interaction between p97 and UBXD8 specifically increases on chromatin, but decreases in the cytosol around 30 minutes after treatment and then only slightly increases over 8 hours (figure 3-1).

UBXD8 itself has two known ways in which it affects cancer cells. The first one is outlined in this study, where it controls the levels of SUMO on DNA damage sites by aiding its extraction. UBXD8 thereby could influence the dynamic assembly and disassembly of DDR proteins after DNA damage induction. However, it is reported to also have a role in the activation of the oncogene RAS-mediated ERK and PKB signalling pathways, and inhibition of UBXD8 leads to down-regulation of these oncogenic pathways (Phan et al., 2010). RAS is considered as a fundamental oncogene inducing genomic instability in cancer, because its activation leads to DNA replication stress and eventual hyperproliferation of cancer cells (Halazonetis et al., 2008). Based on these observations, inhibiting UBXD8 in cancer cells would lead on the one hand to SUMO and ubiquitin retention after DNA damage induction by ionising radiation, possibly slowing down DNA repair, and on the other hand to the downregulation of two major oncogenic signalling pathways. Extensive biochemical work is needed to better understand whether UBXD8 can be used as a possible cancer treatment in the future in combination with ionising radiation. It is firstly important to study the effects of UBXD8 depletion on cell viability

after IR by clonogenic assays, and to see whether UBXD8 depleted cells become hypersensitive to IR. This study provided preliminary data to show that this is likely to be the case.

References

Acs, K., M.S. Luijsterburg, L. Ackermann, F.A. Salomons, T. Hoppe, and N.P. Dantuma. 2011. The AAA-ATPase VCP/p97 promotes 53BP1 recruitment by removing L3MBTL1 from DNA double-strand breaks. *Nat Struct Mol Biol*. 18:1345-1350.

Ahnesorg, P., P. Smith, and S.P. Jackson. 2006. XLF interacts with the XRCC4-DNA ligase IV complex to promote DNA nonhomologous end-joining. *Cell*. 124:301-313.

Alexandru, G., J. Graumann, G.T. Smith, N.J. Kolawa, R. Fang, and R.J. Deshaies. 2008. UBXD7 binds multiple ubiquitin ligases and implicates p97 in HIF1alpha turnover. *Cell*. 134:804-816.

Alt, F.W., Y. Zhang, F.L. Meng, C. Guo, and B. Schwer. 2013. Mechanisms of programmed DNA lesions and genomic instability in the immune system. *Cell*. 152:417-429.

Amerik, A.Y., and M. Hochstrasser. 2004. Mechanism and function of deubiquitinating enzymes. *Biochim Biophys Acta*. 1695:189-207.

Anderson, D.J., R. Le Moigne, S. Djakovic, B. Kumar, J. Rice, S. Wong, J. Wang, B. Yao, E. Valle, S. Kiss von Soly, A. Madriaga, F. Soriano, M.K. Menon, Z.Y. Wu, M. Kampmann, Y. Chen, J.S. Weissman, B.T. Aftab, F.M. Yakes, L. Shawver, H.J. Zhou, D. Wustrow, and M. Rolfe. 2015. Targeting the AAA ATPase p97 as an Approach to Treat Cancer through Disruption of Protein Homeostasis. *Cancer Cell*. 28:653-665.

Antoniou, A.C., A.P. Cunningham, J. Peto, D.G. Evans, F. Lalloo, S.A. Narod, H.A. Risch, J.E. Eyfjord, J.L. Hopper, M.C. Southey, H. Olsson, O. Johannsson, A. Borg, B. Pasini, P. Radice, S. Manoukian, D.M. Eccles, N. Tang, E. Olah, H. Anton-Culver, E. Warner, J. Lubinski, J. Gronwald, B. Gorski, L. Tryggvadottir, K. Syrjakoski, O.P. Kallioniemi, H. Eerola, H. Nevanlinna, P.D. Pharoah, and D.F. Easton. 2008. The BOADICEA model of genetic susceptibility to breast and ovarian cancers: updates and extensions. *Br J Cancer*. 98:1457-1466.

Audebert, M., B. Salles, and P. Calsou. 2004. Involvement of poly(ADP-ribose) polymerase-1 and XRCC1/DNA ligase III in an alternative route for DNA double-strand breaks rejoining. *J Biol Chem*. 279:55117-55126.

Bartkova, J., N. Rezaei, M. Liontos, P. Karakaidos, D. Kletsas, N. Issaeva, L.V. Vassiliou, E. Kolettas, K. Niforou, V.C. Zoumpourlis, M. Takaoka, H. Nakagawa, F. Tort, K. Fugger, F. Johansson, M. Sehested, C.L. Andersen, L. Dyrskjot, T. Orntoft, J. Lukas,

C. Kittas, T. Helleday, T.D. Halazonetis, J. Bartek, and V.G. Gorgoulis. 2006. Oncogene-induced senescence is part of the tumorigenesis barrier imposed by DNA damage checkpoints. *Nature*. 444:633-637.

Bennardo, N., A. Cheng, N. Huang, and J.M. Stark. 2008. Alternative-NHEJ is a mechanistically distinct pathway of mammalian chromosome break repair. *PLoS Genet*. 4:e1000110.

Bergink, S., T. Ammon, M. Kern, L. Schermelleh, H. Leonhardt, and S. Jentsch. 2013. Role of Cdc48/p97 as a SUMO-targeted segregase curbing Rad51-Rad52 interaction. *Nat Cell Biol*. 15:526-532.

Bergink, S., and S. Jentsch. 2009. Principles of ubiquitin and SUMO modifications in DNA repair. *Nature*. 458:461-467.

Bodnar, N.O., and T.A. Rapoport. 2017. Molecular Mechanism of Substrate Processing by the Cdc48 ATPase Complex. *Cell*. 169:722-735 e729.

Bologna, S., V. Altmannova, E. Valtorta, C. Koenig, P. Liberali, C. Gentili, D. Anrather, G. Ammerer, L. Pelkmans, L. Krejci, and S. Ferrari. 2015. Sumoylation regulates EXO1 stability and processing of DNA damage. *Cell Cycle*. 14:2439-2450.

Branigan, E., A. Plechanovova, E.G. Jaffray, J.H. Naismith, and R.T. Hay. 2015. Structural basis for the RING-catalyzed synthesis of K63-linked ubiquitin chains. *Nat Struct Mol Biol*. 22:597-602.

Brown, J.S., N. Lukashchuk, M. Sczaniecka-Clift, S. Britton, C. le Sage, P. Calsou, P. Beli, Y. Galanty, and S.P. Jackson. 2015. Neddylation promotes ubiquitylation and release of Ku from DNA-damage sites. *Cell Rep*. 11:704-714.

Bryant, H.E., N. Schultz, H.D. Thomas, K.M. Parker, D. Flower, E. Lopez, S. Kyle, M. Meuth, N.J. Curtin, and T. Helleday. 2005. Specific killing of BRCA2-deficient tumours with inhibitors of poly(ADP-ribose) polymerase. *Nature*. 434:913-917.

Buchberger, A., H. Schindelin, and P. Hanzelmann. 2015. Control of p97 function by cofactor binding. *FEBS Lett*. 589:2578-2589.

Bunting, S.F., E. Callen, N. Wong, H.T. Chen, F. Polato, A. Gunn, A. Bothmer, N. Feldhahn, O. Fernandez-Capetillo, L. Cao, X. Xu, C.X. Deng, T. Finkel, M. Nussenzweig, J.M. Stark, and A. Nussenzweig. 2010. 53BP1 inhibits homologous recombination in Brca1-deficient cells by blocking resection of DNA breaks. *Cell*. 141:243-254.

Burrell, R.A., N. McGranahan, J. Bartek, and C. Swanton. 2013. The causes and consequences of genetic heterogeneity in cancer evolution. *Nature*. 501:338-345.

Cahill, D.P., K.W. Kinzler, B. Vogelstein, and C. Lengauer. 1999. Genetic instability and darwinian selection in tumours. *Trends Cell Biol*. 9:M57-60.

Cancer Genome Atlas Research, N., J.N. Weinstein, E.A. Collisson, G.B. Mills, K.R. Shaw, B.A. Ozenberger, K. Ellrott, I. Shmulevich, C. Sander, and J.M. Stuart. 2013. The Cancer Genome Atlas Pan-Cancer analysis project. *Nat Genet*. 45:1113-1120.

Cannavo, E., and P. Cejka. 2014. Sae2 promotes dsDNA endonuclease activity within Mre11-Rad50-Xrs2 to resect DNA breaks. *Nature*. 514:122-125.

Cao, L., X. Xu, S.F. Bunting, J. Liu, R.H. Wang, L.L. Cao, J.J. Wu, T.N. Peng, J. Chen, A. Nussenzweig, C.X. Deng, and T. Finkel. 2009. A selective requirement for 53BP1 in the biological response to genomic instability induced by Brca1 deficiency. *Mol Cell*. 35:534-541.

Ceccaldi, R., P. Sarangi, and A.D. D'Andrea. 2016. The Fanconi anaemia pathway: new players and new functions. *Nat Rev Mol Cell Biol*. 17:337-349.

Chapman, E., A.N. Fry, and M. Kang. 2011. The complexities of p97 function in health and disease. *Mol Biosyst*. 7:700-710.

Chauhan, D., Z. Tian, B. Nicholson, K.G. Kumar, B. Zhou, R. Carrasco, J.L. McDermott, C.A. Leach, M. Fulcinniti, M.P. Kodrasov, J. Weinstock, W.D. Kingsbury, T. Hideshima, P.K. Shah, S. Minvielle, M. Altun, B.M. Kessler, R. Orlowski, P. Richardson, N. Munshi, and K.C. Anderson. 2012. A small molecule inhibitor of ubiquitin-specific protease-7 induces apoptosis in multiple myeloma cells and overcomes bortezomib resistance. *Cancer Cell*. 22:345-358.

Chen, W.T., A. Alpert, C. Leiter, F. Gong, S.P. Jackson, and K.M. Miller. 2013. Systematic identification of functional residues in mammalian histone H2AX. *Mol Cell Biol*. 33:111-126.

Chen, X., C. Ruggiero, and S. Li. 2007. Yeast Rpb9 plays an important role in ubiquitylation and degradation of Rpb1 in response to UV-induced DNA damage. *Mol Cell Biol*. 27:4617-4625.

Chen, Z.J., and L.J. Sun. 2009. Nonproteolytic functions of ubiquitin in cell signaling. *Mol Cell*. 33:275-286.

Chow, K.H., S. Elgort, M. Dasso, M.A. Powers, and K.S. Ullman. 2014. The SUMO proteases SENP1 and SENP2 play a critical role in nucleoporin homeostasis and nuclear pore complex function. *Mol Biol Cell*. 25:160-168.

Christianson, J.C., J.A. Olzmann, T.A. Shaler, M.E. Sowa, E.J. Bennett, C.M. Richter, R.E. Tyler, E.J. Greenblatt, J.W. Harper, and R.R. Kopito. 2011. Defining human ERAD networks through an integrative mapping strategy. *Nat Cell Biol*. 14:93-105.

Christianson, J.C., and Y. Ye. 2014. Cleaning up in the endoplasmic reticulum: ubiquitin in charge. *Nat Struct Mol Biol*. 21:325-335.

Ciccia, A., and S.J. Elledge. 2010. The DNA damage response: making it safe to play with knives. *Mol Cell*. 40:179-204.

Costantini, S., L. Woodbine, L. Andreoli, P.A. Jeggo, and A. Vindigni. 2007. Interaction of the Ku heterodimer with the DNA ligase IV/Xrcc4 complex and its regulation by DNA-PK. *DNA Repair (Amst)*. 6:712-722.

Danielsen, J.R., L.K. Povlsen, B.H. Villumsen, W. Streicher, J. Nilsson, M. Wikstrom, S. Bekker-Jensen, and N. Mailand. 2012. DNA damage-inducible SUMOylation of HERC2 promotes RNF8 binding via a novel SUMO-binding Zinc finger. *J Cell Biol*. 197:179-187.

Deans, A.J., and S.C. West. 2011. DNA interstrand crosslink repair and cancer. *Nat Rev Cancer*. 11:467-480.

DeLaBarre, B., and A.T. Brunger. 2003. Complete structure of p97/valosin-containing protein reveals communication between nucleotide domains. *Nat Struct Biol*. 10:856-863.

Deshaies, R.J. 2014. Proteotoxic crisis, the ubiquitin-proteasome system, and cancer therapy. *BMC Biol*. 12:94.

Desterro, J.M., M.S. Rodriguez, and R.T. Hay. 1998. SUMO-1 modification of IkappaBalpha inhibits NF-kappaB activation. *Mol Cell*. 2:233-239.

Diehl, C., M. Akke, S. Bekker-Jensen, N. Mailand, W. Streicher, and M. Wikstrom. 2016. Structural Analysis of a Complex between Small Ubiquitin-like Modifier 1 (SUMO1) and the ZZ Domain of CREB-binding Protein (CBP/p300) Reveals a New Interaction Surface on SUMO. *J Biol Chem*. 291:12658-12672.

Dikic, I., S. Wakatsuki, and K.J. Walters. 2009. Ubiquitin-binding domains - from structures to functions. *Nat Rev Mol Cell Biol*. 10:659-671.

Dou, H., C. Huang, M. Singh, P.B. Carpenter, and E.T. Yeh. 2010. Regulation of DNA repair through deSUMOylation and SUMOylation of replication protein A complex. *Mol Cell*. 39:333-345.

Eid, W., M. Steger, M. El-Shemerly, L.P. Ferretti, J. Pena-Diaz, C. Konig, E. Valtorta, A.A. Sartori, and S. Ferrari. 2010. DNA end resection by CtIP and exonuclease 1 prevents genomic instability. *EMBO Rep*. 11:962-968.

Escribano-Diaz, C., A. Orthwein, A. Fradet-Turcotte, M. Xing, J.T. Young, J. Tkac, M.A. Cook, A.P. Rosebrock, M. Munro, M.D. Canny, D. Xu, and D. Durocher. 2013. A cell cycle-dependent regulatory circuit composed of 53BP1-RIF1 and BRCA1-CtIP controls DNA repair pathway choice. *Mol Cell*. 49:872-883.

Farmer, H., N. McCabe, C.J. Lord, A.N. Tutt, D.A. Johnson, T.B. Richardson, M. Santarosa, K.J. Dillon, I. Hickson, C. Knights, N.M. Martin, S.P. Jackson, G.C. Smith, and A. Ashworth. 2005. Targeting the DNA repair defect in BRCA mutant cells as a therapeutic strategy. *Nature*. 434:917-921.

Feng, L., and J. Chen. 2012. The E3 ligase RNF8 regulates KU80 removal and NHEJ repair. *Nat Struct Mol Biol*. 19:201-206.

Forbes, S.A., N. Bindal, S. Bamford, C. Cole, C.Y. Kok, D. Beare, M. Jia, R. Shepherd, K. Leung, A. Menzies, J.W. Teague, P.J. Campbell, M.R. Stratton, and P.A. Futreal. 2011. COSMIC: mining complete cancer genomes in the Catalogue of Somatic Mutations in Cancer. *Nucleic Acids Res*. 39:D945-950.

Franz, A., L. Ackermann, and T. Hoppe. 2016. Ring of Change: CDC48/p97 Drives Protein Dynamics at Chromatin. *Front Genet*. 7:73.

Galanty, Y., R. Belotserkovskaya, J. Coates, and S.P. Jackson. 2012. RNF4, a SUMO-targeted ubiquitin E3 ligase, promotes DNA double-strand break repair. *Genes Dev*. 26:1179-1195.

Galanty, Y., R. Belotserkovskaya, J. Coates, S. Polo, K.M. Miller, and S.P. Jackson. 2009. Mammalian SUMO E3-ligases PIAS1 and PIAS4 promote responses to DNA double-strand breaks. *Nature*. 462:935-939.

Gareau, J.R., and C.D. Lima. 2010. The SUMO pathway: emerging mechanisms that shape specificity, conjugation and recognition. *Nat Rev Mol Cell Biol*. 11:861-871.

Garvin, A.J., R.M. Densham, S.A. Blair-Reid, K.M. Pratt, H.R. Stone, D. Weekes, K.J. Lawrence, and J.R. Morris. 2013. The deSUMOylase SENP7 promotes chromatin relaxation for homologous recombination DNA repair. *EMBO Rep*. 14:975-983.

Garvin, A.J., and J.R. Morris. 2017. SUMO, a small, but powerful, regulator of double-strand break repair. *Philos Trans R Soc Lond B Biol Sci*. 372.

Gibbs-Seymour, I., Y. Oka, E. Rajendra, B.T. Weinert, L.A. Passmore, K.J. Patel, J.V. Olsen, C. Choudhary, S. Bekker-Jensen, and N. Mailand. 2015. Ubiquitin-SUMO circuitry controls activated fanconi anemia ID complex dosage in response to DNA damage. *Mol Cell*. 57:150-164.

Goodarzi, A.A., T. Kurka, and P.A. Jeggo. 2011. KAP-1 phosphorylation regulates CHD3 nucleosome remodeling during the DNA double-strand break response. *Nat Struct Mol Biol*. 18:831-839.

Gottlich, B., S. Reichenberger, E. Feldmann, and P. Pfeiffer. 1998. Rejoining of DNA double-strand breaks in vitro by single-strand annealing. *Eur J Biochem*. 258:387-395.

Grabbe, C., K. Husnjak, and I. Dikic. 2011. The spatial and temporal organization of ubiquitin networks. *Nat Rev Mol Cell Biol*. 12:295-307.

Grundy, G.J., H.A. Moulding, K.W. Caldecott, and S.L. Rulten. 2014. One ring to bring them all--the role of Ku in mammalian non-homologous end joining. *DNA Repair (Amst)*. 17:30-38.

Grundy, G.J., S.L. Rulten, Z. Zeng, R. Arribas-Bosacoma, N. Iles, K. Manley, A. Oliver, and K.W. Caldecott. 2013. APLF promotes the assembly and activity of non-homologous end joining protein complexes. *EMBO J*. 32:112-125.

Guervilly, J.H., A. Takedachi, V. Naim, S. Scaglione, C. Chawhan, Y. Lovera, E. Despras, I. Kuraoka, P. Kannouche, F. Rosselli, and P.H. Gaillard. 2015. The SLX4 complex is a SUMO E3 ligase that impacts on replication stress outcome and genome stability. *Mol Cell*. 57:123-137.

Guzzo, C.M., C.E. Berndsen, J. Zhu, V. Gupta, A. Datta, R.A. Greenberg, C. Wolberger, and M.J. Matunis. 2012. RNF4-dependent hybrid SUMO-ubiquitin chains are signals for RAP80 and thereby mediate the recruitment of BRCA1 to sites of DNA damage. *Sci Signal*. 5:ra88.

Guzzo, C.M., A. Ringel, E. Cox, I. Uzoma, H. Zhu, S. Blackshaw, C. Wolberger, and M.J. Matunis. 2014. Characterization of the SUMO-binding activity of the myeloproliferative and mental retardation (MYM)-type zinc fingers in ZNF261 and ZNF198. *PLoS One*. 9:e105271.

Haince, J.F., D. McDonald, A. Rodrigue, U. Dery, J.Y. Masson, M.J. Hendzel, and G.G. Poirier. 2008. PARP1-dependent kinetics of recruitment of MRE11 and NBS1 proteins to multiple DNA damage sites. *J Biol Chem*. 283:1197-1208.

Haines, D.S. 2010. p97-containing complexes in proliferation control and cancer: emerging culprits or guilt by association? *Genes Cancer*. 1:753-763.

Halazonetis, T.D., V.G. Gorgoulis, and J. Bartek. 2008. An oncogene-induced DNA damage model for cancer development. *Science*. 319:1352-1355.

Hanahan, D., and R.A. Weinberg. 2011. Hallmarks of cancer: the next generation. *Cell*. 144:646-674.

Hannich, J.T., A. Lewis, M.B. Kroetz, S.J. Li, H. Heide, A. Emili, and M. Hochstrasser. 2005. Defining the SUMO-modified proteome by multiple approaches in Saccharomyces cerevisiae. *J Biol Chem*. 280:4102-4110.

Hanzelmann, P., A. Buchberger, and H. Schindelin. 2011. Hierarchical binding of cofactors to the AAA ATPase p97. *Structure*. 19:833-843.

Harper, J.W., and S.J. Elledge. 2007. The DNA damage response: ten years after. *Mol Cell*. 28:739-745.

Hashimoto, K., and A.R. Panchenko. 2010. Mechanisms of protein oligomerization, the critical role of insertions and deletions in maintaining different oligomeric states. *Proc Natl Acad Sci U S A*. 107:20352-20357.

Heaton, S.M., N.A. Borg, and V.M. Dixit. 2016. Ubiquitin in the activation and attenuation of innate antiviral immunity. *J Exp Med*. 213:1-13.

Heideker, J., J. Prudden, J.J. Perry, J.A. Tainer, and M.N. Boddy. 2011. SUMO-targeted ubiquitin ligase, Rad60, and Nse2 SUMO ligase suppress spontaneous Top1-mediated DNA damage and genome instability. *PLoS Genet*. 7:e1001320.

Helleday, T., E. Petermann, C. Lundin, B. Hodgson, and R.A. Sharma. 2008. DNA repair pathways as targets for cancer therapy. *Nat Rev Cancer*. 8:193-204.

Hendriks, I.A., R.C. D'Souza, J.G. Chang, M. Mann, and A.C. Vertegaal. 2015. System-wide identification of wild-type SUMO-2 conjugation sites. *Nat Commun*. 6:7289.

Hendriks, I.A., D. Lyon, C. Young, L.J. Jensen, A.C. Vertegaal, and M.L. Nielsen. 2017. Site-specific mapping of the human SUMO proteome reveals co-modification with phosphorylation. *Nat Struct Mol Biol*. 24:325-336.

Hendriks, I.A., and A.C. Vertegaal. 2016. A comprehensive compilation of SUMO proteomics. *Nat Rev Mol Cell Biol*. 17:581-595.

Hoeller, D., C.M. Hecker, and I. Dikic. 2006. Ubiquitin and ubiquitin-like proteins in cancer pathogenesis. *Nat Rev Cancer*. 6:776-788.

Hoeller, D., C.M. Hecker, S. Wagner, V. Rogov, V. Dotsch, and I. Dikic. 2007. E3-independent monoubiquitination of ubiquitin-binding proteins. *Mol Cell*. 26:891-898.

Hu, X., A. Paul, and B. Wang. 2012. Rap80 protein recruitment to DNA double-strand breaks requires binding to both small ubiquitin-like modifier (SUMO) and ubiquitin conjugates. *J Biol Chem*. 287:25510-25519.

Hu, Y., and J.D. Parvin. 2014. Small ubiquitin-like modifier (SUMO) isoforms and conjugation-independent function in DNA double-strand break repair pathways. *J Biol Chem*. 289:21289-21295.

Hudson, J.J., S.C. Chiang, O.S. Wells, C. Rookyard, and S.F. El-Khamisy. 2012. SUMO modification of the neuroprotective protein TDP1 facilitates chromosomal single-strand break repair. *Nat Commun*. 3:733.

Ishiai, M., M. Kimura, K. Namikoshi, M. Yamazoe, K. Yamamoto, H. Arakawa, K. Agematsu, N. Matsushita, S. Takeda, J.M. Buerstedde, and M. Takata. 2004. DNA cross-link repair protein SNM1A interacts with PIAS1 in nuclear focus formation. *Mol Cell Biol*. 24:10733-10741.

Ishigaki, S., N. Hishikawa, J. Niwa, S. Iemura, T. Natsume, S. Hori, A. Kakizuka, K. Tanaka, and G. Sobue. 2004. Physical and functional interaction between Dorfin and Valosin-containing protein that are colocalized in ubiquitylated inclusions in neurodegenerative disorders. *J Biol Chem*. 279:51376-51385.

Ismail, I.H., J.P. Gagne, M.M. Genois, H. Strickfaden, D. McDonald, Z. Xu, G.G. Poirier, J.Y. Masson, and M.J. Hendzel. 2015. The RNF138 E3 ligase displaces Ku to promote DNA end resection and regulate DNA repair pathway choice. *Nat Cell Biol*. 17:1446-1457.

Jackson, S.P., and J. Bartek. 2009. The DNA-damage response in human biology and disease. *Nature*. 461:1071-1078.

Jackson, S.P., and D. Durocher. 2013. Regulation of DNA damage responses by ubiquitin and SUMO. *Mol Cell*. 49:795-807.

Jentsch, S., and I. Psakhye. 2013. Control of nuclear activities by substrate-selective and protein-group SUMOylation. *Annu Rev Genet*. 47:167-186.

Jiang, H., H.C. Reinhardt, J. Bartkova, J. Tommiska, C. Blomqvist, H. Nevanlinna, J. Bartek, M.B. Yaffe, and M.T. Hemann. 2009. The combined status of ATM and p53 link tumor development with therapeutic response. *Genes Dev*. 23:1895-1909.

Jiang, N., Y. Shen, X. Fei, K. Sheng, P. Sun, Y. Qiu, J. Larner, L. Cao, X. Kong, and J. Mi. 2013. Valosin-containing protein regulates the proteasome-mediated degradation of DNA-PKcs in glioma cells. *Cell Death Dis*. 4:e647.

Jiricny, J. 2006. The multifaceted mismatch-repair system. *Nat Rev Mol Cell Biol*. 7:335-346.

Kanchi, K.L., K.J. Johnson, C. Lu, M.D. McLellan, M.D. Leiserson, M.C. Wendl, Q. Zhang, D.C. Koboldt, M. Xie, C. Kandoth, J.F. McMichael, M.A. Wyczalkowski, D.E. Larson, H.K. Schmidt, C.A. Miller, R.S. Fulton, P.T. Spellman, E.R. Mardis, T.E. Druley, T.A. Graubert, P.J. Goodfellow, B.J. Raphael, R.K. Wilson, and L. Ding. 2014. Integrated analysis of germline and somatic variants in ovarian cancer. *Nat Commun*. 5:3156.

Kastan, M.B. 2008. DNA damage responses: mechanisms and roles in human disease: 2007 G.H.A. Clowes Memorial Award Lecture. *Mol Cancer Res*. 6:517-524.

Kerscher, O. 2007. SUMO junction-what's your function? New insights through SUMO-interacting motifs. *EMBO Rep*. 8:550-555.

Khanna, K.K., and S.P. Jackson. 2001. DNA double-strand breaks: signaling, repair and the cancer connection. *Nat Genet*. 27:247-254.

Kim, H., H. Zhang, D. Meng, G. Russell, J.N. Lee, and J. Ye. 2013. UAS domain of Ubxd8 and FAF1 polymerizes upon interaction with long-chain unsaturated fatty acids. *J Lipid Res*. 54:2144-2152.

Kim, J.S., T.B. Krasieva, H. Kurumizaka, D.J. Chen, A.M. Taylor, and K. Yokomori. 2005. Independent and sequential recruitment of NHEJ and HR factors to DNA damage sites in mammalian cells. *J Cell Biol*. 170:341-347.

Kim, W., E.J. Bennett, E.L. Huttlin, A. Guo, J. Li, A. Possemato, M.E. Sowa, R. Rad, J. Rush, M.J. Comb, J.W. Harper, and S.P. Gygi. 2011. Systematic and quantitative assessment of the ubiquitin-modified proteome. *Mol Cell*. 44:325-340.

Kloppsteck, P., C.A. Ewens, A. Forster, X. Zhang, and P.S. Freemont. 2012. Regulation of p97 in the ubiquitin-proteasome system by the UBX protein-family. *Biochim Biophys Acta*. 1823:125-129.

Kohler, J.B., M.L. Jorgensen, G. Beinoraite, M. Thorsen, and G. Thon. 2013. Concerted action of the ubiquitin-fusion degradation protein 1 (Ufd1) and Sumo-targeted ubiquitin ligases (STUbLs) in the DNA-damage response. *PLoS One*. 8:e80442.

Komander, D., and M. Rape. 2012. The ubiquitin code. *Annu Rev Biochem*. 81:203-229.

Kong, X., S.K. Mohanty, J. Stephens, J.T. Heale, V. Gomez-Godinez, L.Z. Shi, J.S. Kim, K. Yokomori, and M.W. Berns. 2009. Comparative analysis of different laser systems to study cellular responses to DNA damage in mammalian cells. *Nucleic Acids Res*. 37:e68.

Kuo, C.Y., X. Li, J.M. Stark, H.M. Shih, and D.K. Ann. 2016. RNF4 regulates DNA double-strand break repair in a cell cycle-dependent manner. *Cell Cycle*. 15:787-798.

Lamoliatte, F., F.P. McManus, G. Maarifi, M.K. Chelbi-Alix, and P. Thibault. 2017. Uncovering the SUMOylation and ubiquitylation crosstalk in human cells using sequential peptide immunopurification. *Nat Commun*. 8:14109.

Lee, J.W., L. Blanco, T. Zhou, M. Garcia-Diaz, K. Bebenek, T.A. Kunkel, Z. Wang, and L.F. Povirk. 2004. Implication of DNA polymerase lambda in alignment-based gap filling for nonhomologous DNA end joining in human nuclear extracts. *J Biol Chem*. 279:805-811.

Lee, K.J., J. Saha, J. Sun, K.R. Fattah, S.C. Wang, B. Jakob, L. Chi, S.Y. Wang, G. Taucher-Scholz, A.J. Davis, and D.J. Chen. 2016. Phosphorylation of Ku dictates DNA double-strand break (DSB) repair pathway choice in S phase. *Nucleic Acids Res*. 44:1732-1745.

Lessel, D., B. Vaz, S. Halder, P.J. Lockhart, I. Marinovic-Terzic, J. Lopez-Mosqueda, M. Philipp, J.C. Sim, K.R. Smith, J. Oehler, E. Cabrera, R. Freire, K. Pope, A. Nahid, F. Norris, R.J. Leventer, M.B. Delatycki, G. Barbi, S. von Ameln, J. Hogel, M. Degoricija, R. Fertig, M.D. Burkhalter, K. Hofmann, H. Thiele, J. Altmuller, G. Nurnberg, P. Nurnberg, M. Bahlo, G.M. Martin, C.M. Aalfs, J. Oshima, J. Terzic, D.J.

Amor, I. Dikic, K. Ramadan, and C. Kubisch. 2014. Mutations in SPRTN cause early onset hepatocellular carcinoma, genomic instability and progeroid features. *Nat Genet*. 46:1239-1244.

Lieber, M.R., Y. Ma, U. Pannicke, and K. Schwarz. 2003. Mechanism and regulation of human non-homologous DNA end-joining. *Nat Rev Mol Cell Biol*. 4:712-720.

Limoli, C.L., and J.F. Ward. 1993. A new method for introducing double-strand breaks into cellular DNA. *Radiat Res*. 134:160-169.

Liu, C., S. Srihari, K.A. Cao, G. Chenevix-Trench, P.T. Simpson, M.A. Ragan, and K.K. Khanna. 2014. A fine-scale dissection of the DNA double-strand break repair machinery and its implications for breast cancer therapy. *Nucleic Acids Res*. 42:6106-6127.

Lord, C.J., and A. Ashworth. 2012. The DNA damage response and cancer therapy. *Nature*. 481:287-294.

Lord, C.J., A.N. Tutt, and A. Ashworth. 2015. Synthetic lethality and cancer therapy: lessons learned from the development of PARP inhibitors. *Annu Rev Med*. 66:455-470.

Lukas, J., C. Lukas, and J. Bartek. 2011. More than just a focus: The chromatin response to DNA damage and its role in genome integrity maintenance. *Nat Cell Biol*. 13:1161-1169.

Luo, K., H. Zhang, L. Wang, J. Yuan, and Z. Lou. 2012. Sumoylation of MDC1 is important for proper DNA damage response. *EMBO J*. 31:3008-3019.

Mahajan, K.N., S.A. Nick McElhinny, B.S. Mitchell, and D.A. Ramsden. 2002. Association of DNA polymerase mu (pol mu) with Ku and ligase IV: role for pol mu in end-joining double-strand break repair. *Mol Cell Biol*. 22:5194-5202.

Maison, C., K. Romeo, D. Bailly, M. Dubarry, J.P. Quivy, and G. Almouzni. 2012. The SUMO protease SENP7 is a critical component to ensure HP1 enrichment at pericentric heterochromatin. *Nat Struct Mol Biol*. 19:458-460.

Mari, P.O., B.I. Florea, S.P. Persengiev, N.S. Verkaik, H.T. Bruggenwirth, M. Modesti, G. Giglia-Mari, K. Bezstarosti, J.A. Demmers, T.M. Luider, A.B. Houtsmuller, and D.C. van Gent. 2006. Dynamic assembly of end-joining complexes requires interaction between Ku70/80 and XRCC4. *Proc Natl Acad Sci U S A*. 103:18597-18602.

Marteijn, J.A., H. Lans, W. Vermeulen, and J.H. Hoeijmakers. 2014. Understanding nucleotide excision repair and its roles in cancer and ageing. *Nat Rev Mol Cell Biol*. 15:465-481.

Matic, I., M. van Hagen, J. Schimmel, B. Macek, S.C. Ogg, M.H. Tatham, R.T. Hay, A.I. Lamond, M. Mann, and A.C.O. Vertegaal. 2008. In vivo identification of human small ubiquitin-like modifier polymerization sites by high accuracy mass spectrometry and an in vitro to in vivo strategy. *Mol Cell Proteomics*. 7:132-144.

Meerang, M., D. Ritz, S. Paliwal, Z. Garajova, M. Bosshard, N. Mailand, P. Janscak, U. Hubscher, H. Meyer, and K. Ramadan. 2011. The ubiquitin-selective segregase VCP/p97 orchestrates the response to DNA double-strand breaks. *Nat Cell Biol*. 13:1376-1382.

Meray, R.K., and P.T. Lansbury, Jr. 2007. Reversible monoubiquitination regulates the Parkinson disease-associated ubiquitin hydrolase UCH-L1. *J Biol Chem*. 282:10567-10575.

Mevissen, T.E.T., and D. Komander. 2017. Mechanisms of Deubiquitinase Specificity and Regulation. *Annu Rev Biochem*. 86:159-192.

Meyer, H., M. Bug, and S. Bremer. 2012. Emerging functions of the VCP/p97 AAA-ATPase in the ubiquitin system. *Nat Cell Biol*. 14:117-123.

Minty, A., X. Dumont, M. Kaghad, and D. Caput. 2000. Covalent modification of p73alpha by SUMO-1. Two-hybrid screening with p73 identifies novel SUMO-1-interacting proteins and a SUMO-1 interaction motif. *J Biol Chem*. 275:36316-36323.

Mishina, Y., E.M. Duguid, and C. He. 2006. Direct reversal of DNA alkylation damage. *Chem Rev*. 106:215-232.

Mo, Y.Y., and S.J. Moschos. 2005. Targeting Ubc9 for cancer therapy. *Expert Opin Ther Targets*. 9:1203-1216.

Morris, J.R., C. Boutell, M. Keppler, R. Densham, D. Weekes, A. Alamshah, L. Butler, Y. Galanty, L. Pangon, T. Kiuchi, T. Ng, and E. Solomon. 2009. The SUMO modification pathway is involved in the BRCA1 response to genotoxic stress. *Nature*. 462:886-890.

Moschos, S.J., and Y.Y. Mo. 2006. Role of SUMO/Ubc9 in DNA damage repair and tumorigenesis. *J Mol Histol*. 37:309-319.

Motycka, T.A., T. Bessho, S.M. Post, P. Sung, and A.E. Tomkinson. 2004. Physical and functional interaction between the XPF/ERCC1 endonuclease and hRad52. *J Biol Chem*. 279:13634-13639.

Mueller, B., E.J. Klemm, E. Spooner, J.H. Claessen, and H.L. Ploegh. 2008. SEL1L nucleates a protein complex required for dislocation of misfolded glycoproteins. *Proc Natl Acad Sci U S A*. 105:12325-12330.

Munoz, M.C., C. Laulier, A. Gunn, A. Cheng, D.F. Robbiani, A. Nussenzweig, and J.M. Stark. 2012. RING finger nuclear factor RNF168 is important for defects in homologous recombination caused by loss of the breast cancer susceptibility factor BRCA1. *J Biol Chem*. 287:40618-40628.

Nayak, A., and S. Muller. 2014. SUMO-specific proteases/isopeptidases: SENPs and beyond. *Genome Biol*. 15:422.

Nick McElhinny, S.A., J.M. Havener, M. Garcia-Diaz, R. Juarez, K. Bebenek, B.L. Kee, L. Blanco, T.A. Kunkel, and D.A. Ramsden. 2005. A gradient of template dependence defines distinct biological roles for family X polymerases in nonhomologous end joining. *Mol Cell*. 19:357-366.

Nie, M., A. Aslanian, J. Prudden, J. Heideker, A.A. Vashisht, J.A. Wohlschlegel, J.R. Yates, 3rd, and M.N. Boddy. 2012. Dual recruitment of Cdc48 (p97)-Ufd1-Npl4 ubiquitin-selective segregase by small ubiquitin-like modifier protein (SUMO) and ubiquitin in SUMO-targeted ubiquitin ligase-mediated genome stability functions. *J Biol Chem*. 287:29610-29619.

Nijman, S.M., T.T. Huang, A.M. Dirac, T.R. Brummelkamp, R.M. Kerkhoven, A.D. D'Andrea, and R. Bernards. 2005. The deubiquitinating enzyme USP1 regulates the Fanconi anemia pathway. *Mol Cell*. 17:331-339.

Nimonkar, A.V., J. Genschel, E. Kinoshita, P. Polaczek, J.L. Campbell, C. Wyman, P. Modrich, and S.C. Kowalczykowski. 2011. BLM-DNA2-RPA-MRN and EXO1-BLM-RPA-MRN constitute two DNA end resection machineries for human DNA break repair. *Genes Dev*. 25:350-362.

Noon, A.T., A. Shibata, N. Rief, M. Lobrich, G.S. Stewart, P.A. Jeggo, and A.A. Goodarzi. 2010. 53BP1-dependent robust localized KAP-1 phosphorylation is essential for heterochromatic DNA double-strand break repair. *Nat Cell Biol*. 12:177-184.

O'Connor, M.J. 2015. Targeting the DNA Damage Response in Cancer. *Mol Cell*. 60:547-560.

Ochi, T., A.N. Blackford, J. Coates, S. Jhujh, S. Mehmood, N. Tamura, J. Travers, Q. Wu, V.M. Draviam, C.V. Robinson, T.L. Blundell, and S.P. Jackson. 2015. DNA repair. PAXX, a paralog of XRCC4 and XLF, interacts with Ku to promote DNA double-strand break repair. *Science*. 347:185-188.

Olzmann, J.A., C.M. Richter, and R.R. Kopito. 2013. Spatial regulation of UBXD8 and p97/VCP controls ATGL-mediated lipid droplet turnover. *Proc Natl Acad Sci U S A*. 110:1345-1350.

Ouyang, K.J., L.L. Woo, J. Zhu, D. Huo, M.J. Matunis, and N.A. Ellis. 2009. SUMO modification regulates BLM and RAD51 interaction at damaged replication forks. *PLoS Biol*. 7:e1000252.

Paul, K., M. Wang, E. Mladenov, A. Bencsik-Theilen, T. Bednar, W. Wu, H. Arakawa, and G. Iliakis. 2013. DNA ligases I and III cooperate in alternative non-homologous end-joining in vertebrates. *PLoS One*. 8:e59505.

Pearl, L.H., A.C. Schierz, S.E. Ward, B. Al-Lazikani, and F.M. Pearl. 2015. Therapeutic opportunities within the DNA damage response. *Nat Rev Cancer*. 15:166-180.

Perry, J.J., J.A. Tainer, and M.N. Boddy. 2008. A SIM-ultaneous role for SUMO and ubiquitin. *Trends Biochem Sci*. 33:201-208.

Phan, V.T., V.W. Ding, F. Li, R.J. Chalkley, A. Burlingame, and F. McCormick. 2010. The RasGAP proteins Ira2 and neurofibromin are negatively regulated by Gpb1 in yeast and ETEA in humans. *Mol Cell Biol*. 30:2264-2279.

Postow, L., C. Ghenoiu, E.M. Woo, A.N. Krutchinsky, B.T. Chait, and H. Funabiki. 2008. Ku80 removal from DNA through double strand break-induced ubiquitylation. *J Cell Biol*. 182:467-479.

Povirk, L.F., T. Zhou, R. Zhou, M.J. Cowan, and S.M. Yannone. 2007. Processing of 3'-phosphoglycolate-terminated DNA double strand breaks by Artemis nuclease. *J Biol Chem*. 282:3547-3558.

Puumalainen, M.R., D. Lessel, P. Ruthemann, N. Kaczmarek, K. Bachmann, K. Ramadan, and H. Naegeli. 2014. Chromatin retention of DNA damage sensors DDB2 and XPC through loss of p97 segregase causes genotoxicity. *Nat Commun*. 5:3695.

Rabouille, C., H. Kondo, R. Newman, N. Hui, P. Freemont, and G. Warren. 1998. Syntaxin 5 is a common component of the NSF- and p97-mediated reassembly pathways of Golgi cisternae from mitotic Golgi fragments in vitro. *Cell*. 92:603-610.

Ramadan, K., R. Bruderer, F.M. Spiga, O. Popp, T. Baur, M. Gotta, and H.H. Meyer. 2007. Cdc48/p97 promotes reformation of the nucleus by extracting the kinase Aurora B from chromatin. *Nature*. 450:1258-1262.

Raman, M., C.G. Havens, J.C. Walter, and J.W. Harper. 2011. A genome-wide screen identifies p97 as an essential regulator of DNA damage-dependent CDT1 destruction. *Mol Cell*. 44:72-84.

Ramanathan, H.N., and Y. Ye. 2011. Revoking the cellular license to replicate: yet another AAA assignment. *Mol Cell*. 44:3-4.

Ramanathan, H.N., and Y. Ye. 2012. The p97 ATPase associates with EEA1 to regulate the size of early endosomes. *Cell Res*. 22:346-359.

Reverter, D., and C.D. Lima. 2005. Insights into E3 ligase activity revealed by a SUMO-RanGAP1-Ubc9-Nup358 complex. *Nature*. 435:687-692.

Ribar, B., L. Prakash, and S. Prakash. 2007. ELA1 and CUL3 are required along with ELC1 for RNA polymerase II polyubiquitylation and degradation in DNA-damaged yeast cells. *Mol Cell Biol*. 27:3211-3216.

Ritz, D., M. Vuk, P. Kirchner, M. Bug, S. Schutz, A. Hayer, S. Bremer, C. Lusk, R.H. Baloh, H. Lee, T. Glatter, M. Gstaiger, R. Aebersold, C.C. Weihl, and H. Meyer. 2011. Endolysosomal sorting of ubiquitylated caveolin-1 is regulated by VCP and UBXD1 and impaired by VCP disease mutations. *Nat Cell Biol*. 13:1116-1123.

Robertson, A.B., A. Klungland, T. Rognes, and I. Leiros. 2009. DNA repair in mammalian cells: Base excision repair: the long and short of it. *Cell Mol Life Sci*. 66:981-993.

Rogakou, E.P., D.R. Pilch, A.H. Orr, V.S. Ivanova, and W.M. Bonner. 1998. DNA double-stranded breaks induce histone H2AX phosphorylation on serine 139. *J Biol Chem*. 273:5858-5868.

Rothenberg, E., J.M. Grimme, M. Spies, and T. Ha. 2008. Human Rad52-mediated homology search and annealing occurs by continuous interactions between overlapping nucleoprotein complexes. *Proc Natl Acad Sci U S A*. 105:20274-20279.

Rustgi, A.K. 2014. Familial pancreatic cancer: genetic advances. *Genes Dev*. 28:1-7.

Sampson, D.A., M. Wang, and M.J. Matunis. 2001. The small ubiquitin-like modifier-1 (SUMO-1) consensus sequence mediates Ubc9 binding and is essential for SUMO-1 modification. *J Biol Chem*. 276:21664-21669.

Sauer, R.T., and T.A. Baker. 2011. AAA+ proteases: ATP-fueled machines of protein destruction. *Annu Rev Biochem*. 80:587-612.

Schrul, B., and R.R. Kopito. 2016. Peroxin-dependent targeting of a lipid-droplet-destined membrane protein to ER subdomains. *Nat Cell Biol*. 18:740-751.

Schuberth, C., and A. Buchberger. 2008. UBX domain proteins: major regulators of the AAA ATPase Cdc48/p97. *Cell Mol Life Sci*. 65:2360-2371.

Schulz, S., G. Chachami, L. Kozaczkiewicz, U. Winter, N. Stankovic-Valentin, P. Haas, K. Hofmann, H. Urlaub, H. Ovaa, J. Wittbrodt, E. Meulmeester, and F. Melchior. 2012. Ubiquitin-specific protease-like 1 (USPL1) is a SUMO isopeptidase with essential, non-catalytic functions. *EMBO Rep*. 13:930-938.

Schwertman, P., S. Bekker-Jensen, and N. Mailand. 2016. Regulation of DNA double-strand break repair by ubiquitin and ubiquitin-like modifiers. *Nat Rev Mol Cell Biol*. 17:379-394.

Seeler, J.S., and A. Dejean. 2003. Nuclear and unclear functions of SUMO. *Nat Rev Mol Cell Biol*. 4:690-699.

Shin, E.J., H.M. Shin, E. Nam, W.S. Kim, J.H. Kim, B.H. Oh, and Y. Yun. 2012. DeSUMOylating isopeptidase: a second class of SUMO protease. *EMBO Rep*. 13:339-346.

Sims, J.J., and R.E. Cohen. 2009. Linkage-specific avidity defines the lysine 63-linked polyubiquitin-binding preference of rap80. *Mol Cell*. 33:775-783.

Song, J., L.K. Durrin, T.A. Wilkinson, T.G. Krontiris, and Y. Chen. 2004. Identification of a SUMO-binding motif that recognizes SUMO-modified proteins. *Proc Natl Acad Sci U S A*. 101:14373-14378.

Song, J., Z. Zhang, W. Hu, and Y. Chen. 2005. Small ubiquitin-like modifier (SUMO) recognition of a SUMO binding motif: a reversal of the bound orientation. *J Biol Chem*. 280:40122-40129.

Spasser, L., and A. Brik. 2012. Chemistry and biology of the ubiquitin signal. *Angew Chem Int Ed Engl*. 51:6840-6862.

Spratt, D.E., H. Walden, and G.S. Shaw. 2014. RBR E3 ubiquitin ligases: new structures, new insights, new questions. *Biochem J*. 458:421-437.

Stark, J.M., A.J. Pierce, J. Oh, A. Pastink, and M. Jasin. 2004. Genetic steps of mammalian homologous repair with distinct mutagenic consequences. *Mol Cell Biol*. 24:9305-9316.

Stolz, A., W. Hilt, A. Buchberger, and D.H. Wolf. 2011. Cdc48: a power machine in protein degradation. *Trends Biochem Sci*. 36:515-523.

Storchova, Z., and D. Pellman. 2004. From polyploidy to aneuploidy, genome instability and cancer. *Nat Rev Mol Cell Biol*. 5:45-54.

Stratton, M.R., P.J. Campbell, and P.A. Futreal. 2009. The cancer genome. *Nature*. 458:719-724.

Sun, H., J.D. Leverson, and T. Hunter. 2007. Conserved function of RNF4 family proteins in eukaryotes: targeting a ubiquitin ligase to SUMOylated proteins. *EMBO J*. 26:4102-4112.

Suzuki, M., T. Otsuka, Y. Ohsaki, J. Cheng, T. Taniguchi, H. Hashimoto, H. Taniguchi, and T. Fujimoto. 2012. Derlin-1 and UBXD8 are engaged in dislocation and degradation of lipidated ApoB-100 at lipid droplets. *Mol Biol Cell*. 23:800-810.

Tatham, M.H., M.C. Geoffroy, L. Shen, A. Plechanovova, N. Hattersley, E.G. Jaffray, J.J. Palvimo, and R.T. Hay. 2008. RNF4 is a poly-SUMO-specific E3 ubiquitin ligase required for arsenic-induced PML degradation. *Nat Cell Biol*. 10:538-546.

Tatham, M.H., E. Jaffray, O.A. Vaughan, J.M. Desterro, C.H. Botting, J.H. Naismith, and R.T. Hay. 2001. Polymeric chains of SUMO-2 and SUMO-3 are conjugated to protein substrates by SAE1/SAE2 and Ubc9. *J Biol Chem*. 276:35368-35374.

Taylor, E.B., and J. Rutter. 2011. Mitochondrial quality control by the ubiquitin-proteasome system. *Biochem Soc Trans*. 39:1509-1513.

Tighe, A., O. Staples, and S. Taylor. 2008. Mps1 kinase activity restrains anaphase during an unperturbed mitosis and targets Mad2 to kinetochores. *J Cell Biol*. 181:893-901.

Torrecilla, I., J. Oehler, and K. Ramadan. 2017. The role of ubiquitin-dependent segregase p97 (VCP or Cdc48) in chromatin dynamics after DNA double strand breaks. *Philos Trans R Soc Lond B Biol Sci*. 372.

Truong, L.N., Y. Li, L.Z. Shi, P.Y. Hwang, J. He, H. Wang, N. Razavian, M.W. Berns, and X. Wu. 2013. Microhomology-mediated End Joining and Homologous Recombination share the initial end resection step to repair DNA double-strand breaks in mammalian cells. *Proc Natl Acad Sci U S A*. 110:7720-7725.

Uematsu, N., E. Weterings, K. Yano, K. Morotomi-Yano, B. Jakob, G. Taucher-Scholz, P.O. Mari, D.C. van Gent, B.P. Chen, and D.J. Chen. 2007. Autophosphorylation of DNA-PKCS regulates its dynamics at DNA double-strand breaks. *J Cell Biol*. 177:219-229.

Ulrich, H.D. 2008. The fast-growing business of SUMO chains. *Mol Cell*. 32:301-305.

van den Boom, J., M. Wolf, L. Weimann, N. Schulze, F. Li, F. Kaschani, A. Riemer, C. Zierhut, M. Kaiser, G. Iliakis, H. Funabiki, and H. Meyer. 2016. VCP/p97 Extracts Sterically Trapped Ku70/80 Rings from DNA in Double-Strand Break Repair. *Mol Cell*. 64:189-198.

Verma, R., R. Oania, R. Fang, G.T. Smith, and R.J. Deshaies. 2011. Cdc48/p97 mediates UV-dependent turnover of RNA Pol II. *Mol Cell*. 41:82-92.

Verma, R., R.S. Oania, N.J. Kolawa, and R.J. Deshaies. 2013. Cdc48/p97 promotes degradation of aberrant nascent polypeptides bound to the ribosome. *Elife*. 2:e00308.

Vogelstein, B., N. Papadopoulos, V.E. Velculescu, S. Zhou, L.A. Diaz, Jr., and K.W. Kinzler. 2013. Cancer genome landscapes. *Science*. 339:1546-1558.

Wagner, S.A., P. Beli, B.T. Weinert, M.L. Nielsen, J. Cox, M. Mann, and C. Choudhary. 2011. A proteome-wide, quantitative survey of in vivo ubiquitylation sites reveals widespread regulatory roles. *Mol Cell Proteomics*. 10:M111 013284.

Walden, H., and A.J. Deans. 2014. The Fanconi anemia DNA repair pathway: structural and functional insights into a complex disorder. *Annu Rev Biophys*. 43:257-278.

Wang, A.T., and A. Smogorzewska. 2015. SnapShot: Fanconi anemia and associated proteins. *Cell*. 160:354-354 e351.

Wang, C.W., and S.C. Lee. 2012. The ubiquitin-like (UBX)-domain-containing protein Ubx2/Ubxd8 regulates lipid droplet homeostasis. *J Cell Sci*. 125:2930-2939.

Wang, Y., and M. Dasso. 2009. SUMOylation and deSUMOylation at a glance. *J Cell Sci*. 122:4249-4252.

Watts, G.D., J. Wymer, M.J. Kovach, S.G. Mehta, S. Mumm, D. Darvish, A. Pestronk, M.P. Whyte, and V.E. Kimonis. 2004. Inclusion body myopathy associated with Paget

disease of bone and frontotemporal dementia is caused by mutant valosin-containing protein. *Nat Genet*. 36:377-381.

Weinstock, J., J. Wu, P. Cao, W.D. Kingsbury, J.L. McDermott, M.P. Kodrasov, D.M. McKelvey, K.G. Suresh Kumar, S.J. Goldenberg, M.R. Mattern, and B. Nicholson. 2012. Selective Dual Inhibitors of the Cancer-Related Deubiquitylating Proteases USP7 and USP47. *ACS Med Chem Lett*. 3:789-792.

Wright, W.D., and W.D. Heyer. 2014. Rad54 functions as a heteroduplex DNA pump modulated by its DNA substrates and Rad51 during D loop formation. *Mol Cell*. 53:420-432.

Wu, C.S., J. Ouyang, E. Mori, H.D. Nguyen, A. Marechal, A. Hallet, D.J. Chen, and L. Zou. 2014. SUMOylation of ATRIP potentiates DNA damage signaling by boosting multiple protein interactions in the ATR pathway. *Genes Dev*. 28:1472-1484.

Wu, N., X. Kong, Z. Ji, W. Zeng, P.R. Potts, K. Yokomori, and H. Yu. 2012. Scc1 sumoylation by Mms21 promotes sister chromatid recombination through counteracting Wapl. *Genes Dev*. 26:1473-1485.

Xie, A., A. Hartlerode, M. Stucki, S. Odate, N. Puget, A. Kwok, G. Nagaraju, C. Yan, F.W. Alt, J. Chen, S.P. Jackson, and R. Scully. 2007. Distinct roles of chromatin-associated proteins MDC1 and 53BP1 in mammalian double-strand break repair. *Mol Cell*. 28:1045-1057.

Yano, K., K. Morotomi-Yano, S.Y. Wang, N. Uematsu, K.J. Lee, A. Asaithamby, E. Weterings, and D.J. Chen. 2008. Ku recruits XLF to DNA double-strand breaks. *EMBO Rep*. 9:91-96.

Ye, Y., H.H. Meyer, and T.A. Rapoport. 2003. Function of the p97-Ufd1-Npl4 complex in retrotranslocation from the ER to the cytosol: dual recognition of nonubiquitinated polypeptide segments and polyubiquitin chains. *J Cell Biol*. 162:71-84.

Yin, Y., A. Seifert, J.S. Chua, J.F. Maure, F. Golebiowski, and R.T. Hay. 2012. SUMO-targeted ubiquitin E3 ligase RNF4 is required for the response of human cells to DNA damage. *Genes Dev*. 26:1196-1208.

Zhang, F., Q. Fan, K. Ren, and P.R. Andreassen. 2009. PALB2 functionally connects the breast cancer susceptibility proteins BRCA1 and BRCA2. *Mol Cancer Res*. 7:1110-1118.

Zhang, W., Z. Qin, X. Zhang, and W. Xiao. 2011. Roles of sequential ubiquitination of PCNA in DNA-damage tolerance. *FEBS Lett*. 585:2786-2794.

Zhou, H.L., C. Geng, G. Luo, and H. Lou. 2013. The p97-UBXD8 complex destabilizes mRNA by promoting release of ubiquitinated HuR from mRNP. *Genes Dev*. 27:1046-1058.

Zhu, Y., and L.F. Parada. 2001. Neurofibromin, a tumor suppressor in the nervous system. *Exp Cell Res*. 264:19-28.